Varga, Dániel, Dipl.- Ing.

Impregnation of Polycarbonate in Supercritical Carbon Dioxide

DOCTORAL THESIS

to achieve the university degree of

Doktor der technischen Wissenschaften

submitted to

Graz University of Technology

Supervisor

Gamse, Thomas, Ao.Univ.-Prof. Dipl.-Ing. Dr.techn.

Institute of Chemical Engineering and Environmental Technology

Graz University of Technology

Graz, October 2016

AFFIDAVIT

I declare that I have authored this thesis independently, that I have not used other than the declared sources/resources, and that I have explicitly indicated all material which has been quoted either literally or by content from the sources used. The text document uploaded to TUGRAZonline is identical to the present doctoral thesis.

Date

Signature

This project was financially supported by the Marie Curie Initial Training Networks (ITN) via "DoHip − Training Program for the Design of Resource and Energy Efficient Products by High Pressure Processes", project number PITN-GA-2012-316959.

DoHip Training

- Life Long Learning (LLL) Intensive Course, **"Process Intensification by High Pressure Technologies – Actual Strategies for Energy and Resources Conservation"**, Darmstadt, (Germany). June 30 – July 17, 2013.

- Workshop I: **"Project Management, Intellectual Property Rights (IPR) and Tools for Literature and Patent Survey"** and Initial Exchange Program between partner universities and institutes; Bochum, Oberhausen (Germany), Valladolid (Spain), Graz (Austria), Maribor (Slovenia) and Budapest (Hungary). November 20 – December 6, 2013.

- Workshop II: **"Business and Communication Skills in English"**, Graz, (Austria). July 14-17, 2014. **"DoHip Analytical Course"**, Maribor (Slovenia). July 21-26, 2014.

- Workshop III: **"Academic Career Planing"**, Darmstadt, Frankfurt (Germany). June 15-19, 2015.

Publications

D. Varga, S. Alkin, P. Gluschitz, B. Péter-Szabó, E. Székely, T. Gamse: *Supercritical Fluid Dyeing of Polycarbonate in Carbon Dioxide,* Journal of Supercritical Fluids 116 (2016) 111–116.

Contributions

- Jahrestreffen der Fachgruppe Hochdruckverfahrenstechnik, March 13-14, 2014. Merseburg (Germany). **Poster presentation**: D. Varga, T. Gamse: *Supercritical impregnation and surface modification of natural products and polymers*

- 10th Minisymposium Verfahrenstechnik, June 17-18, 2014. Vienna (Austria). **Poster presentation**: D. Varga, T. Gamse: *The idea of creating reinforced polymers by supercritical fluid impregnation*

- Jahrestreffen der Fachgruppe Hochdruckverfahrenstechnik, March 4-5, 2015. Darmstadt (Germany). **Poster presentation**: D. Varga, T. Gamse: *Supercritical fluid impregnation for creating fiber reinforced polymers*

- Hungarian National Conference on Supercritical Fluids, 21th May 2015. Budapest (Hungary). **Oral presentation**: D. Varga, S. Alkin, T. Gamse: *Dyeing of Polycarbonate in Supercritical Carbon Dioxide*

- 10th European Congress of Chemical Engineering (ECCE2015), Sept. 27th – October 1st 2015. Nice (France). **Oral presentation**: D. Varga, T. Gamse: *Dyeing of Polycarbonate in Supercritical Carbon Dioxide*

- 12th Minisymposium Verfahrenstechnik, March 30-31, 2016. Graz (Austria). **Oral presentation:** *Impregnation of Polycarbonate with Copper Nanoparticles in Supercritical Carbon Dioxide*

- 15th European Meeting on Supercritical Fluids (EMSF2016), May 8-11, **2016**. Essen (Germany). **Oral presentation**: D. Varga, M. Giebler, T. Gamse: *Modification of Polycarbonate with Metal Impregnation in Supercritical Carbon Dioxide*

Acknowledgements

An dieser Stelle möchte ich all jenen danken, die mich während der Erstellung dieser Dissertation unterstützt haben. Zuallererst gebührt mein Dank Prof. Dr. Thomas Gamse, der mich während meiner Arbeit mit zahlreichen Ratschlägen versorgt hat. Dank seiner Expertise und Geduld war diese Forschung erst möglich. Ich möchte mich auch für seine Unterstützung abseits dieser Arbeit bedanken.
Dr. Helmar Wiltsche danke ich für die ICP–OES/MS Messungen. Ein besonderer Dank gilt Dr. Julian Wagner und dem Team des FELMI – ZFE Graz für die Rasterelektronmikroskopie Analyse. Ich danke unseren Technikern, Rene Fras und Johann Grubbauer für ihre Hilfe während des Aufbauens der Versuchshalle. Ich danke meinen Studenten für ihre Mithilfe: Simon Alkin, Peter Gluschitz, Rafael Halb, Lukas Koller, Michael Giebler und Simone Schiavo.

This project was financially supported by the Marie Curie Initial Training Networks (ITN) via "DoHip − Training Program for the Design of Resource and Energy Efficient Products by High Pressure Processes". I would like to acknowledge the DoHip coworkers for providing me this outstanding opportunity, and a very special thanks goes to Edit Székely and to Diego Castaneda for their support. I am grateful to Matjaž Finsgar and to Amra Perva Uzunalić from the University of Maribor for providing me the opportunity to carry out several analytical measurements at their faculty. Further on, of course, I have to mention all the Ph.D. students of the Marie Curie project, or the *DoHippies*, as we have named ourselves. Thanks for their support as well as the forever good mood and lovely spirit; I had so much fun at every project meeting and conference. Amongst them, I would specifically like to mention my colleague, Candela Campos Domínguez for her support; she always had an answer for my questions in connection with personal matters in everyday life or with high pressure fluid phase equilibria for ethanol–supercritical carbon dioxide system.

Végezetül pedig szeretném megköszönni a családomnak, hogy minden döntésemben messzemenőkig támogattak, a barátaimnak pedig mindazt a segítséget és türelmet, amit az elmúlt években adtak nekem. Nélkülük nagyon kevés dolog sikerült volna.

Abstract

In this work, investigations for polymer modification in supercritical media have been carried out. Being one of nowadays' most important technical plastic, polycarbonate was used for the study, which was impregnated in supercritical carbon dioxide. These sorption processes took place in a high pressure vessel in batch mode.

First, the colorability of this raw material was studied by the use of two azo-disperse dyes; disperse red 1 and disperse red 13. After investigating the properties of the raw polycarbonate, impregnation was carried out in the range of 100–300 bar and 3–24 hours sorption time at 40 to 60°C. During these experiments sorption kinetics were studied in detail and the solubility of the applied dyes were determined. In addition, equilibrium constants for the dyes between the polymer and the supercritical phase were calculated. As an outcome, entirely, deep dyed polymer pellets were obtained with excellent dyeing fixation, using only supercritical carbon dioxide as impregnation media. Maximal dye uptakes obtained were 0.010 wt % and 0.055 wt % for disperse red 1 and disperse red 13, respectively, with respect to the mass of the polymer. Having achieved these promising results, a calculation was made in order to scale up the impregnation device for a yearly production of 5 000 tons dyed polycarbonate. Moreover, cost estimation for the scaled up process was carried out.

As a second part of the work, different ways of metal modification of polycarbonate were explored. In the first approach, polycarbonate pellets were impregnated with dithizone, a chelate ligand capable to react with several metal ions. At this step, impregnation kinetics were studied in detail and diffusion coefficients of dithizone in polycarbonate and its solubility in supercritical carbon dioxide were determined. As a second step, the possible chelation of metal ions using these impregnated pellets was investigated. By this technique, a maximum copper load of 109±3 ppm and a zinc load of 21±3 ppm inside the polymer matrix were achieved. Samples were measured by scanning electron microscopy, which showed copper clusters having a size of 5 to 400 nanometers, equally distributed deep inside in the entire polymer matrix. Using a different, second approach, two dithizonate complexes of copper were synthesized in the lab and used for the impregnation. Highest copper load obtained by this way was 5±1 ppm. In order to compare the results achieved by using dithizonate complexes, the modification has also been carried out by applying a commercially available copper complex, the copper(hexafluoroacetylacetonate)-hydrate. By this, impregnation yielded to a maximum 5.0±0.7 ppm metal load in the polymer.

Kurzfassung

In dieser Arbeit wurden Untersuchungen zur Modifizierung von Polymeren mittels eines überkritischen Lösemittels durchgeführt. Als eines der wichtigsten Polymere heutzutage wurde Polykarbonat verwendet. Dieses wurde mit überkritischem Kohlenstoffdioxid imprägniert, wobei dieser Prozess in einem Hochdruckbehälter in diskontinuierlichem Betrieb stattgefunden hat.

Im ersten Teil der Arbeit wurde die Färbbarkeit vom Polykarbonat mit zwei Azo-Farbstoffen (disperse red 1 und disperse red 13) erforscht. Nachdem die Eigenschaften des Rohmaterials in überkritischem CO_2 geprüft wurden, erfolgte die Imprägnierung im Druckbereich von 100 bis 300 bar für 3 bis 24 Stunden bei Temperaturen von 40–60°C. Dabei wurde die Kinetik der Imprägnierung geprüft und die Löslichkeit der Farbstoffe in überkritischem CO_2 bestimmt. Zusätzlich erfolgte die Berechnung der Gleichgewichtskonstante von den Farbstoffen zwischen der Polymer- und Fluidphase. Aus dem in überkritischem CO_2 durchgeführten Färbeprozess resultierten vollständig und homogen eingefärbte Polykarbonatpellets mit einer extrem guten Farbfixierung. Die höchste Farbstoffaufnahmen waren 0.010 % und 0.055 % Massenanteil für disperse red 1 bzw. disperse red 13 bezogen auf das Polymergewicht. Aufgrund der guten Ergebnisse wurde die Versuchsanlage auf eine Industrieanlage für die Herstellung von 5000 Jahrestonnen gefärbten Polymers hochgerechnet inklusive einer Kostenrechnung.

Danach wurde die Vorgehensweisen bezüglich der Herstellung von mit Nanopartikeln imprägnierten Polykarbonaten erforscht. Als erstes Verfahren wurde ein zweistufiger Prozess entwickelt. In der ersten Stufe erfolgte die Imprägnierung von Polykarbonat mit Dithizon, einer Substanz, die mit verschiedenen Metallen Komplexe bilden kann. Hierbei wurde die Imprägnierkinetik untersucht und der Diffusionskoeffizient vom Dithizon im Polykarbonat bzw. die Gleichgewichtskonstante wurden bestimmt. Im zweiten Schritt diente das mit Dithizon imprägnierte Polykarbonat als Trägermaterial für Metalle. Durch diesen Prozess wurden Polykarbonate mit Beladungen von max. 109±3 ppm Kupfer und 21±3 ppm Zinkhergestellt. Die Proben wurden durch Rasterelektronmikroskopie untersucht, wobei sich Kupfercluster mit einer Größe von 5 bis 400 nm zeigten, die gleichmäßig in der gesamten Polymermatrix verteilt waren. Mit Hilfe einer anderen Methode wurden zwei Kupfer-Dithizonate-Komplexe hergestellt und für die Imprägnierung verwendet, wobei eine höchste

Kupferkonzentration von 5±1 ppm erreicht wurde. Diese Kupfermodifizierung wurde auch mit einem kommerziell erhältlichen Kupferkomplex, dem Kupfer(II)-(hexafluoracetylacetonat)-hydrat, durchgeführt. Dieser Komplex ergab eine maximale Kupferbeladung von 5.0±0.7 ppm in der Polymermatrix.

Preface

The modification of different raw materials via surface treatment or impregnation is a possible way to change their original characteristics. By impregnating natural products or polymers with different modifiers, virtually new products can be created. This occurs by introducing a specific chemical compound (which has practical properties) into their matrix. This process generally takes place in an appropriate chemical solvent, in which the dissolved additive is contacted with the matrix to be modified. Instead of liquid solvents also supercritical fluids (e.g. supercritical carbon dioxide, $scCO_2$) can be used. In this case, the method is called supercritical fluid impregnation (SFI). Supercritical fluids (SCFs) have tunable properties which means, by changing temperature and pressure, the properties like viscosity, diffusivity and dissolving capacity can be fine tuned. By the use of $scCO_2$ the organic solvent consumption can be reduced or in some processes even fully eliminated.

Since there is always a growing demand from the industry for developing new methods that can replace old techniques and overcome the drawbacks of recent processes, investigating and understanding the application of SFI for natural products and polymers is an important issue of nowadays chemical industry. There are numerous examples in the scientific literature where the SFI method was successfully used for substrate modification and some processes already have industrial applications.

Taking a polymer as a solid matrix for the impregnation in supercritical media also has a high importance. By using the benign properties of $scCO_2$ the production of new polymer mixtures, drug impregnation and metal modification of the matrix has already been realized. Supercritical fluid dyeing (SFD) is a particular case of SFI where the modifier is a dyestuff. Unlike conventional dyeing methods, this process does not require large amount of water and the use of heavy metals and surfactants. For coloring textile fibers SFD proved to be an appropriate process and it is already applied in industry. The applicability of SFD on polymers has already been an object of several investigations and it turned out that many polymers can be dyed in supercritical media. Most of the available studies provide elaborated data, but examples for successful polycarbonate dyeing with detailed data analysis and process optimization cannot be found in opened literature.

Polymer containing nanoparticles are also receiving growing interest in the recent years [1]. Due to their unique properties, they can be used in microelectronics and for optical and catalytic applications. The modification of polycarbonate with metal nanoparticles has already

been a scope of some studies. However, the main goal of these investigations was the surface modification of the polymer instead of the incorporation of different compounds deep into the polymer matrix.

Polycarbonate is a polymeric material that has high importance nowadays. It is an impact resistant, thermally stable, optically clear polymer. It has many practical applications and is mainly used in electronics and in the automotive industry. In 2011 approximately 3.5 million tons polycarbonate were end-used worldwide, out of which approx. half million tons in Europe. With an average growth of approx. 4 % per year, worldwide demand on polycarbonate is expected to increase up to 4.2 million tons by the end of 2016 [2].

Therefore, the aim of this work is to study the applicability of SFI on polycarbonate and provide new experimental data by understanding its behavior in the impregnation process. The first part of this work is focusing on polycarbonate dyeing via SFD, while the second part deals with investigations in order to create metal impregnated polycarbonate by using the SFI method.

Table of contents

I. Introduction to supercritical fluids

Gases can be liquefied below their critical temperature (T_c) by increasing their pressure. A pressure required in order to obtain liquefied gas at its T_c is called the critical pressure (p_c). A supercritical fluid (SCF) is a substance (liquid or gas) which is in a state above its T_c and p_c (i.e., above the critical point) [3]. In this supercritical (fluid) phase, the solvent has properties that are different from those of liquids or gases at standard conditions. This region can be observed in figure 1 on a schematic phase diagram; the critical point is marked with "**C**".

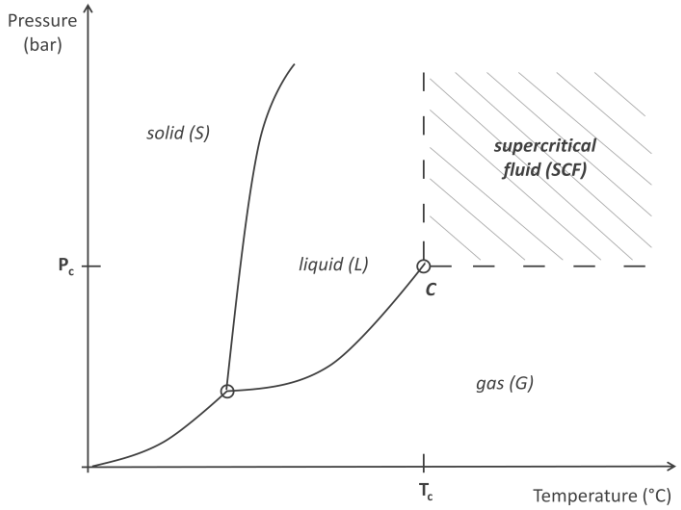

Figure 1: Schematic phase diagram with the critical point and supercritical phase

SCFs have similar density, thus solvating power, like several organic solvents, but their higher diffusivities, lower viscosity and surface tension make them in some cases much more effective. For some applications, several organic solvents (such as hexane, methanol, methylene chloride, chloroform) can be replaced by SCFs. Table 1 shows some physical parameters of the SCFs compared to liquid and gas phases.

Table 1: fluid densities and diffusivities [3]

parameter	gas	SCF	liquid
density (g/cm^3)	(10)E-3	0.2–0.9	0.8–1.0
diffusivity (cm^2/s)	0.01–1.0	(0.1–3.3)E-4	(0.5–2.0)E-5
viscosity	(0.5–3.5)E-4	(0.2–1.0)E-3	(0.3–2.4)E-2

SCFs are generally cheap, safe to use and have minimal disposal or regeneration costs. Moreover, only by changing their physical parameters like temperature and pressure, due to

the changes in density, the solvent power can be fine-tuned. These changes predominates more close to the critical point of a given fluid. The ability of adding cosolvents to SCFs, for example to change their polarity, further enhances their solvating properties. Table 2 shows the critical parameters of most common solvents used as SCF.

Table 2: critical parameters of some common used solvents [4]

Solvent	T_c [K]	P_c [bar]
methane	191	46.0
ethane	305	48.8
ethylene	282	50.3
propane	370	42.4
propylene	365	46.2
n-pentane	470	33.7
carbon dioxide	**304**	**73.8**
water	647	220.0

Processes applying SCFs are in operation for a long time. Residuum Oil Supercritical Extraction Process (ROSE) is used to extract deasphalted oils that can be used for fluid catalytic crackers and hydrocrackers. In this process, the extraction solvent is recovered and recycled after the separation [5]. Low density polyethylene (LDPE) is made via a free radical initiated polymerization process, which is carried out in supercritical ethylene [6]. Sub- and supercritical water is also used as cooling media for some reactors and as an oxidation media. [7,8]. Due to their low critical pressures, alkanes and alkenes are mostly used in the oil industry, which is well prepared for the security issues arising from the high flammability of such chemicals [4]. However, supercritical ethane and near-critical propane can also be used for oil and fat extraction from natural products [9], even their flammability is a considerable drawback.

For many practical reasons, the most commonly used supercritical solvent is supercritical carbon dioxide ($scCO_2$). Due to its low critical parameters (p_c = 73.8 bar and T_c = 31.1°C [10]), working with $scCO_2$ does not require very special equipment. Based on the relatively high fluid density it is a good solvent for non-polar substances and by adding some modifier this dissolving capacity, even for certain polar substances, can be fine tuned. $ScCO_2$ is not flammable, has a low toxicity and is available in high quantity and purity at a low costs. Being

a gas under ambient conditions favors its easy removal from the product, thus saving costs and energy on secondary down-stream processes such as drying and solvent removal. Since CO_2 is a by-product of other chemical syntheses, its use does not contribute to the net global warming effect hence it can be easily recovered in several industrial processes.

1. Applications of supercritical fluids

Supercritical fluids as solvent are used in several fields of chemical industry. Only between 1980 and 2003 more than 1100 patents were registered worldwide in connection with novel use of supercritical fluids. By 2007, more than 150 industrial high pressure extraction pants have already been in operation out of which approx. 100 work with extractor volumes of more than 500 liters [11]. Since the applications are numerous, only the most common methods involving SCFs are being briefly discussed here. A schematic draw in figure 2 shows an overview of the different applications.

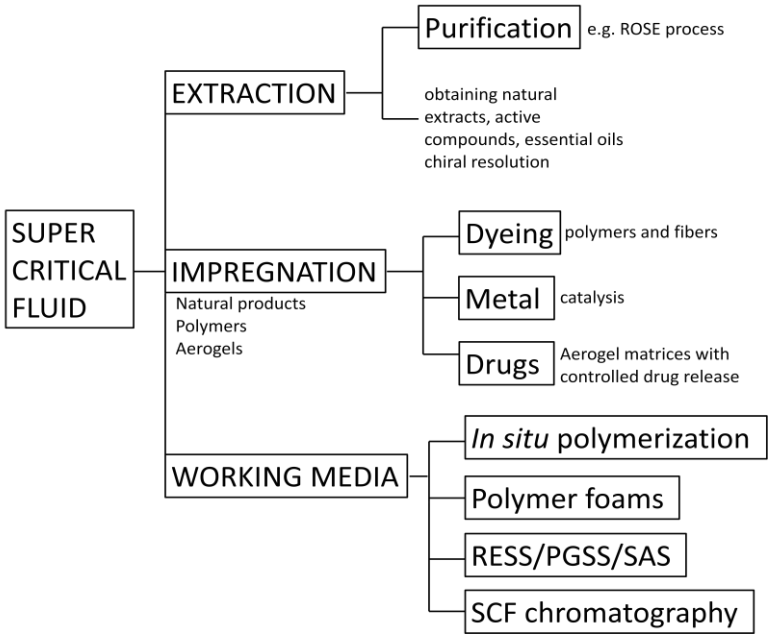

Figure 2: Applications of SCFs in chemical industry

1.1 Supercritical Fluid Extraction (SFE)

One of these applications is the supercritical fluid extraction (SFE). Examples for extraction of different compounds from natural products by SFE using CO_2 as a fluid are numerous. Round one hundred examples are listed by Reverchon and De Marco [12] reviewing research papers only between 1996 and 2006. Besides the above mentioned benign properties, the

biggest advantage of using $scCO_2$ for plant extraction is, that by the use of relatively low extraction temperature, essential oils and other heat sensitive compounds can be extracted. Data published in this field are numerous [13]. Extraction of alkaloids (e.g. decaffeination of coffee beans and nicotine removal from tobacco), herbs and spices, hop extraction and cork purification are the most common industrial examples of plant extraction [14]. Some of such extractions are also realized in industrial scale by Natex Prozesstechnologie GmbH, a leading company in supercritical technologies nowadays. The company has designed and built several supercritical plants, which are in operation worldwide, in India, Taiwan, Denmark, New Zealand and in Spain with extractor size varying between 200 and 20 000 liters [15]. However, SFE can also be carried out in really small, moreover, in *micro* scale plants. Instead of using huge extraction columns, ethanol – water separation can also be carried out by the use of micro devices. In a work published very recently ethanol was extracted from its aqueous solution by the use of a micro mixer operating in a continuous mode using $scCO_2$ as a fluid phase. By this process the authors proposed, that one theoretical stage of extraction could be achieved within this micro-mixer [16].

Figure 3: Supercritical extraction plant (600 liters, 550 bar) for spices and herbs, India [15]

The biggest advantage of using $scCO_2$ in extraction processes comes from the fact that its solvent power can be continuously varied by temperature and pressure. Therefore, it is possible to carry out two extraction steps for a given compound using the same batch. In the first step, by applying low density CO_2, the most soluble compounds (e.g. essential oils) can be extracted while the second step carried out at higher CO_2 density yields the less soluble

ones (for example, antioxidants). This makes it possible for instance, using the $scCO_2$ method, only the caffeine is gathered from coffee beans while the large-molecule flavor compounds remains behind [12]. Further on, CO_2 leaves the extract in gaseous form after decompression. Thus one of the main advantages is that the products are completely solvent free, without further treatment. $ScCO_2$ can also be used in enantiomer separation based on a diastereomer salt formation [17]. In some cases, the diastereomer salt can be formed in supercritical media (without adding any organic solvent) and subsequently, the unreacted enantiomer can be removed by SFE [18,19]. Interestingly, the structure of a diastereomer salt formed in supercritical media can be different from that of crystallized from organic solvent. This means, by using $scCO_2$, new crystal structures of some compounds can be obtained.

Using the supercritical fluids in purification techniques has also been of interest in the recent years. Probably, the highest importance has the already mentioned ROSE process for oil purification [5]. The extraction of heavy metals from water is also a highly investigated field. It is realized by adding different chelating agents to the aqueous solution of heavy metals which is capable of building a complex with the specific metals. This complex can be extracted by SFE later on. Erkey [20] suggests that there are numerous advantages of using supercritical fluids instead of an organic solvent, such as,

- the amount of extracting solvent can be decreased,
- residual contamination of the aqueous solution by the organic solvent can also be avoided,
- possible enhancement of extraction rate by the better mass transfer properties of SCFs,
- since SCFs have lower surface tension than organic solvents, the extraction requires smaller equipment for a given solvent to feed ratio compared to organic solvent extraction,
- selectivity of the process can be set by changing supercritical solvent properties by pressure and temperature,
- being inert, $scCO_2$ may not be degraded in some nuclear applications, such as Uranium extraction.

1.2 Supercritical Fluid Impregnation (SFI)

Contrary to the extraction, the aim of impregnation is to introduce certain compounds into a given material (that is, into a solid matrix). When using supercritical solvents for the process,

the method is called supercritical fluid impregnation (SFI). This is a convenient and environmentally friendly way for creating impregnated materials. The mostly common fluid is $scCO_2$ and thus applications of other supercritical fluids are not discussed in this section. Matrices that can be treated with impregnation additives are wood [21], polymers [22], aerogels [23,24], textile fibers [25] and many more. The impregnation additive (solute) can be basically anything. However, there is one general requirement: it has to have at least a slight solubility in the applied fluid [22]. SFI is a batch process which takes place in a high pressure vessel. The sorption itself is carried out in one single step: after placing the raw materials in the tempered vessel, it is sealed, pressurized up to the desired pressure and being held under pressure for a given impregnation time (typically for several hours).

It is important to distinguish between two different mechanisms of SFI of additives into polymer matrices.

- The first involves the simple deposition of a compound soluble in a SCF into the matrix. This happens when the solute is highly soluble in the SCF. When the vessel is decompressed, CO_2 molecules leave the polymer quickly (in gas form), leaving the solute molecules trapped inside the matrix.
- A different mechanism applies to compounds having very low solubility in the supercritical phase, as in the case of polymer dyeing, for example. In such cases the high affinity of these solutes for certain matrices can result in the preferential partitioning of a solute in favor of matrix over the fluid phase [26].

Irrespective of which mechanism governs the sorption, the most determinative parameters of the SFI are the density of $scCO_2$ (related to applied pressure and temperature conditions), sorption time and the depressurization rate [26]. This process has several advantages upon conventional technologies based on the fact that $scCO_2$ is an environmentally benign solvent and thus it can replace some other harmful chemicals. With this method, several polymer blends can be formed which theoretically could not be produced by other techniques because carbon dioxide acts as a plasticizing agent and decreases the glass transition temperature (T_g) thus enables an efficient mixing of the two polymers [26]. After the impregnation process during the depressurization step CO_2 leaves as a gas. So the product is solvent free at the end and the gaseous CO_2 can be cooled down and re-used by cleaning and recirculation. By this method, polymers with high crystallinity and really high molecular weight such as UHMW-PE can also be impregnated [27].

Water used in the conventional dyeing technologies of textile yarns or polymers contains at the end of the process large quantities of chemicals, salts and alkali, which is a chemical

waste really difficult to treat. By using a particular case of solute impregnation, the supercritical fluid dyeing (SFD), both the water consumption and the waste production can be eliminated, because supercritical fluids can replace water in the dyeing processes [25]. The first patent in connection with polymer dyeing by $scCO_2$ was published in 1988 [28] where a technique was proposed for polyethylene terephthalate (PET) dyeing which was thoughtfully investigated in the next years [29,30].

The use of SFI has also a high importance in forestry including paper and pulp industry [31]. Chemically, wood mostly consists of cellulose, hemicelluloses and lignin. Arising from their orientation, wood has a dense but relatively porous structure. Whatever the impregnation solute is, accessibility of wood components with this modifying material is a key factor. These chemicals must be able to enter the cell walls and to diffuse into the middle lamella region. Having low viscosities (which enhance penetration) and liquid-like densities (which improve dissolution) a SCF is an appropriate media for wood treatment. Wood matrices can easily be percolated by $scCO_2$ with only a minimal damage to the cellulosic fractions. Many examples are given in literature for wood impregnation, such as incorporation of chemical preservatives or impregnation by high molecular weight polymers for increase its mechanical strength [21]. Wood extraction (such as delignification) by using supercritical fluids has also been explored [31].

1.3 Supercritical carbon dioxide ($scCO_2$) as working media

Due to the already mentioned individual properties of SCFs, they can also be used in several different processes. For example, a supercritical fluid, which has the higher diffusivity and the lower viscosity than a liquid solvent, will function much better than a liquid solvent as a mobile phase in chromatography. Therefore, a chromatography method that uses SCF (i.e., supercritical fluid chromatography, SFC) was invented in the sixties. The biggest technical advantage of SFC over liquid chromatography is that the pressure can also be set (nevertheless, it can be gradually controlled) during separation which also influences the retention and by this leading to a better separation of the different compounds [32].

Different types of polymerization reactions carried out in $scCO_2$ media became also of interest [33]. Whatever the type of the polymerization is (chain- or step-grow), due to its tunable properties applying $scCO_2$ has substantial effects on the reaction setup. It can enhance the separation of the polymer from the monomer and from the catalyst and hence a molecular weight fractionation of the polymer can be realized during polymerization. The only

drawback is that in case of anionic polymerization the reactive anions would attack the Lewis acid CO_2 (unless there are extremely weak nucleophils involved). Thus in such cases, the usage of $scCO_2$ is problematic. For other applications (such as melt condensation polymerizations, in particular) the advantage of the plasticizing effect of the CO_2 is used. Based on the capability of plasticizing the polymer melt phase, it increases the free volume of the melt and lowers its viscosity, which translates into a more easily processed material. This advantage is used also in the $scCO_2$ aided polycarbonate (PC) synthesis, where CO_2 solubilize phenol to extract the by product and thus driving the reaction to higher conversation [34]. Another example for *in situ* polymerization is creating polystyrene blends with several polymers, aided by $scCO_2$ [35].

Polymer foams have several applications, depending mostly upon their structure. Foams may be flexible or rigid, depending upon whether their T_g are below or above room temperature, which depends upon their chemical composition, degree of crystallinity and crosslinking. The cell geometry, i.e. open or closed cell, size and shape, greatly affect the foam properties. Closed cell foams are most suitable for thermal insulation, while open cell foams are best for acoustical insulation. There are several ways to produce polymer foams, such as

1) thermal decomposition of chemical blowing agents which then generate nitrogen or carbon dioxide during polymerization,
2) mechanical whipping of gases into a polymer system (melt or solution),
3) expansion of gas filled beads by application of heat and many more.

However, all these techniques require either high temperatures or organic solvents. Polycarbonate foams are good alternative to metal for some components in the automotive industry, since this resin combines a good mixture of rigidity, impact strength and toughness with good flammability values [36]. Formation of microcellular polymer foams is also of great interest. These materials have a cell size equal or less than 10 μm and can be used mainly as separation media, adsorbents or controlled release devices.

Besides using $scCO_2$ as an aid in polymerization reactions in order to create such foams, a number of research groups have investigated the use of $scCO_2$ as a foaming agent for non-reactive processing of polymers after their production. This method takes advantage of the large depression in T_g found for many polymers in the presence of a compressed gas (such as CO_2), which means that the polymer may be kept in the liquid or rubbery state at relatively low temperatures. By lowering the pressure at a fixed temperature the amount of gas absorbed by the polymer is decreased. Thus, T_g begins to rise again, eventually to the point where T_g for

the polymer is higher than the foaming temperature: at this point the cellular structure can grow no further and is locked in. The sudden reduction in pressure on a fixed temperature leads to the generation of nuclei due to supersaturation, and these nuclei grow to form the cellular structure until vitrification occurs inside the polymer [37].

Particle formation by the use of supercritical fluids is also a broad area of research. There are several ways for the preparation using SCFs which can be divided into two sub-categories: those which involve precipitation from a homogeneous supercritical solution by rapid expansion and those which use the SCF as an antisolvent.

The process of particle formation by rapid expansion of supercritical solutions (RESS) begins with a homogeneous solution of a compound dissolved in a SCF which is then expanded rapidly through a suitable noozle. The gas loses its solvent power and the dissolved material precipitates. By this, micrometer range particles can be formed. This technique requires that the compound has reasonable solubility in the SCF, thus this process is limited to such materials and hence the knowledge of the phase behavior of the given binary mixture is inevitable [37]. To date, more than 100 substances were micronized by RESS process. However, due to the relatively high amount of SCF related to the amount of product and the difficulties of particle separation in μm range or smaller from huge gaseous CO_2 volumes the industrial application of RESS is rather uneconomical [38].

Contrary to RESS, antisolvent processes are using a supercritical solvent as an antisolvent for particle production. In the supercritical antisolvent (SAS) process, a given compound is dissolved in an organic solvent to create a solution which is contacted subsequently with a supercritical fluid. Depending on pressure, temperature and mass transfer, the SCF can remove the organic solvent. Therefore, the concentration of the solute increases, it becomes supersaturated and finally crystallizes by forming nano- or micro sized particles. The phase behavior of the substances is really complicated during the process, since the knowledge of ternary diagrams is required. The example of producing powder lecithin from raw lecithin should be noted as an important industrial application of the SAS technique, with a productivity of approx. 200 kg/day [38].

Figure 4: Industrial scale antisolvent process for powderous dried lecithin production, Uhde GmbH, Hagen, Germany [38]

Supercritical fluid extraction of emulsions (SFEE) can be considered as an improved SAS technology, which is especially suitable to encapsulate poorly water soluble drugs in an aqueous suspension. The process consists of forming an oil-in-water emulsion, containing the water-insoluble drug in the dispersed organic phase. The organic solvent is than extracted from this emulsion by the supercritical solvent, which quickly extracts the organic solvent from the emulsion and leads to the rapid supersaturation and a fast precipitation of the compound of interest. Contrary to the SAS antisolvent precipitation method where particle nucleation and growth occur across the whole solution volume, in the case of SFEE the formation of particles is confined within the emulsion droplets [39].

While the applicability of SAS and RESS processes is highly dependent on the solubility of a given compound in a SCF, a third technique called particle from gas saturated solutions (PGSS) is slightly different. Generally, this process is working with substances containing the solute of interest mixed with $scCO_2$. This mixing occurs at high pressure with the help of a static mixer. After the mixing zone, this gas-saturated solution is rapidly expanded to atmospheric pressure through a nozzle. During the expansion, the gas dissolved in the solution is suddenly vaporized, enhancing the atomization of the solution, therefore in some cases this technique is referred as PGSS-drying. Moreover, the intense cooling due to Joule–Thomson effect during CO_2 expansion promotes particle formation. By this process, particles in the micrometer range can be created and hence their size distribution can be controlled [40]. The technique can also be used for polymer particle production. In such case, the polymer has to be introduced in a molten state into the mixer [38].

Although supercritical water is highly corrosive and has relatively high critical pressure and temperature, it has some very practical properties. At supercritical conditions water is a nonpolar solvent completely miscible with organics. It also presents complete miscibility with oxygen, creating a homogeneous reaction medium, which makes it an excellent medium for the oxidation of organics. This process is known as supercritical water oxidation (SCWO) and consists of the homogeneous oxidation of chemical compounds in aqueous medium using oxygen (or air) as the oxidizing agent, at temperatures and pressures above the critical point of water. The main application of the SCWO is the wastewater and sludge treatment. With the appropriate reaction temperatures, pressures and residence time almost any pollutant can be completely transformed into harmless products by SCWO, with residence times lower than 1 min. Up to the present, a wide range of organic and inorganic substances have been converted into CO_2, water and N_2 using SCWO [8].

1.4 Polymer impregnation in scCO_2 atmosphere

As it was shown, the application of the supercritical fluids is numerous. This work deals with polymer impregnation in scCO_2 as sorption media, therefore the knowledge of polymer behavior under high pressure and of the possible interactions with CO_2 is essential. This chapter gives an overview of phenomena when contacting supercritical fluids with polymers with a main focus on glassy polymers and polycarbonate.

It is known, that exposure of glassy polymers to vapors or liquids which are highly adsorbed cause significant change in polymers' behavior since such penetrants can perturb the local chain configurations [41]. Even if some gases are sparingly soluble in polymers at atmospheric conditions, an increase of pressure can remarkably enhance this solubility. Koros *et al.* [42] measured the solubility, permeability and diffusion time lag for different gases (CH_4, Ar, N_2, CO_2 and He) in polycarbonate at 35°C for pressures ranging from 1 to 20 atm. Some gases, such as CO_2, showed a remarkable sorption in polycarbonate (10 cm^3 gas (STP)/cm^3 polymer) already at 4 atm. Other gases, such as He showed almost no sorption even on pressure levels as high as 20 atm. In a separate work, CO_2 sorption in PC was determined to be around 40 cm^3 gas (STP)/cm^3 polymer at 30 atm [43]. Authors found that the sorption (C) could be described by the following equation which can be derived from Langmuir and Henry's law:

$$C = k_{DP}\frac{C'_H bp}{1+bp} \quad (1)$$

Where k_D is the Henry's law solubility coefficient, C'_H is the Langmuir capacity constant and b is an affinity constant. Henry's law describes the gas sorption equilibrium in polymers above their T_g, while Langmuir term applies for amorphous polymers below T_g (where chain mobility is highly restricted) [42]. Due to the changes in chain configurations of polymers, the structure of some polymers can change remarkably. In several cases, the interchain distance grows and the segmental and chain mobility also increases, which results in a higher free volume of the polymer [26] and therefore the polymer starts to swell. By placing a polymer in compressed or supercritical CO_2, gas sorption takes place which induces swelling. During the swelling of glassy and rubbery polymers their viscosity can be reduced by up to an order of magnitude, which facilitates the mass transport inside the matrix. Therefore, the impregnation of solutes into polymers is accelerated in $scCO_2$-swollen polymers [44].

The amount of *gas sorbed* in polymers can be measured either by quartz crystal microbalance (QCM) [45] or by magnetic suspension balance (MSB) [46]. These gravimetric methods can provide really accurate sorption data. MSB was first described by Schnitzler and Eggers [47] and developed by Rubotherm Präzisionsmesstechnik GmbH in Germany. It is basically a combination of a very sensitive balance and a high pressure view cell. Its biggest advantage is the *in situ* data collection, that is, the sample is in the supercritical phase (under high pressure) meanwhile sorption data being measured. From the data collected, the Non-Random Hydrogen-Bonding (NRHB) model of fluid mixtures can be used to give a reasonably good estimation for the swelling behavior of the polymer. An elaborated mathematical description of this model is described in details elsewhere [45].

Measuring the *swelling behavior* and data collection is a rather complicated task and methods invented for such measurements are often highly inaccurate and tedious. However, from the swelling data of a given polymer, sorption data can also be calculated by using the Peng–Robinson equation of state and the Flory equation for binary fluid–polymer system by assuming isotropic swelling (that is, equal volume change of the polymer in all the three dimensions) [48]. Generally, rubbery polymers reach the maximal gas saturation much faster than glassy polymers and the amount of swelling is usually higher. However, interestingly, poly(methyl methacrylate) (PMMA), a glassy polymer, has a larger sorption of CO_2 than some rubbery polymers. This can be explained by the favorable π-interactions between the

CO_2 molecules and PMMA, which means that besides physical phenomenon, a possibility of chemical interaction of the polymer with the CO_2 have to be taken into account [48].

Wissinger and Paulaitis [49] measured the gas sorption and consequently the swelling under CO_2 of PMMA, polystyrene and polycarbonate at elevated pressures as high as 100 bar and temperatures from 33 to 65°C. Swelling determination here had an uncertainty of ±0.3% (V/V), while sorption could be determined with ±1 cm^3(STP)CO_2/g polymer accuracy. The authors pointed out, that in case of applying different polymers, CO_2 sorption amount is not necessarily proportional to the swelling behavior. The amount of gas sorbed may be the same for distinct polymers but the swelling behavior is different arising from the various chemical structures. The authors observed two distinct types of swelling and sorption isotherms, depending on the *depressed* T_g of the polymer. In the absence of a glass transition under CO_2, sorption isotherms begin to level off and reach limiting values at higher pressures. The equilibrium solubility of a gas in a polymer will show a maximum with increasing pressure due to free volume effects. A different characteristic can be observed if the depressed T_g of the polymer is exceeded during sorption. In this case sorption amount further increases with pressure from the point where glass transition of the polymer occurred. This can be clearly demonstrated by the example of PMMA's behavior shown in figure 5. Below 42°C glass transition of PMMA does not occur, the curve levels off (data for 32.7°C). However, at higher temperatures sorption (and consequently swelling) continues to increase with increasing pressure. This indicates that PMMA undergoes a glass transition in this range. Figure 5 shows a CO_2 sorption and swelling curve of PMMA [49], which are really similar.

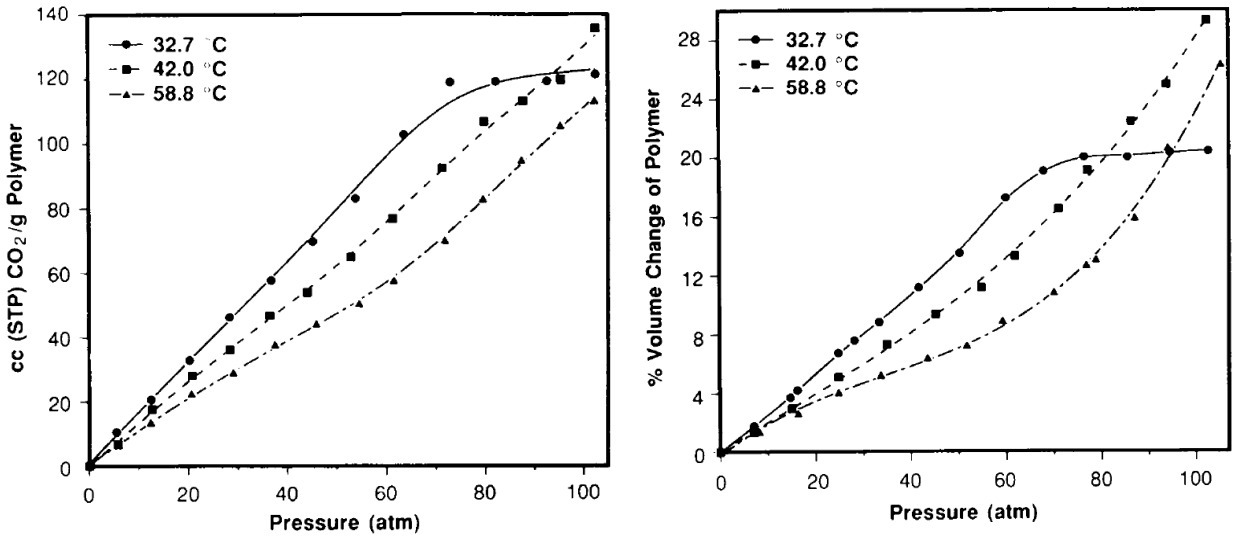

Figure 5: CO_2 sorption (left) and swelling (right) curves of PMMA, measured by [49]

Investigating the degree of swelling, which is the volume change of a polymer under high pressure as a function of carbon dioxide pressure, rubbery and crystalline polymers show different behavior. Rubbery polymers show sigmoidal behavior, while polymers having greater degree of crystalline first show linear change in volume which levels off after a certain pressure [48]. Figure 6 shows swelling of polycarbonate in CO_2 at 35°C. From the figure it can be seen, that PC does not undergo a glass transition at measurement conditions.

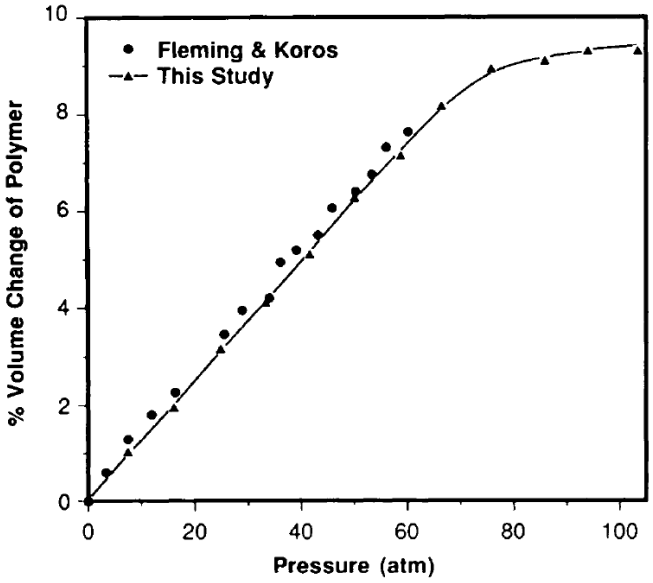

Figure 6: Swelling behavior of polycarbonate at 35°C by [49]

The authors determined the T_g of PMMA at atmospheric conditions via differential scanning calorimetry (DSC) and it was found to be around 105°C. This is remarkably higher, than temperatures used during CO_2-sorption experiments, however, glass transition was observed upon sorption. Taking this into account, a new phenomenon has to be discussed.

Besides swelling, gas sorption causes one another important change in polymer properties, which is called sorption induced glass transition (SIGT). Caused by sorption, plasticization of the glassy polymer occurs which results in a remarkable *decrease* of the T_g. To evaluate this change, an accurate model is given for predicting the glass transition temperature as a function of the amount of gas adsorbed by the polymer. This thermodynamic based-on mathematical model has two specific parameters to describe the systems that are not at equilibrium. In this glassy state, the fraction of holes in the polymer (1) and the number of nearest-neighbor contacts between polymers segments per polymer molecule (2) describe the thermodynamic properties. The accurate mathematical interpretation can be found elsewhere

[50]. The already mentioned NRHB model has also been found adequate to determine the depressed T_g of both glassy and rubbery polymers [45].

The glass transition temperature for polymers in equilibrium with $scCO_2$ can be fitted to the Cha-Yoon equation [51]:

$$T_{g(d)} = T_g exp\left\{-M_w^{-\frac{1}{3}}(\rho_p)^{-\frac{1}{4}}\alpha\omega\right\} \quad (2)$$

Where T_g is the glass transition temperature of the pure polymer, $T_{g(d)}$ is the glass transition temperature of polymer in equilibrium with carbon dioxide, M_w is the polymer molecular weight, ρ_p is the polymer density, ω is the absorbed carbon dioxide in percentage of weight, and α is a parameter for the model. According to Beckman and Porter [52], $T_{g(d)}$ should pass through a minimum value versus sorption pressure and starts increasing then by approx. 5°C/100 bar in case of PC.

Diffusion of different gases in polymers has already been in focus of several studies. Diffusion within polymers is a really complicated issue and is controlled by temperature, pressure, polymer composition, morphological features (such as crystallinity and cross-linking), possible chemical interactions between the penetrant and the matrix and many more. Measuring the diffusion coefficient is in several cases easier than giving predictions by mathematical models because mass transport within polymers does not necessarily follow the laws of classical molecular diffusion [53]. Berens [54] suggested a sigmoidal form isotherm for sorption of swelling penetrants in PVC matrix. This theory was confirmed later on by Pantoula [45]. Webb [55] determined the CO_2 solubility and its diffusion coefficient in several polymers at 40°C and at 100 bar. In this work, Fickian diffusion was found to be adequate to describe the polymer behavior. Tang *et al.* [56] investigated the sorption and diffusion of $scCO_2$ in polycarbonate at temperature ranged from 40 to 60°C and pressures from 100 to 400 bar. Authors concluded that, because of the linear relationship observed between mass gain of the polymer during sorption and square root of time, the $scCO_2$ conducted Fickian sorption (and desorption) in the investigated range within the polymer. In their work sorption diffusivity (D) was calculated as:

$$\frac{M_s}{M_\infty} = 1 - \frac{8}{\pi^2}\exp\left(\frac{-D_s\pi^2 t_s}{l^2}\right) \quad (3)$$

Where M_s is the sorption amount at time t_s, M_∞ is the saturated (equilibrium) sorption amount at a larger sorption time and l is the thickness of the planar polymer sample. Sun *et al.* [57] measured the diffusion coefficients of $scCO_2$ in polycarbonate from 75 to 175°C and up to 200 bar by MSB. The authors also took the assumption, that the diffusion obeys Fick's second law and D was calculated also by the equation (3). The diffusion coefficient increased with pressure at constant temperature unless crystallization of the PC in $scCO_2$ occurred. Sorption and diffusion data are commonly measured by MSB and the assumption that $scCO_2$ has a Fickian diffusion in polymer matrices is generally taken in other studies [58,59,60,61]. However, it should be noted, that in case of polymers with high crystallinity (such as high-density polyethylene (HDPE) and polypropylene (PP)) the measurements were conducted in the molten phase of the polymers. Although there is no data given for crystalline polymers at lower temperatures, one would certainly assume that the diffusion has anomalous behavior in the crystalline regions. Sun *et al.* [57] observed for example a change in diffusion kinetics from the point where PC became crystalline due to CO_2 sorption. Table 3 shows diffusion coefficients of CO_2 within several polymers at various conditions.

Table 3: diffusion coefficients of CO_2 in polymers

Polymer	Diff. coeff. (cm^2/s)	Conditions		Literature reference
		P (bar)	T (°C)	
PC	(1.22)E-7	200	40	[56]
PC	(8.74)E-7	200	75	[57]
PC	(2.88)E-6	200	150	[57]
PMMA	(1.04)E-6	100	40	[55]
HDPE	(9.10)E-5	110	180	[59]
PS	(1.67)E-6	83	100	[61]

Unfortunately, literature data for the same experimental conditions but for different polymers are scarce. Therefore it is hard to give a clear overview on the different effects that can determine diffusivity in distinct polymers. However, it can be observed, that on a fixed pressure, temperature causes increment in the diffusivity due to the higher chain mobility. Comparing the data measured at 40°C in case of PMMA and PC, it can be seen, that even on lower pressures, PMMA has an order of magnitude higher diffusivity due to the favorable π-

bonding of the $scCO_2$ to the polymer chains. Table 3 also shows that generally the diffusivity of CO_2 in polymer matrices is rather low.

As it was mentioned, anomalous diffusion in polymers can occur due to the structural changes caused by sorption. The crystallization of polycarbonate induced by CO_2 sorption and consequently plasticization at high pressures was already investigated in literature. First, Chiou *et al.* [62] showed that CO_2 plasticizes polycarbonate, but not to that extent which causes crystallization. This phenomenon was then investigated by Beckmann and Porter [52] in the range of 100–600 bar and at 50–87.5°C. Authors did not observe crystallinity in the investigated pressure range after 4 hours of sorption time for temperatures as low as 50 and 62.5°C. However, at 75°C 25 % crystallinity was determined by DSC already at 100 bar after 1 hour of soaking time. PC was observed to degas quickly (within two hours at atmospheric conditions) and therefore polymer regained its original T_g after sorption. Tang *et al.* [56] observed that at 400 bar and 60°C after 4 hours sorption on polycarbonate sheets (having an average molecular weight (M_w) of 64 000 g/mol) turned opaque. This effect was highly time dependent: after 40 minutes of soaking PC specimen in $scCO_2$ almost no changes were observed while after one hour samples lost their transparency. However, a sample measured at lower temperature of 40°C at 400 bar for 4 hours remained fully transparent. Therefore, authors concluded, that the depressed T_g of PC can be below 60°C at 400 bar. Mascia *et al.* [63] produced polycarbonate foams by using $scCO_2$ as foaming agent. M_w of the applied polymer was 25 000 g/mol. During experimentation authors observed the onset of the polymer crystallization induced by $scCO_2$ during soaking which varied between 8 and 24 hours. According to DSC and X-ray diffraction (XRD) examinations, crystallization started around 80°C at 300 bar and was favored at higher sorption times. As for the highest crystallinity, 24.3 % was measured at 300 bar, 180°C and after 24 hours of soaking time. Gross and coworkers [64] investigated the pressure, temperature, time and polycarbonate's M_w effect on crystallinity. The authors observed that the lower the molecular weight is, the earlier crystallization starts and occurs within less time. For instance, for molecular weights as low as 2 500 g/mol, 5 % crystallinity was observed after 2 hours of sorption time at 204 bar readily at 40°C. Applying the same CO_2 pressure for PC having a M_w of 44 000 g/mol, 120°C was required to reach the same crystallinity of 5 % after 2 hours of sorption. The highest crystallinity determined was around 27 % for M_w of 2 500 g/mol at 204 bar and 70°C for 4–12 hours. Crystalline samples lost their transparency and turned to white-opaque. Sun *et al.* [57] used PC sheets having a M_w of 41 900 g/mol for their work. Authors investigated the kinetics of the crystallization of PC in $scCO_2$. Studying the effect of pressure and temperature, it was

concluded, that crystallization only occurs if the *difference* between the applied sorption temperature and the depressed T_g of the PC exceeds 40°C. At higher temperatures crystallinity was generally higher and was determined to be slightly above 30 % as highest at 175°C between 100 and 200 bar. It was observed, that crystallization occurs slowly: at 100°C and 125 bar final crystallinity of ~25 % was reached after 100 hours of sorption time. The crystallization rate of PC can be determined by the Avrami equation [57]:

$$ln\left\{1 - \frac{X_c(t)}{X_C(\infty)}\right\} = -k(t - t_0)^n \quad (4)$$

Where X_c is the crystallinity, k is the crystallization kinetic constant, n is the Avrami exponent, and t_0 is the induction time of crystallization. The parameters k, n, and t_0 can be determined by a non-linear least square method and are available in literature [57]. Table 4 contains experimental data on PC swelling and its depressed T_g measured by different research groups.

Table 4: PC swelling and T_g in $scCO_2$ atmosphere

p (bar)	M_w	sorption time	lit. reference	depressed T_g (°C)	swelling (V/V) %
400	64000	after 4 hours	Tang [56]	below 60	(nd)
300	(nd)	(nd)	Schnitzler [47]	around 70	up to 16 %
100	(nd)	(nd)	Schnitzler [47]	around 70	up to 11 %
90	(nd)	(nd)	Zhang [65]	65	(nd)

*(nd, no data): original work does not provide this particular data

According to Zhang and Handa [65], T_g depression of PC is a linear function of the time measured up to 90 bar. In absence of a crystal structure change upon sorption, original T_g of the polymer is regained [52] after the polymer sample degas (typically, after several hours).

1.5 Polymer dyeing in supercritical media

As it was already presented, $scCO_2$ is an applicable medium for polymer modification by impregnation. By taking a dyestuff as an impregnation solute and applying the SFD method, conventional techniques for polymer dyeing (which have several drawbacks mentioned earlier) can be replaced. SFD has already industrial applications for textile dyeing, first applied in 1991 [28]. The device had a volume of 67 liter and it could operate with 2 kg yarn

load. More recently, Dyecoo, a Dutch company, realized textile dyeing in industrial scale and their CO_2-dyeing technology is applied in clothes coloring for costumers such as Nike, one of the world's leading suppliers of athletic clothes and sports equipment. However, the investment costs for a CO_2-dyeing plant is rather high, but on the other side the operation costs are much lower which results in lower overall costs by approx. 50% [66]. Therefore, apart from the clearly positive environmental impact that CO_2-dyeing does not produce waste water, from the economical point of view, it is much cheaper than conventional processes when designing its operation for longer time.

1.5.1 Dyes and their behavior

In order to carry out a successful dyeing, a scCO_2 soluble dyestuff is necessary for the process. Therefore, this has been a highly researched field of the chemical industry and by now one can find elaborated data for dyestuffs suitable for CO_2-dyeing and their solubility [67]. Chrastil [68] investigated the dissolution of many different solid materials in high pressure gases and he proposes an empirical equation to predict their solubility as a function of the gas density, applied temperature and empirical constants:

$$c = \rho^k \exp\left(\frac{a}{T} + b\right) \tag{5}$$

Where c is the concentration of a solute in a gas, ρ is the density of the gas, k is an association number, T is the temperature and a and b are constants and are calculated as:

$$a = \Delta H / R \tag{6}$$

$$b = \ln(M_A + kM_B) \tag{7}$$

Where ΔH is the total reaction heat, R is the ideal gas constant, M_A and M_B are the molecular weights of the solute and of the gas, correspondingly. This equation has been used by many authors, whose experimental data correlated well with this Chrastil model [66,69,70]. However it is not possible to give an accurate prediction for solubility in scCO_2 of a given dye without any measured data. It is known, that dye properties such as melting point, molecular weight, heat and entropy of fusion do not correlate with their dissolution properties. Generally, dye structures have the most important effect on their solubility, whereas it is clearly increased e.g. in case of dyes containing halogen groups [71]. Shinoda [72] provided

an equation for calculating the solubility of DR1 and DR13 in $scCO_2$, whereas the model has several empirical parameter and many constants were obtained from experimental results. From their work it can be seen, that dye solubility is a really strong function of $scCO_2$ density (see figure 7).

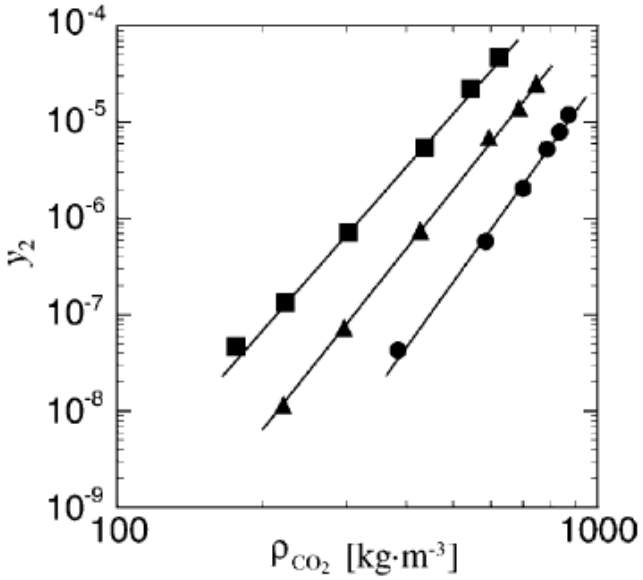

Figure 7: Solubility of DR13 dyestuff in $scCO_2$ versus its density measured at 50 (circle marker), 80 (triangle) and at 110°C (square marker) [72]

In an ideal case, the mass transfer of the dye in a swollen polymer phase follows a Fickian model for diffusion (just as CO_2 molecules diffuses within the matrix) and can be described by eq. (3). However, it has to be noted, that the specific interactions of the dye with the polymer matrix (such as dipole-dipole or the possibility of forming hydrogen bonding) can strongly affect this ideal behavior and eq. (3) should only be used in a very ideal case.

1.5.2 The dyeing process

Dyeing in supercritical media is a particular case of solute impregnation. In principle, a suitable dye is dissolved in a supercritical fluid (in our case, in $scCO_2$) and by simultaneously contacting this solution with a polymer matrix in a high pressure vessel the dye penetrates into the polymer phase. The dye uptake proceeds in four steps:

(1) dissolution of the dye in CO_2,
(2) dye transport to the material,
(3) adsorption on the surface,
(4) finally diffusion of the dye into the matrix.

This batch process is mainly controlled by diffusion, and in an ideal case, the Fick law of diffusion can be applied. The fluid phase has always to be saturated and cannot be exhausted by the uptake of the polymer during the impregnation. This is achieved by creating a saturated phase in the impregnation vessel with high excess of dye – remarkably higher than the maximum theoretical solubility of the dye in $scCO_2$ at given conditions. Although, generally the solubility of the dyes in $scCO_2$ is rather low (~ 10^{-7} – 10^{-6} mol/mol [72]), a preferable partition of the dye towards the polymer phase over the fluid phase can drive the dye into the polymer matrix. This partitioning coefficient K_c is defined as the ratio of the saturated concentration of the dye in the polymer phase to the saturated concentration of the dye in the fluid phase.

$$K_c = \frac{c_{dye,polym}}{c_{dye,fluid}} \tag{8}$$

The concentration in each phase at equilibrium is dependent upon the solubility of the dye in each phase [73]. If K_c is high enough (thus the partition is favored towards the polymer phase), the dye concentration in the applied polymer can be remarkably higher than in the dye bath (fluid phase) [28].

Although several polymers had already been colored by SFD [26], there are no detailed experimental data in the open literature on successful PC dyeing by SFD technique was found. However, the work of West *et al.* [74] should be noted who reported the dye impregnation of PMMA films with two disperse dyes. Authors achieved remarkable dye uptake (approx. 0.5 wt%) of the PMMA film at 40°C and 91 bar. However, they could only achieve very poor coloring on PC sample at these conditions. They mention, that by the use of disperse red 1 dyestuff PC samples were colored slightly pink contrary to PMMA's dark red color. Accordingly, in that article, dyeing of PC turned out to be complicated which was explained by the relatively nonpolar environment.

1.5.3 Dithizone impregnation

It is known from literature, that dithizone reacts with a high variety of metals and can be used for instance in spectrophotometrical detection [75]. For instance, Ag(I), Hg(II) and Pb(II) can be determined by using silica gel (SG) loaded with dithizone and zinc dithizonate. Authors achieved 40 μmol (~ 10 mg) dithizone load per g SG and with this loading they achieved 39.5 μmol Pb(II) adsorbed on the membrane [76]. Dithizone impregnated SG membranes were

reported to be good chelating agent also for Cu^{2+} ions. They were used in a sample preparation step before spectroscopic measurements of water samples [77]. In connection with supercritical fluids, dithizone can be used as a chelating agent in $scCO_2$ extraction of heavy metals from aqueous solutions [78]. Since in this work, during preliminary experimentation dithizone was found to be slightly soluble in $scCO_2$ with green color, it can be considered (and its impregnation kinetic can be investigated) as a dyestuff. No work in connection with dithizone impregnation by using SFI is reported. However, literature proved that dithizone has a capacity of chelating different heavy metals and hence it can be impregnated into some matrices. These properties can be used in order to create dithizone impregnated PC as a sensor or to impregnate PC by metal particles by the use of dithizone.

Therefore, the first goal of this thesis is to successfully apply the SFD on PC by using two commercially available dyestuffs (DR1 and DR13) and additional dithizone. Furthermore, the aim is to give a data evaluation and a detailed explanation of phenomena experienced during experimental work.

1.6 Polymer impregnation with nanoparticles using supercritical fluids

Polymer containing nanoparticles are receiving growing interest in the recent years [1]. Due to their unique properties, they can be used in microelectronics and for optical and catalytic applications. Their properties can be fine tuned by the size and the amount of the incorporated nanoparticles, since the surface of the nanoparticles plays an important role for their catalytic properties. There are several ways to synthesize polymer-supported nanoparticles; however all the conventional techniques (sol–gel processes, deposition–precipitation, co–precipitation, etc.) have several drawbacks. These are e.g. aggregation, dispersing uniformly the particles within the polymer matrix is also difficult, and as a major drawback, the size of the particles cannot be controlled. SFI is an alternative and promising way to deposit metal nanoparticles onto surfaces of porous solid supports or into polymers. In this approach, a metallic precursor is used as an impregnation material which is dissolved in a supercritical fluid and this solution is then contacted with a substrate. After incorporation, this metallic precursor can be converted (reduced) to its metal form [79]. Figure 8 shows a scheme of using the SFI method for metal impregnation. There are different ways to obtain the reduced form of the metal:

(1) chemical reduction *in situ* in the SCF with a reducing agent (e.g. hydrogen),

(2) thermal reduction in the SCF at higher temperatures,

(3) thermal decomposition in an inert atmosphere or chemical conversion with hydrogen or air *after* the depressurization step.

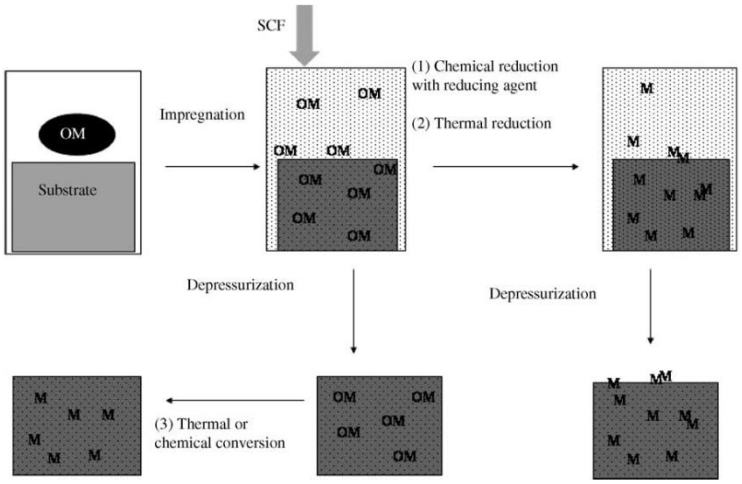

Figure 8: Impregnation or deposition of metals from SCFs [79]

The first study of using SCF as a media for metal deposition was reported by Watkins and McCarthy [80]. The authors impregnated Pt nanoparticles from dimethyl(1,5-cyclooctadiene)platinum(II) (Pt(cod)me_2) precursor into poly(4-methylpent-1-ene) (PMP) and poly(tetraflouroethylene) (PTFE) matrices. This study was performed in 1995 and since then many examples have been reported in literature on successful metal impregnation into polymers or onto solid porous supports using SCFs (mostly $scCO_2$). Such metals are e.g. Pt, Ru, Pd, Rh, Cu, Ni, Au and Ag using their various, commercially available $scCO_2$ soluble metallic precursors for the sorption (such as -(cod)me_2, -acetylacetate (acac) or -hexafluoroacetylacetate (hfac)) [79,81]. However, such $scCO_2$ soluble complexes can also be synthesized in laboratory scale. Said-Galiyev and coworkers [82] synthesized new iron and copper complexes for polyarylate (PAR) film impregnation. The authors achieved copper and iron contents in PAR films as high as 6.3 and 4.5 wt%, respectively.

1.6.1 Nanoparticle impregnation of polycarbonate

Generally, literature data on PC impregnation with metal nanoparticles are scarce. Hasell *et al.* [83] embedded silver nanoparticles by using (1,5-cyclooctadiene)(1,1,1,5,5,5-hexafluoro-acetylacetonate)silver(I), (Ag(hfac)cod) as a precursor via SFI. The authors impregnated PC strips at 103 and 90 bar and at 40°C between 1 and 24 hours sorption times, which were then characterized by transmission electron microscopy (TEM). TEM pictures revealed a uniform

distribution of silver particles having a 2–10 nm diameter approximately with a penetration deepness of ~6.5 μm within the matrix after 24 hours of sorption. The authors pointed out, that at the lower pressure of 90 bar a deeper impregnation depth was achieved. This was explained by the lower solubility of the complex (due to the lower $scCO_2$ density) at this pressure. Because the solubility in the $scCO_2$ phase decreased, the partition coefficient was slightly shifted towards to the polymer phase causing a deeper penetration of the nanoparticles into the polymer matrix.

The only study, in which polycarbonate films were impregnated by copper nanoparticles, was carried out by an ion implantation method, not using any supercritical fluids [84]. By this, authors achieved nanoparticles sized between 3–15 nm; however particle distribution (homogeneity) and impregnation depth was not investigated in that work.

Although PC is an important technical plastic and metal nanoparticles impregnated polymers have high importance, data in the literature on metal impregnation of PC in $scCO_2$ are very scarce. Therefore, the second part of this thesis focuses on PC modification by SFI using mainly copper as a model compound.

II. Materials and Methods

1. Prime materials and reagents

Disperse red 1 (N-Ethyl-N-(2-hydroxy ethyl)4-(4-nitrophenylazo)aniline) and disperse red 13 (2-[4-(2-Chloro-4-nitrophenylazo)-N-ethylphenylamino] ethanol), DR1 and DR13, respectively, were supplied from Sigma Aldrich. They are common chromophores for nonlinear optic (NLO) materials and only differ in one chlorine group (see figure 9). Since it is known that the presence of halogen groups increases the solubility in $scCO_2$ atmosphere [71], they are appropriate for a comparison in their dyeing efficiency. Polycarbonate (Lexan® resin 121) was kindly provided by Saudi Basic Industries Corporation (SABIC) in pelletized form with a diameter of approx. 1.5 mm and a length of 3 mm, see figure 10.

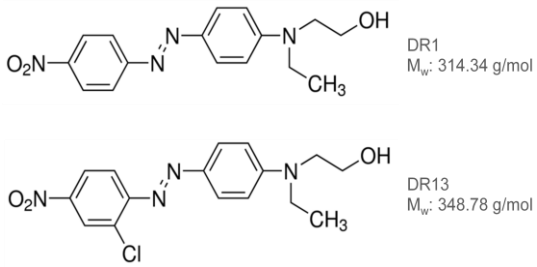

Figure 9: Chemical structure of dyes' DR1 and DR13

Carbon dioxide was ordered from Linde Gas GmbH. and had a purity of 99.5 %. Organic solvents (e. g. cleaning ethanol and dichloromethane) were supplied from Sigma Aldrich and had a purity of >99.5 %. Copperhexafluoroacetylacetonte-hydrate ($Cu(hfac)_2$) and dithizone (H_2Dz, melting point 168°C) (chemical structures are shown in figure 11) were ordered also from Sigma Aldrich, just as all other chemicals (e.g. copper salts) used in our experiments.

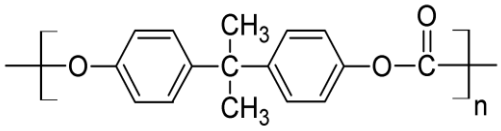

Figure 10: Chemical structure of Lexan® resin 121

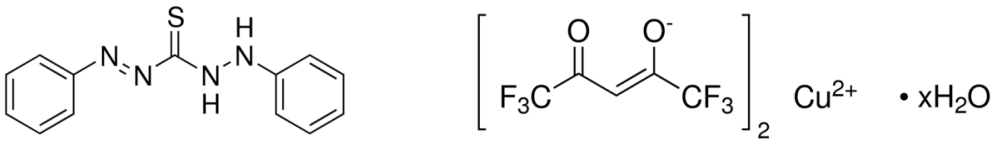

Figure 11: Chemical structure of dithizone (left) and $Cu(hfac)_2$ (right)

2. Experimental apparatus

The experimental hall at the Institute of Chemical Engineering and Environmental Technology had been completely reconstructed and renovated from summer 2012 – 2014 February. This thorough construction included the re-arrangement of all the existing plants, creating new, individual laboratory boxes for the different research groups and renovating several parts of the laboratory equipment. After the construction works in the experimental hall was finished and was ready for use, the high pressure equipment had to be reinstalled. This meant the assembly of the impregnation plant and to fix it into its final place into the box. The supply of CO_2 and other necessary connections for operating the plant (e.g. pressurized air, cooling water and electricity) have also been installed. Taking special care to safety and health instructions, a safety box for the storage of CO_2 cylinders and a continuous ventilation system in the box was fixed. All the connections for the impregnation plant such as high pressure tubes and fittings, valves etc. were carefully cleaned and tested before use. Each high pressure vessel was checked for sealing before taking them into operation. A complete control and display system was installed to the devices in order to monitor pressures and temperatures. This involved the programming of each individual controller and pressure or temperature indicators and their connection to a computer program via a previously chosen interface (FieldPoint^{TM} AI 110, National Instruments, USA). Temperature was measured by Pt100 (Lumel N30U) choosing a 0–10 V input signal while pressure data collected (Philips Digital 280) via a 4–20 mA signal were transported to the interface. From the interface, data was sent to the computer by an RS-232 serial port where it was registered by a computer program (LabVIEW 7.0 *Express*).

2.1 Dyeing experiments

The impregnation equipment is shown in figure 12. Carbon dioxide is stored in cylinders equipped with a dip tube (1) and a manometer in a safety box (not pictured). It enters into the system via a liquid CO_2 pump (3, Haskel ASF-100, USA), which operates with pressurized air. CO_2 is cooled below 5°C by a recirculation cooling bath (5) in order to maintain it in liquid form. Pressurized CO_2 leaves the pump through a check valve (6a) and flows into the high pressure vessel (7) which is placed inside a thermostated heating chamber (9, *Spe-ed SFE*, Applied Separations, USA, T_{max} = 250°C). The useful volume of the vessel was 300 ml.

Temperature and pressure were monitored by indicators (8a and 8b) and data were transmitted into the computer (10) via an interface (not pictured). The use of a metering valve (11, Kämmer Typ KA, Flowserve ltd. Germany) connected to the regulators and controlled by the computer allows a controlled depressurization at the end of the process. High pressure tubes, fittings and valves were obtained from SITEC and Nova Swiss, Switzerland.

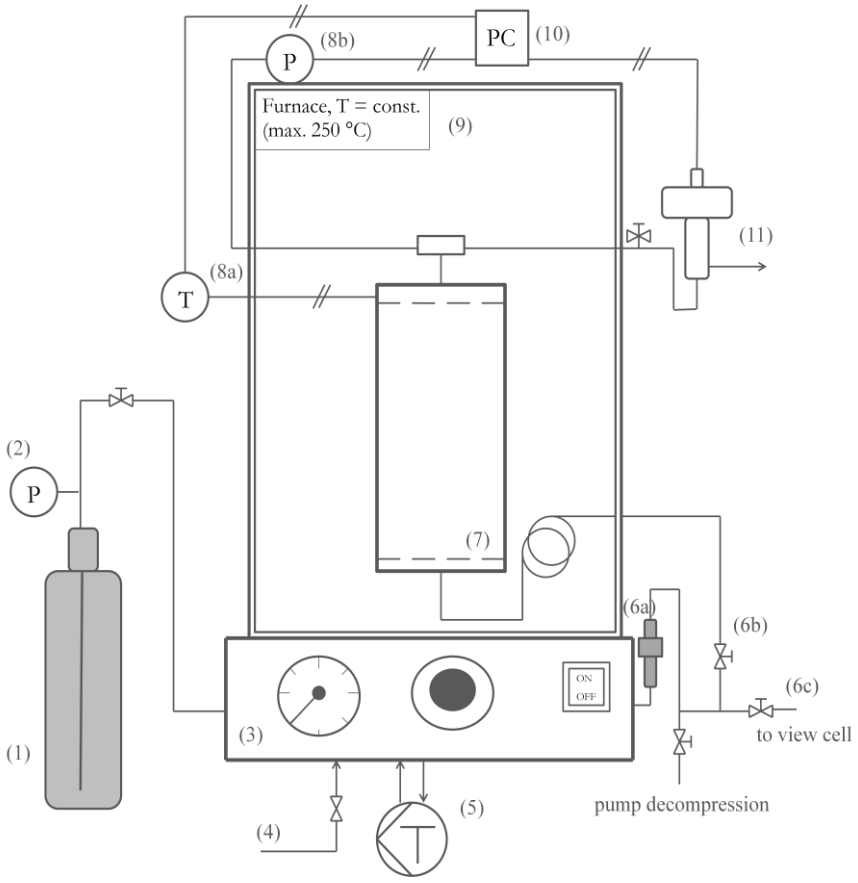

Figure 12: Experimental apparatus for SFD process

2.2 Observations under high pressure CO_2

In order to carry out observations in high pressure CO_2 atmosphere, a view cell was installed, connected with the impregnation device, so it can be pressurized by using the pump of the impregnation plant. By closing valve (6b) and opening (6c), CO_2 flows to the view cell (Natex Prozesstechnologie GmbH, Ternitz, Austria, see figure 13). This view cell can be operated up to 400 bar and ~85°C as the tempering media is water. CO_2 flows through the inlet valve (**A1**) and enters into the cell (**D**). Pressure and temperature are monitored by (**B1**) and (**B2**) indicators, respectively. A magnetic stirrer (**C**) is placed below the cell. The whole apparatus is located in a water bath (**E**) in order to maintain constant temperature controlled by a

thermostat (**F**). It can be simply decompressed by opening the outlet valve (**A2**). The cell has a useful volume of ~140 ml.

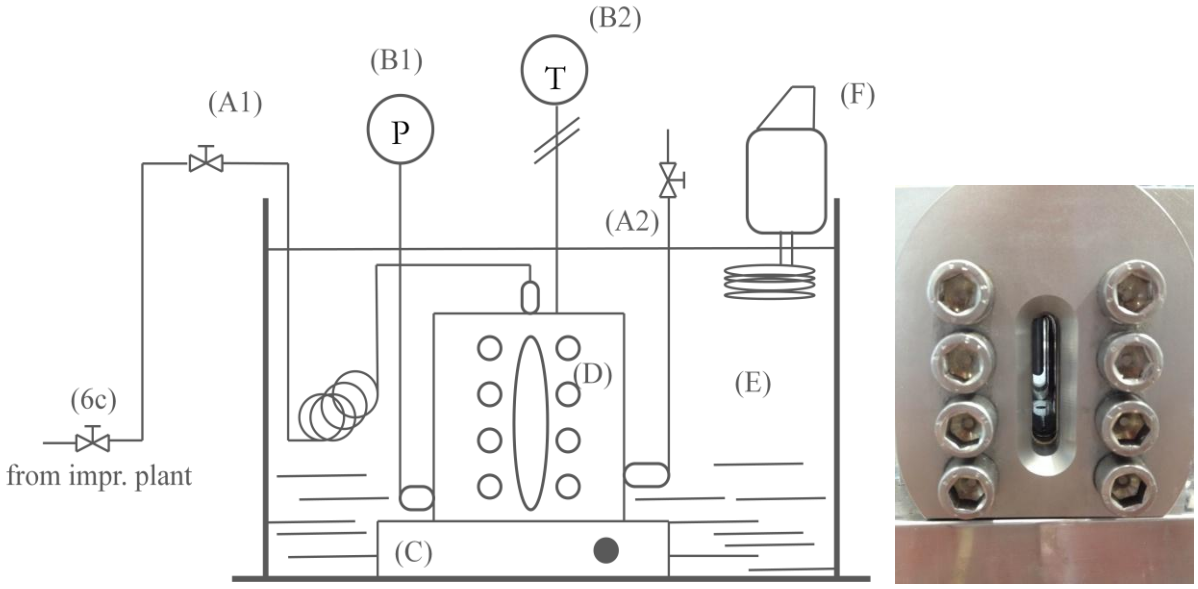

Figure 13: High pressure view cell, schematic draw (left) and picture (right)

2.3 Metal nanoparticle impregnation of polycarbonate

For the metal impregnation study, the same experimental device was used as in the dyeing experiments. However, in this case, a gear pump (12) with a control unit (13) was installed to the system (see figure 14; differences from figure 12 are marked with red). By continuously circulating the content of the reactor during sorption, the mass transport of the compounds in the $scCO_2$ phase is enhanced because the mass transfer in the fluid phase is no longer diffusion limited. This mixing makes it also possible to carry out impregnation in case of such a system, where in the vessel two non-miscible phases are present, which was the case for some of our experiments.

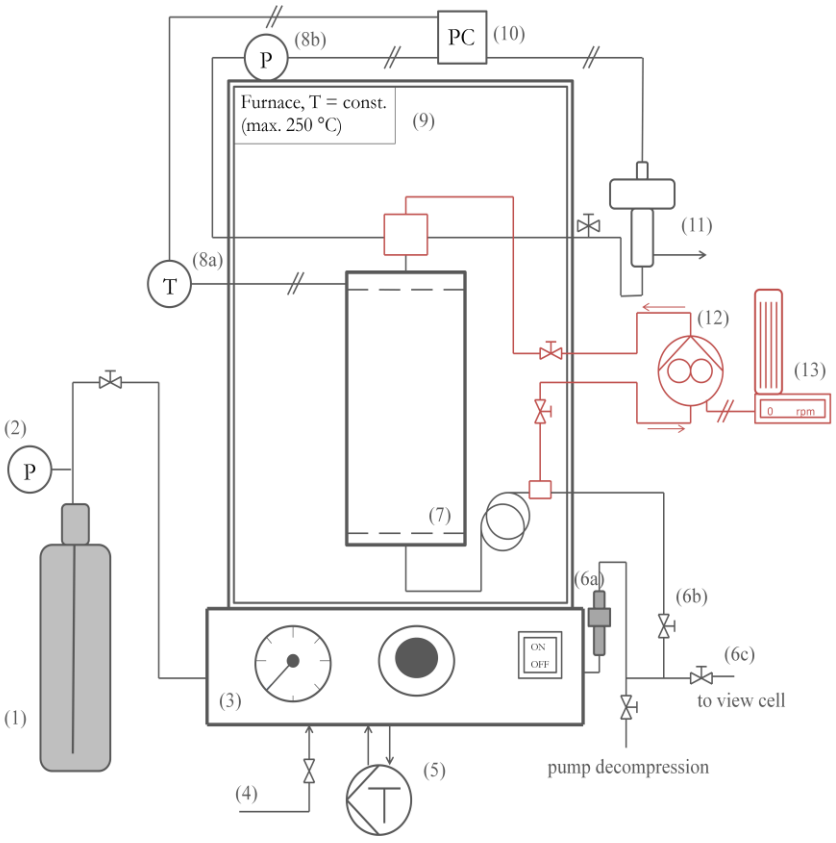

Figure 14: Impregnation plant with a gear pump connected

2.4 Solubility measurements

Measurements were carried out at the Budapest University of Technology and Economics (BUTE) in Budapest, Hungary, in cooperation within the DoHip project. A flow type apparatus, a simplified version of [72], was used to measure the solubility of DR13 in $scCO_2$ for these conditions, where literature data were not available. A JASCO Pu-2080-CO2 Plus liquid pump was used for the measurements.

3. Experimental methods

3.1 Observations under high pressure CO_2

For these observations, materials were placed in a glass vial having a volume of 15 ml and a magnetic stirrer inside. Then this vial was placed into the view cell. This helped to keep the material in the middle of the cell during the experiment and made the cleaning easier and more effective afterwards. Once the desired temperature was reached via tempered water, the cell was pressurized with CO_2. After the observations, the scCO_2 was slowly decompressed within 5-10 minutes by opening the outlet valve.

3.2 Dyeing and dithizone impregnation

The volume of the high pressure vessel can be changed between ~50 and 300 ml by inserting different additional spare parts (rings and cylinders) into the vessel body (see figure 16 and 17). For the dyeing experiments the arrangement (3) was chosen (see figure 17) and by this the volume of the vessel was ~140 ml. Samples of PC and the applied solute (DR1, DR13 or dithizone) were weighted on an analytical balance (Sartorius, ± 0.0001 g) and placed in the high pressure vessel separately from each other. To ensure that the solute is present in high excess 3 wt% of dye with respect to the polymer mass was applied (2.00 g PC and 0.0600 g dyestuff). For the dithizone impregnation experiments 0.0400–0.0600 g dithizone were used. The impregnation material was placed at the bottom, underneath the polymer, which was situated on an upper stainless steel sieve approx. 1 cm above the solute. No additional cosolvents (e.g. water, ethanol) were used for the DR1 and DR13 dyeing experiments, but in some experiments dithizone was impregnated by using ethanol as a cosolvent. After sealing and connecting the vessel to the CO_2 supply, it was heated up to impregnation temperature in the oven. When temperature was reached, the vessel was pressurized up to the desired pressure and the experiment started. During sorption, pressure and temperature were controlled by ± 3.0 bar and ± 1.0°C, respectively. After a given impregnation time, the vessel was depressurized applying linear decompression within 30–60 minutes by using the metering (Kämmer) valve. A typical pressure curve for an experiment is shown in figure 17. The impregnated PC samples were cleaned with ethanol to remove precipitations of the impregnation material from the PC surface. The high pressure vessel was disassembled and thoroughly cleaned with ethanol.

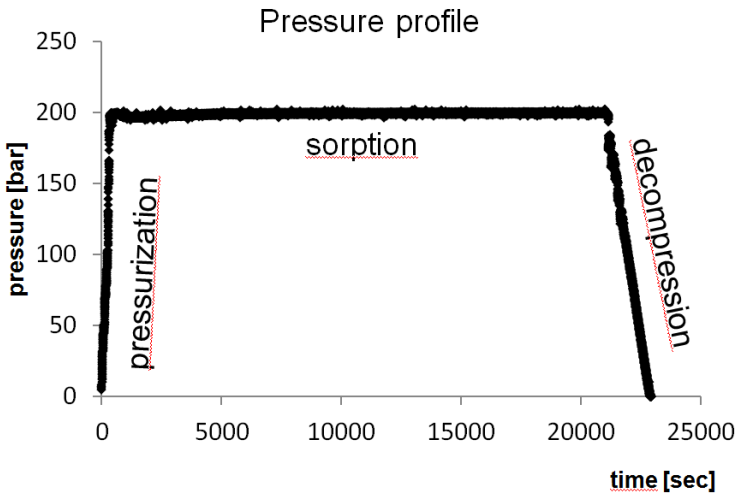

Figure 15: Pressure curve of a dyeing experiment

3.3 Metal nanoparticle impregnation

For the metal impregnation experiments, three different precursors were used and distinct experimental set ups were considered. The spare parts used are shown in figure 16 and 17. In some experiments, the vessel volume was reduced to ~50 ml by inserting a cylindrical spare part into the vessel ((2) and (1), respectively, see figure 16), while in other cases the experimental set up and the arrangement of the materials within the vessel were the same as in the dyeing/dithizone impregnation experiments ((3), figure 17). Spare part (4) was used with (2) in order to further reduce the volume of the vessel (1) and by this the dead zones (where no or only poor mixing occurred by the gear pump) were also reduced. Sieves were used to place the polymers and the metallic precursors onto them. This results in a more homogenous arrangement of the samples and makes the removal of the polymer pellets easier from the vessel after sorption.

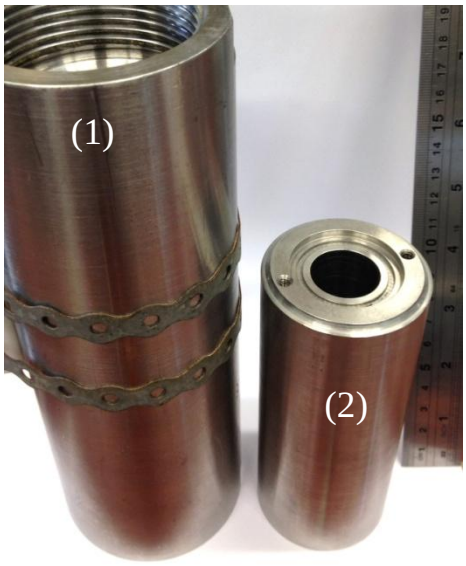

Figure 16: Impregnation vessel (1) with a cylindrical custom made spare part (2)

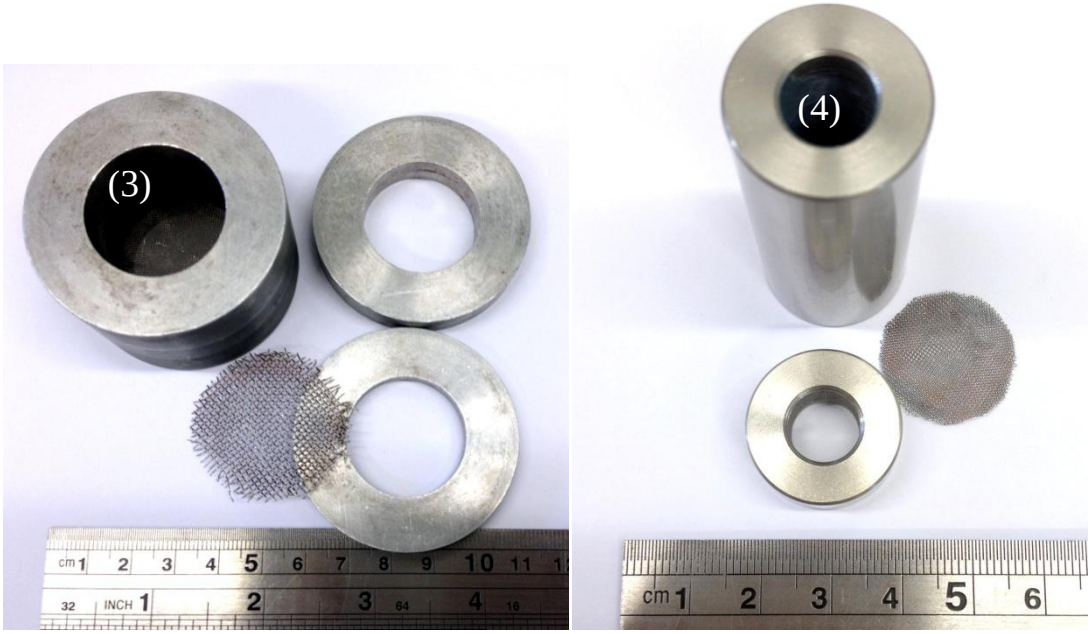

Figure 17: Additional custom made spare parts with grid

First, a commercially available complex with a good solubility in $scCO_2$ ($Cu(hfac)_2$) was used. As a second, two more complexes were synthesized in our lab for comparison. These were the primary and the secondary copper(II) dithizonate ($Cu(HDz)_2$ and CuDz, respectively). $Cu(HDz)_2$ was synthesized according to Irving and Kiwan [85] while CuDz was prepared by the method given by Geiger and Sandell [86]. In some cases, impregnation was carried out only in $scCO_2$ atmosphere while in other cases, water and/or ethanol was used as cosolvent. Ethanol has a good miscibility with $scCO_2$ and it also enhances the solubility of the complexes. In cases where ethanol was used as a cosolvent, ultrasound was applied for a

better dispersion of the complex in the solvent. Ultrasonic device (Hielscher UP400S, Germany) was operated with 400 W power at 24 kHz. Sonication time was 3–10 minutes applying 80–100% amplitude and 1.0 cycle.

In addition, copper modification of the polycarbonate has been tried to carry out by a two step process (figure 18). In this novel approach, first PC pellets were impregnated with dithizone, which was found to be soluble in $scCO_2$ according to high pressure view cell observations (figure 19). By this, *dithizone impregnated PC* (DPC) was obtained. In a second, distinct step, DPC was impregnated with copper nanoparticles by simultaneously contacting a solution containing copper ions with DPC in a high pressure vessel in $scCO_2$ atmosphere. As a copper ion source, $Cu(NO_3)_2$, $CuSO_4$ and $CuCl_2$ was used, dissolved either in ethanol or in water. This two step process is shown on figure 18.

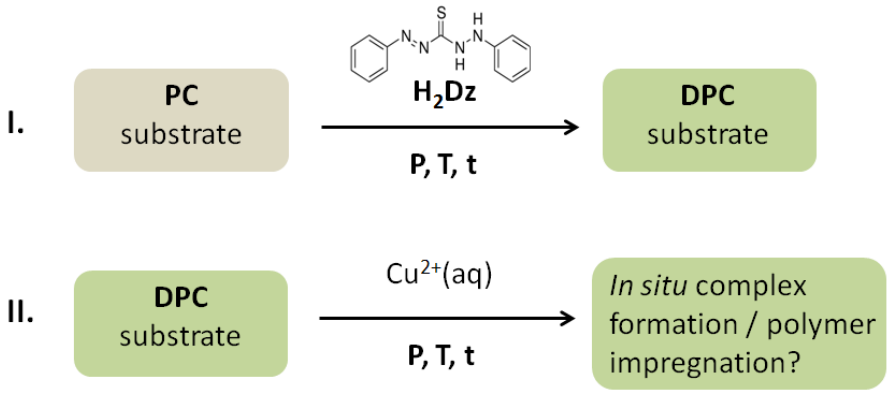

Figure 18: Schematic draw of two step impregnation process

Figure 19: Dithizone dissolves in $scCO_2$ with light green color at 150 bar and 45 °C

3.4 Solubility measurement of dyestuff DR13

The CO_2 liquid pump (JASCO Pu-2080-CO2 Plus) was connected to an extraction column placed in a tempered water bath. The column was filled with 0.020 g dye mixed with 0.150 g

Perfil 100^{TM}, a porous, inert supporting material, in order to obtain a uniform flow distribution of the $scCO_2$. At the end of the column, a filter (pore size 0.5 μm) was placed. Underneath and above the dye-Perfil package, small amount of cotton-wool was placed in order to avoid the possible blocking of the filter. The inner diameter of the column was 4.0 mm and the package length was 9.6 cm. The filled column was pressurized and a sample from the CO_2 phase was taken by firmly opening a needle valve placed after the column while pressure and temperature was kept constant. During sample taking 0.75 ml/min CO_2 flow was maintained by the JASCO pump. Average residence time in the packed part of the column was then calculated as 0.64 minutes assuming 0.4 relative void volume. Each sample was collected for 15 minutes in a liquid ethanol trap. After every sample the needle valve was carefully cleaned and the dye precipitated in the valve upon sample taking was washed into the collected sample by known amount of ethanol. After this, dye content was determined by UV-Vis spectroscopy upon its calibration by using the Lambert-Beer law. According to the data given for a flow type apparatus constructed by [72], the average residence time was calculated to be 0.45 minutes and authors stated that by this time a saturation of the fluid phase with the dye was achieved. Moreover, one solubility measurement was carried out in a stirred high pressure view cell. That is a non-continuous flow type apparatus where the dye-$scCO_2$ (without Perfil) system was held for 120 minutes, thus equilibrium was surely evolved. The result obtained by using the view cell correlated fairly well with literature data and with the solubility measurements carried out in the flow type apparatus. Therefore solubility data measured by the constructed apparatus was accepted as a technical solubility data for DR13 in $scCO_2$.

4. Analytical methods for product characterization

4.1 Dye and dithizone concentration of impregnated PC

After every experiment, eight pellets (approx. 0.15 g, measured on analytical balance) of the impregnated PC were dissolved in 2.000 ml dichloromethane (DCM) and the solution was measured by a double beam UV-Vis spectrophotometer (UV-1800, SHIMADZU Handels GesmbH, Austria) using 1 ml quartz vials. UV measurements were triplicate to ensure the accuracy. The measured absorbance of these three different samples (each of them containing eight pellets) taken from one experiment correlated reasonably well, indicating the uniformity of the impregnation. UV-Vis instrument was calibrated by known amount of dye or dithizone dissolved in DCM. Calibration curves are shown on figure 20 and 21. The dye or dithizone concentration of the impregnated PC samples was calculated by the Lambert-Beer law. Dissolving untreated PC pellets in dichloromethane did not change its absorbance in the 300-800 nm wavelength range thus clean DCM was used as a reference sample. The absorbance maximum was 484 nm and 503 nm for DR1 and DR13, respectively, whereas dithizone had the highest absorbance at 609 nm. Concentrations measured at absorbance maximum are given in [$mg_{(dye)}/g_{(PC)}$] and [$mg_{(dithizone)}/g_{(PC)}$] units.

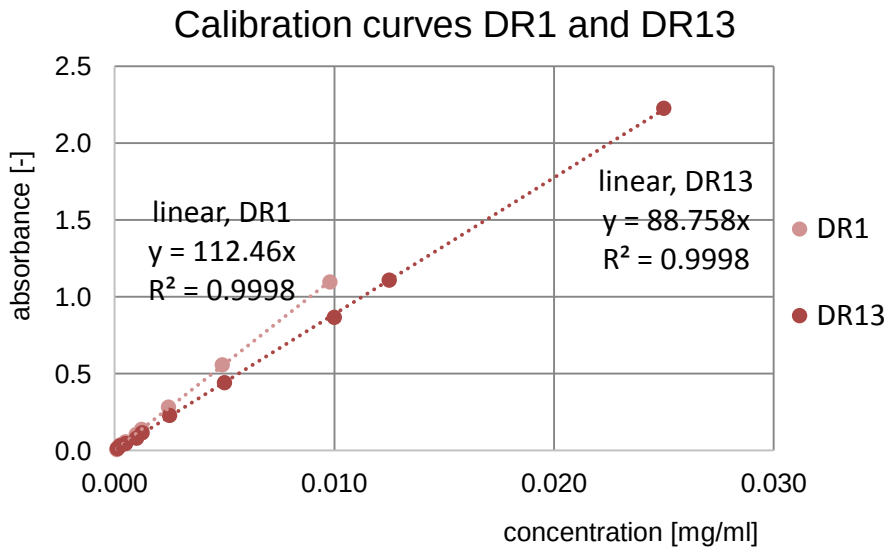

Figure 20: Calibration curve for DR1 and DR13 dyestuff

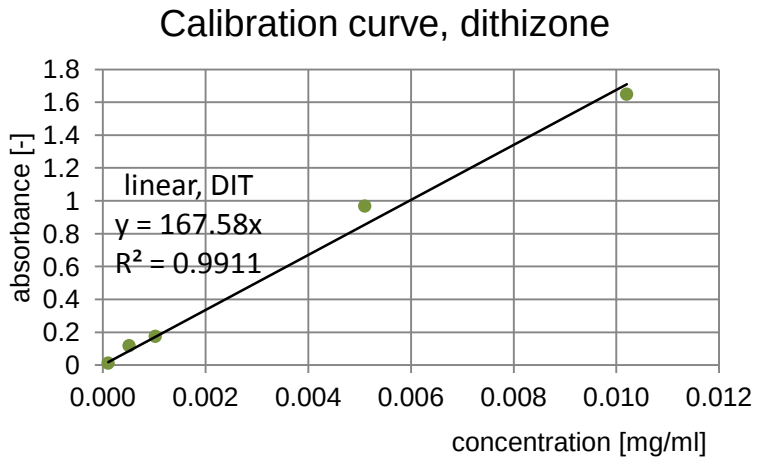

Figure 21: Calibration curve for dithizone

4.2 Overall copper content determination in PC

The copper content of the impregnated samples was measured by ICP-OES and ICP-MS spectroscopy. Samples obtained by the two step process were cleaned either with NH_4OH or with 10 % H_2SO_4 before analysis in order to remove any precipitation from the surface. Other samples were cleaned with ethanol. Measurements were performed at the Institute of Analytical Chemistry and Food Chemistry at the TU Graz by Helmar Wiltsche. PC pellets were digested in aqua regia (4.0 ml HNO_3 and 2.0 ml HCl) at 240°C in closed ceramic crucibles with microwave aid (Anton Paar Multiwave 3000 SOLV, Austria). By temperature increase, pressure increased approximately up to 40 bar. After digestion samples were measured by spectroscopy. For ICP-OES measurements, Spectro Ciros Vision EOP (1350 W power, Spectro, Kleve, Germany) device was used which was calibrated with 1.0 mg/L Sc internal standard. For copper determination λ = 324.754 nm was applied. ICP-MS was measured by Perkin Elmer Elan DRC+ (1400 W power, Perkin Elmer, USA) by using Ge as an internal standard. Limit of quantification (LOQ) for ICP-OES method was *LOQ* = 4 ppm (that is, 4 $mg_{copper}/kg_{PC\ matrix}$) while for ICP-MS it was 0.01 ppm.

4.3 SEM/EDX investigation

In order to determine the homogeneity of the samples, some PC pellets were measured by electron microscopy. First, a cross section of the investigated polymer pellet was cut (Leica Ultracut UCT) by using a diamond knife (Diatome). Sample was then coated with graphite in order to obtain conductivity on the surface and measured by the microscope (Zeiss Ultra 55).

Besides the information provided by the secondary electrons (SE), the microscope is also equipped with a backscattered electron detector (BsE) which makes easier the detection of metal particles since they appear with bright contrast in the matrix. Electron Dispersive X-ray Spectroscopy (EDX) detector provides extra information from the particles. By EDX measurement, each detected point can be identified by measuring its elemental composition. Pictures were obtained and EDX was measured by applying 5 and 20 kV accelerating voltage.

4.4 X-ray photoelectron spectroscopy (XPS)

XPS (sometimes also referred as Electron Spectroscopy for Chemical Analysis, ESCA) measurement was done at the Jožef Stefan Institute in Ljubljana, Slovenia, within the cooperation of DoHip. Polymer pellets were cut and analyzed by a PHI 5700 spectrophotometer in low vacuum (2×10^{-10} mbar). As X-ray source, the K_α radiation of Al (1.4866 keV) was used. The energy of the emitted photoelectron was measured by a hemispherical electron analyzer, operating at 29.3 eV and 58.7 eV pass energy for high-resolution spectra and 187.8 eV for survey spectra with a resolution of 0.2 eV. Sample was measured at 5°, 20°, 45° and 90° take off angles (with respect to the surface of the polymer). At 90° take off angle the analyzed area was r = 0.4 mm with a depth of 1.5 – 5 nm.

4.5 Thermoanalytics

Some thermogravimetric (TG) measurements were carried out at the University of Maribor (UMB) within the cooperation of DoHip project. Samples were measured by Mettler Toledo TGA/DSC 1 STARe Thermogravimetric analyzer (USA). Differential thermal analysis (DTA) curve was obtained by registering the enthalpy signal. Samples were heated by 5°C/min in N_2 atmosphere. Other TG measurements were conducted at our department by using a Netzsch Jupiter STA 449C balance also in N_2 at 10°C/min heating rate. DSC measurements were performed at BUTE within the frame of DoHip by using a TA Instruments DSC 2920 device by applying 10 °C/min heating rate.

4.6 IR measurements

IR spectra of some samples were measured at the UMB within the cooperation of DoHip by using a SHIMADZU IRAffinity-1 device with ATR attachment.

III. Results and Discussion

1. Polycarbonate dyeing by SFD in $scCO_2$

Dyes and pigments are conventionally incorporated into polycarbonate resins during their manufacture. This method suffers from two general drawbacks:

- first, the high melt viscosity of the resin makes it difficult to disperse the color uniformly and
- second, the high temperatures used in molding the resin exclude the use of thermally labile dyes.

Processes invented to overcome these disadvantages consume high amount of organic solvent (containing carriers and surfactants) and hence an additional drying step has to be involved at the end of the dying process [87,88]. Therefore, the goal was to apply the SFD method (see figure 22) for polycarbonate to overcome all the above mentioned drawbacks that conventional techniques have. In this part of the work, two azo-disperse dyes, DR1 and DR13 were used. During experimentation sorption data were collected and evaluated, dyeing kinetics were studied in detail. In case of DR13 no solubility data in $scCO_2$ were available, so the solubility of DR13 was measured and these new data are reported. Equilibrium constants which determine the maximum dye uptake on a given pressure and temperature have also been calculated.

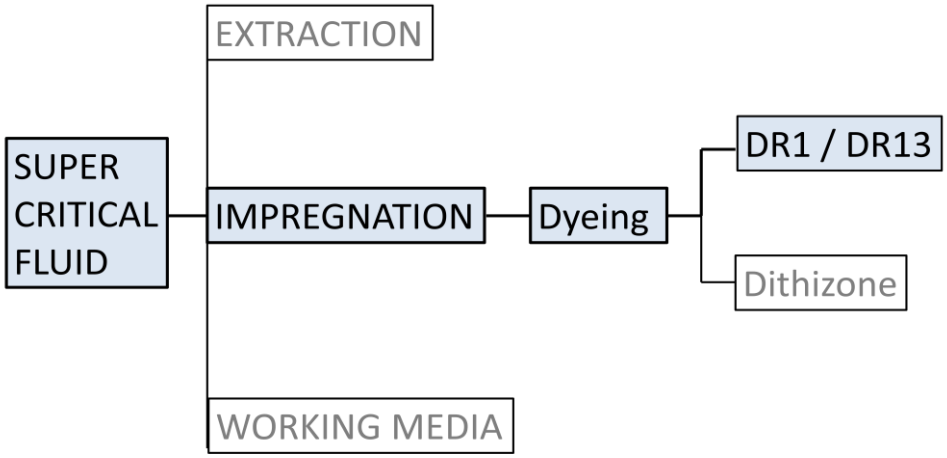

Figure 22: Application of $scCO_2$ for polymer dyeing by DR1 and DR13

1.1 Observations under high pressure CO_2

As it was discussed above, polymers have an uncommon behavior in $scCO_2$ atmosphere. This behavior clearly differs for distinct polymers, but it can also be different for the same type of polymer, arising from their production method and the presence of additives (e.g. flame retardants, softening agents etc.). Therefore, it was essential to observe the PC behavior in $scCO_2$ atmosphere in the high pressure view cell. It should be noted here, that a detailed experimentation such as accurate sorption data collection or measurement of swelling requires very special equipment and was out of the scope of this present study. Polycarbonate sample was used as received. For observations in high pressure CO_2, approx. 4 g polymer pellets were measured in the range of 40–70°C and at pressures up to 150 bar for 4–6 hours of sorption time. Pressurization of the cell was not controlled and took several minutes. No literature reference has been found, in which pressurization rate was reported to be critical in case of using polymers for impregnation. In the investigated range, no visual changes were observed. PC remained transparent after every experiment, no dissolution, foaming, or extraction of additives was observed. However, when weighting a sample right after the experiment, a continuous and relatively fast mass decrease was observed on the analytical balance. This indicated degassing of the sample, which means, that CO_2 sorption had to take place before in the view cell. The amount of sorbed gas was not determined, since CO_2 sorption data for PC are available in literature [49]. Figure 23 shows polycarbonate in $scCO_2$ after six hours of sorption time at 140 bar and 40°C.

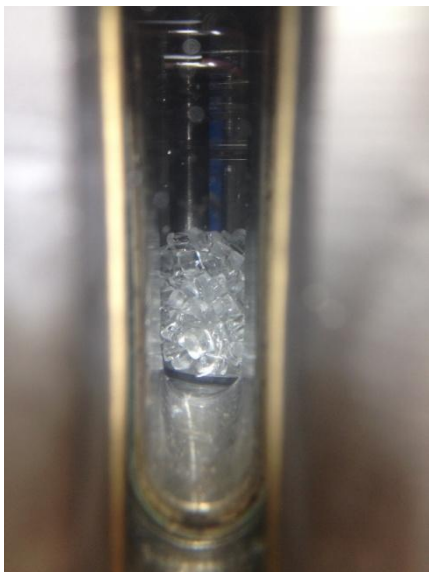

Figure 23: Polycarbonate in the view cell in $scCO_2$ atmosphere

The dissolution of dyestuff DR1 and DR13 has also been observed whereas only one experiment was made with each dye. As described previously in literature [72], these dyestuffs were readily soluble in $scCO_2$. After some minutes the content of the view cell turned to pink/slight red color.

1.2 Analytical studies of polycarbonate

In order to monitor the changes of the pellets upon sorption, thermoanalytical measurements were performed. An untreated PC sample, and one sample after 3 hours of sorption time at 300 bar and 50°C carried out in $scCO_2$, were measured by DSC. These curves are shown in figure 23 and 24. DSC measurements (10°C/min heating rate) and the measured sample with CO_2 sorption were obtained at BUTE within the frame of DoHip. From figure 24 it can be seen that glass transition phenomena of the untreated PC occurs between 144 and 150°C whereas T_g can be determined to be ~148°C, which correlates well with literature data [65]. An endotherm peak at 88.4°C can arise from a chemical transformation of a contaminant or an additive. A sample after 3 hours in $scCO_2$ at 300 bar and 50°C turned opaque after sorption. This can indicate either crystallization or foaming. Since the decompression of the vessel took one hour, phenomenon of foaming was excluded (which could only have been obtained by a rapid decompression of the vessel). Therefore, presumably crystallization of PC took place. DSC curve of this sample is shown in figure 25. Here, T_g of the sample decreased to 138°C, thus original T_g could not be regained this time, which further supports the phenomenon of partly crystallization of the sample. Moreover, glass transition phenomena occurred in a broader temperature range of 132–147°C.

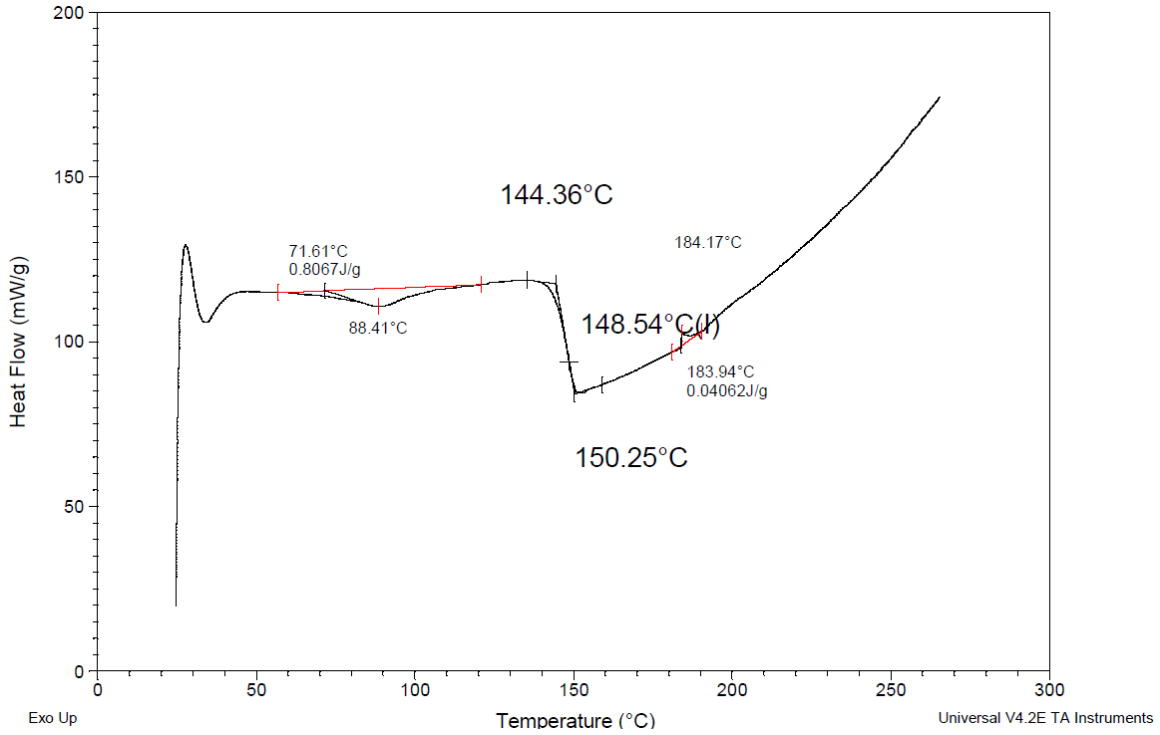

Figure 24: DSC curve of untreated PC pellet

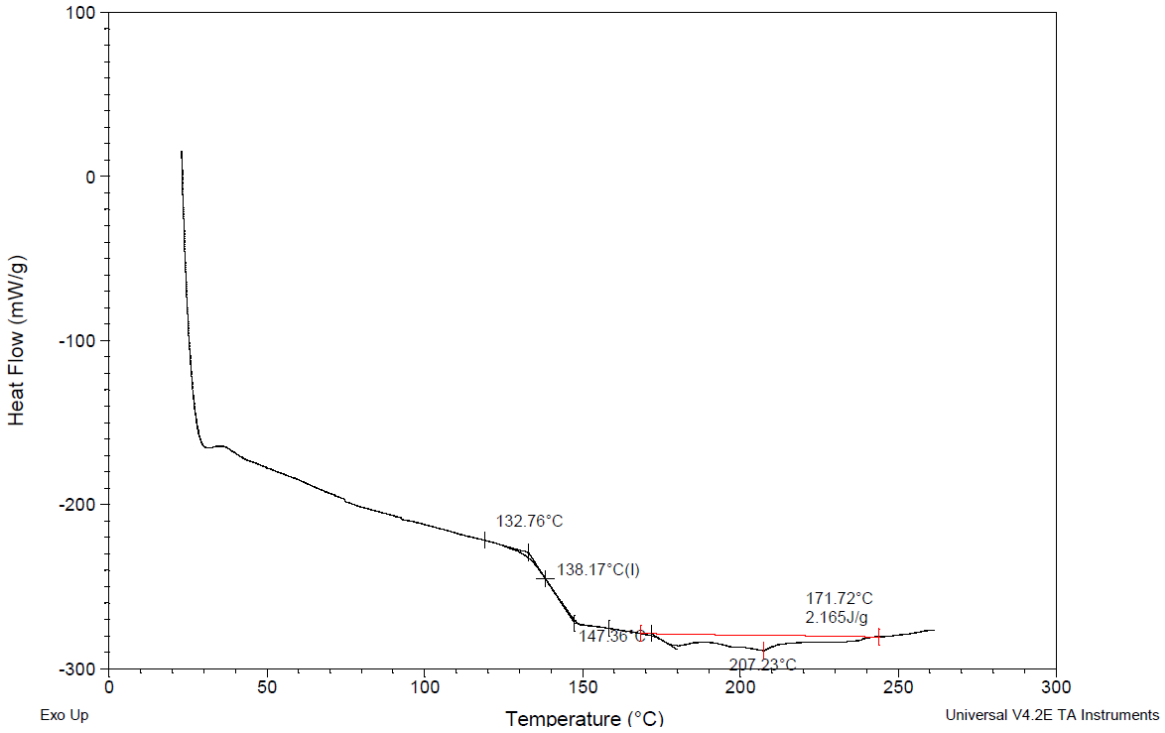

Figure 25: DSC curve of PC in scCO$_2$ for 3 hours at 300 bar and 50°C

After the sorption experiment where this opaque PC samples were produced, the total amount of CO_2 expanded from the system during decompression was collected into a liquid hexane trap. This solution was analyzed by GC later on, and no peaks different from the solvent peak

were found. This means, the possibility of extracting any kind of additives from PC by $scCO_2$ can be excluded. At around 200°C in figure 25 flat, prolonged peaks can be observed which were missing in case of untreated PC (figure 24). Although these peaks correspond to a low specific enthalpy of fusion of 2.16 J/g, these still can indicate melting phenomenon. Arising from the distinct size and the imperfect nature of PC crystals formed during sorption in $scCO_2$, these peaks are not sharp but elongated between approx 170–240°C. Mercier and coworkers [89] determined 26.2 kcal/g (~109 J/g) enthalpy of fusion for 100 % crystalline polycarbonate. Mascia [63] reported a value of 4.5 J/g for PC (M_w = 25 000 g/mol) crystallized under $scCO_2$ (80°C, 300 bar, 12 hours of sorption time) which corresponded to a crystallinity of 4.1 %. Based on calculations from data published for 100 % crystallinity and the enthalpy of fusion measured, PC sample used in this work has a crystallinity of approx. 2.4 %. However, the conditions of 300 bar, 3 hours sorption time and 50°C temperature are relatively mild, here it is proven that crystallization of the PC sample in $scCO_2$ has been occurred. In spite of several authors [52,56,57,63] have not observed crystallization at these mild conditions, Gross *et al.* [64] pointed out, that the crystallization phenomenon also depends upon the average molecular weight of the polymer and is more expressed at lower molecular weights. Unfortunately, the M_w of the PC sample used in our experiments are confidential information and the property of SABIC, therefore the accurate M_w of our sample shall not be reported here. However, from the crystallization behavior is visible, that we are dealing with a material having relatively low molecular weight compared to PC samples used in other studies.

TG measurements were carried out at the UMB from 30 to 300°C with a heating rate of 10°C/min. Figure 26 shows TG curve for an untreated PC sample. Upper curve in figure 26 shows the mass change while the curve below shows the enthalpy signal (DTA curve). From the signal registered it can be seen that there is virtually no mass change (-0.052 %) of the non impregnated polymer. DTA gives a T_g of 145°C which correlates well with literature [65] and data measured by DSC at the BUTE. Apart from the change in glass transition, there are only two other very small elongated peaks visible with a negligible enthalpy of fusion of < 0.3 J/g.

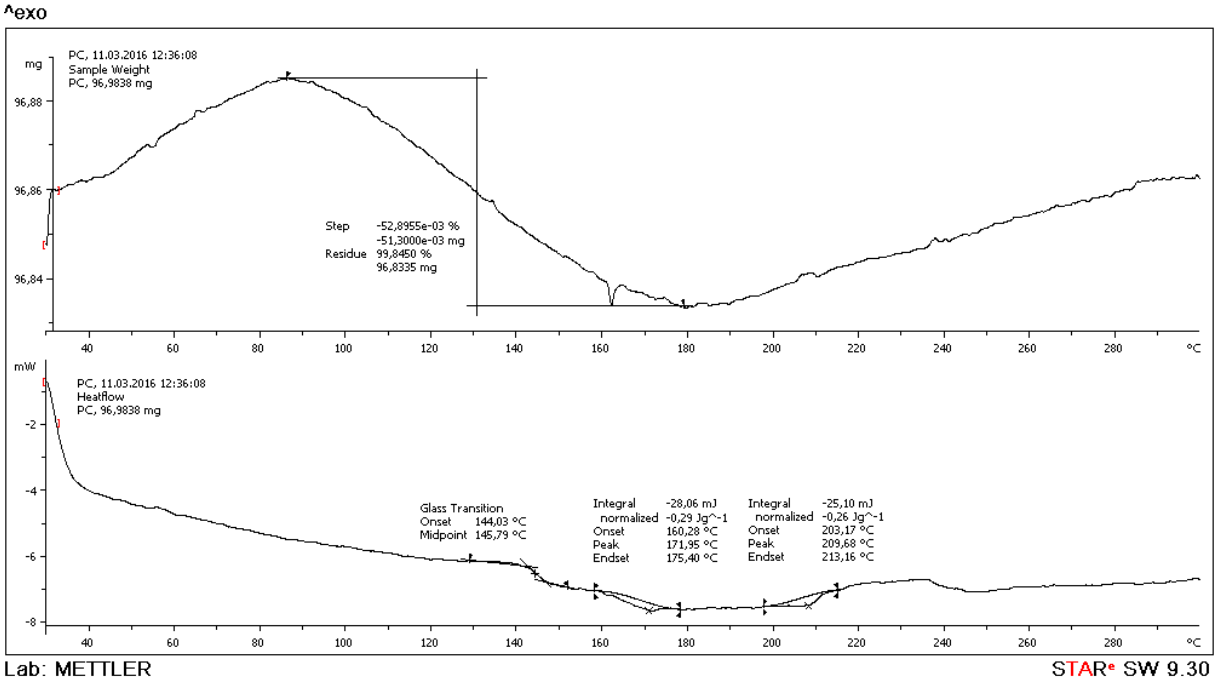

Figure 26: Thermogravimetric curve of untreated PC pellet

1.3 Impregnation parameters

As it was discussed earlier, impregnation time, pressure, temperature, decompression rate and stirring in the vessel influence the dyeing process. Moreover, the fluid phase has to be always saturated and cannot be exhausted by the dye uptake of a polymer as sorption proceeds. Since it was reported that PMMA has an uptake of 0.5 wt% from DR1 in $scCO_2$ at 91 bar and 40°C [74], to ensure that the dyestuff presents in high excess during the experiment, 3.0 wt% of dye to polymer was applied with 0.0600 g dye and 2.00 g polymer inside the high pressure vessel. Experiments were performed in the range of 100–300 bar. As it was shown here, PC becomes crystalline due to sorption induced crystallization in $scCO_2$ already at temperature as low as 50°C at higher pressure of 300 bar. This means an irreversible change in the polymer structure, which has to be avoided since crystalline regions are harder to impregnate and hence an anomalous diffusion of the CO_2 within the polymer matrix occurs which influences the mass transport. Therefore, vessel temperature was fixed with 40 and 50°C. According to Schnitzler [47], polycarbonate reaches its equilibrium sorption amount under $scCO_2$ within 3–6 hours (depending on the temperature) and from 8 to 72 hours for some dyes. Tang *et al.* [56] investigated the PC behavior in $scCO_2$ and reported that a 0.5 mm thick polycarbonate sample reaches the maximum carbon dioxide uptake after approx. 2 hours at 40°C, measured at 200, 300 and 400 bar. This uptake is diffusion controlled. Our cylindrical shaped pellet samples have a remarkably bigger size (approx. 1.5 mm in diameter and 3 mm in length), thus

presumably require more time to reach the equilibrium in $scCO_2$. Therefore a minimum impregnation time of three hours was chosen. Dyeing fixation was tested by inserting some impregnated sample into ethanol for 48 hours. After that, absorption of the ethanol was measured and since no difference from the clean ethanol was found, dyeing efficiency proved to be excellent.

1.4 Results obtained by the use of DR1

Experiments were performed first on 40°C at 3, 6 and 24 hours of sorption time. The dye uptake versus time is shown in figure 27.

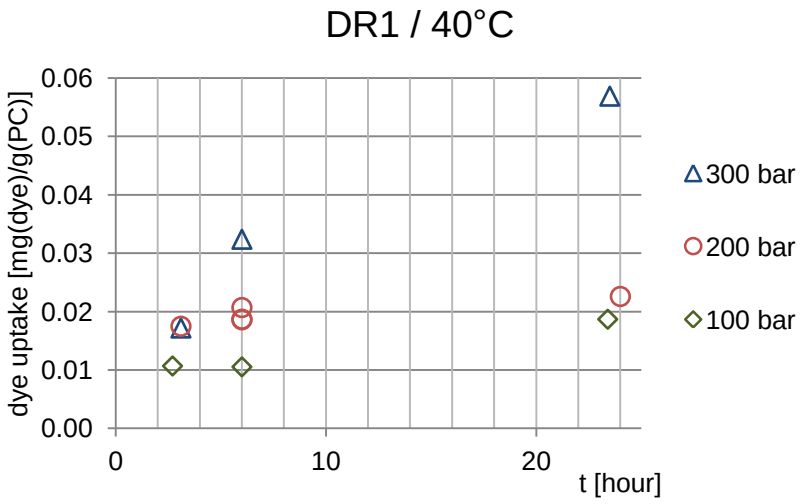

Figure 27: Effect of the CO_2 pressure and temperature on the DR1 dye uptake versus impregnation time at 40°C sorption temperature

The experiment at 200 bar and 40°C and 6 hours was triplicate, the standard deviation was determined as 0.0012 [$mg_{(dye)}/g_{(PC)}$] which is 6.2 % (not pictured in figure 27). Since performing all the impregnation experiments in triplicate would be laborious, this error of 6.2 % was considered to be constant within the pressure and sorption time range in case of using DR1 dyestuff. Since this standard deviation involves all the errors of the whole process, this number was considered to be reasonable. At 100 bar the impregnation is low, experiments performed at 200 bar result in a slightly better dye uptake. This can be due to the higher solubility of the dyestuff caused by the increased density of $scCO_2$. Table 5 shows data obtained upon DR1 impregnation of PC.

Table 5: Tabulated data of dye uptake at various temperature and pressure, DR1 dyestuff

T (°C)	p (bar)	Dye uptake (mg/g)		
		3 hours	6 hours	24 hours
40	100	0.0107	0.0105	0.0187
40	200	0.0175	**0.0193±0.0012**	0.0226
40	300	0.0172	0.0324	0.0569
50	100	0.0283	0.0351	
50	200	0.0590	0.1040	

At these pressures $scCO_2$ swells the polymer remarkably (min. ~ 6.0 vol% depending on temperature, measured by Schnitzler *et al.* [47]). Since from 6 hours to 24 hours the uptake did not change remarkably neither at 100 nor at 200 bar, it is assumed that equilibrium of dye sorption in the polymer phase has been reached. To prove this assumption properly, one would need to perform experiments with longer impregnation time even up to 72 hours since dye uptake can take that long [47]. However, it has to be noted that crystallization of the PC sample is also a function of the time and therefore it possibly takes place after longer sorption times. Therefore, no experiments with more than 24 hours of sorption time were carried out. In the equilibrium, the partition coefficient, K_c, which is the ratio of the saturated concentration of the dye in the polymer phase to the saturated concentration of the dye in the fluid phase, determines the final dye uptake. K_c was calculated from the solubility data of the dyes taken from [90] and from the measured dye concentration in the polymer after 24 hours. They were determined to be 56.7 and 6.2 at 100 and at 200 bar, respectively. These values are low. The coloring of PC with DR1 is rather poor as it was previously reported [74], see figure 28 which also shows impregnated pellets at 40°C. Although the difference between the two samples is not that remarkable for the eye, it can be clearly measured via UV-Vis. It can be observed that impregnation is deep and equal throughout the pellet.

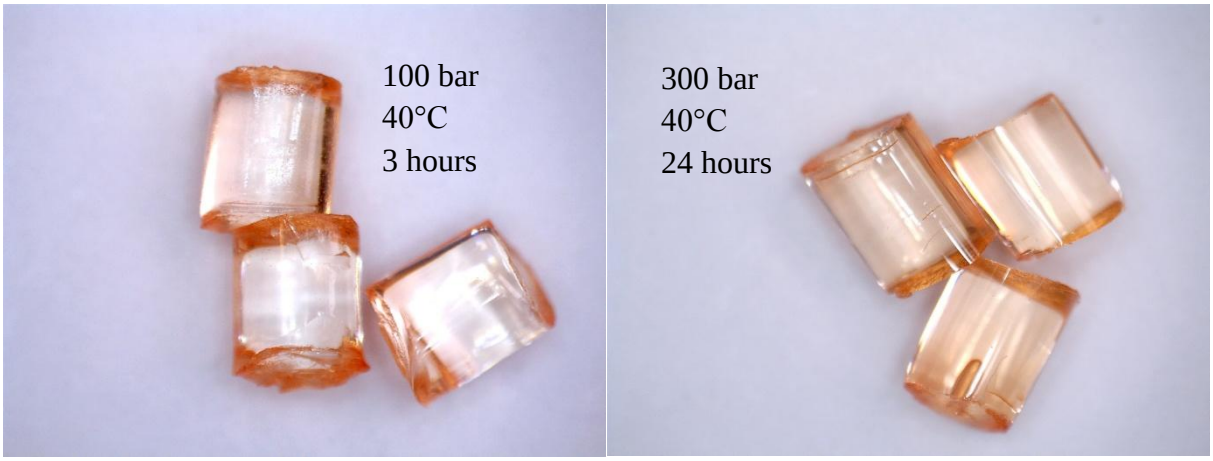

Figure 28: PC pellets impregnated with DR1 at 40°C at various conditions

For PMMA-DR1 system, West *et al.* [74] determined the K_c to be ~10^5 at 91 bar and 40°C. For DO25 dyestuff in PMMA matrix, a similar value at this pressure and temperature for K_c of 5.29×10^4 was found [73]. The calculated partition coefficient is lower at higher pressure. This is expected, because as CO_2 density increases, the solubility of the dye in the fluid phase increases, thus its partition in the polymer phase compared the fluid phase decreases. This correlates to literature data reported elsewhere [73,74]. The diffusion coefficient in $scCO_2$ at a constant temperature increases with pressure [57] thus *D* is higher at 200 bar than at 100 bar. This increased *D* led to a faster process, thus equilibrium uptake seem to be reached already after 6 hours at 200 bar (figure 27). At 300 bar much better results were observed after 24 hours and it is probable, that equilibrium has not been reached. Here, the process is still governed by diffusion and dye uptake can increase by impregnation time as more and more dye diffuses into the polymer matrix. Dye uptake reaches remarkably higher values at 300 bar than at 200 bar – meanwhile dye solubility and polymer behavior under $scCO_2$ do not change much within this range (see table 6. which contains literature data of the dyes' solubility and swelling of the polymer at various pressures and temperatures).

Table 6: Dyes solubility in $scCO_2$ and PC swelling at various pressures and temperatures

T (°C)	p (bar)	CO_2 density (mol/L) [a)]	Solubility DR1 ($\times10^{-7}$ mol/mol)	Swelling V/V % [d)]
40	100	14.283	0.81 [b)]	~ 6.0
40	200	19.082	6.44 [b)]	
40	300	20.675	(no data)	~ 9.5
50	100	8.7328	0.16 [c)]	~ 5.9
50	200	17.821	15.78 [c)]	
50	300	19.778	48.09 [c)]	~ 9.2

a) NIST Standard Reference Database
b) From reference [90]
c) From reference [72]
d) From reference [47]

In general, applying higher temperature (50°C, figure 29, full markers) resulted in a better uptake.

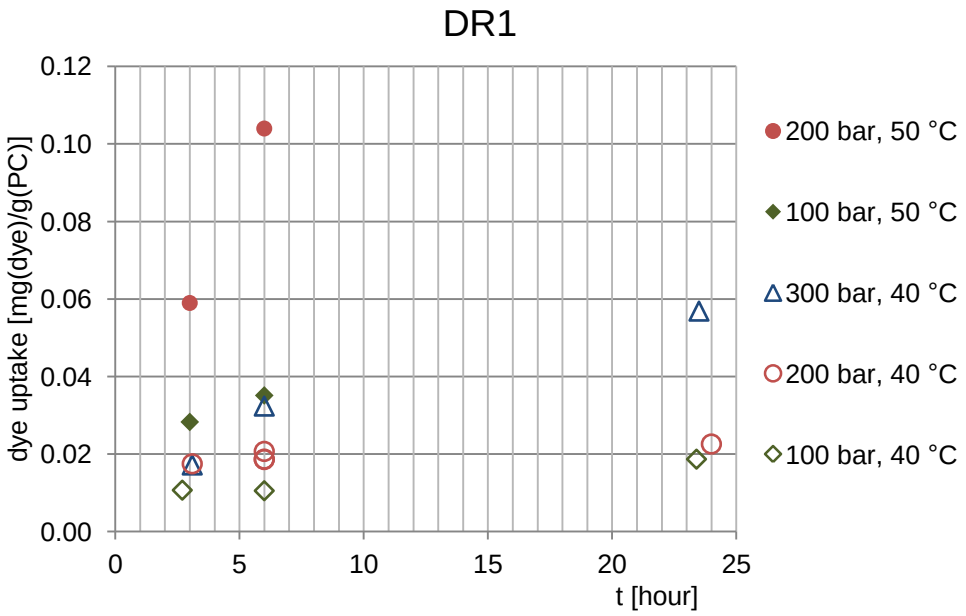

Figure 29: Effect of the CO_2 pressure and temperature on the DR1 dye uptake versus impregnation time

After six hours of impregnation time, similar uptake was achieved at 100 bar, 50°C and at 300 bar, 40°C. The difference in dye uptake between samples measured at these conditions is even higher after three hours. In the former case at 100 bar and 50°C, from solubility data and from data measured via UV-Vis, it can be calculated that here the concentration of the dye in the polymer phase is higher than in the vessel. There are no literature data available for the solubility of DR1 at 300 bar and 40°C. However, generally, the solubility of a given dye increases with the CO_2 density [71,72,90]. Therefore it is assumed, that the solubility is higher at 300 bar and 40°C ($\rho_{(CO2)}$=20.675 mol/l) than at 100 bar and 50°C ($\rho_{(CO2)}$=8.733 mol/l). Tang *et al.* [56] measured the diffusion coefficients in PC at temperature ranges from 40 to 60°C and pressure ranges from 100 to 400 bar. The authors pointed out, that $scCO_2$ sorption diffusivities enhanced with temperature and are the highest at lowest pressures. In addition, by temperature increase the chain mobility and the kinetic motion of the $scCO_2$ within the polymer phase also increases. These factors strongly affect the uptake and the effect of temperature seems to be more important that of the pressure and CO_2 density. At 200 bar and 50°C after six hours an entirely colored but somewhat opaque sample was obtained (see figure 30). As it was described earlier, this behavior of PC indicates the CO_2 sorption induced crystallization. Since this was observed already at 200 bar at 50°C after six hours of sorption time, no further experiments were run with higher impregnation times at 50°C. Figure 30

shows dyed PC pellets applying 200 bar, 50°C and three (left) and six (right) hours of sorption time.

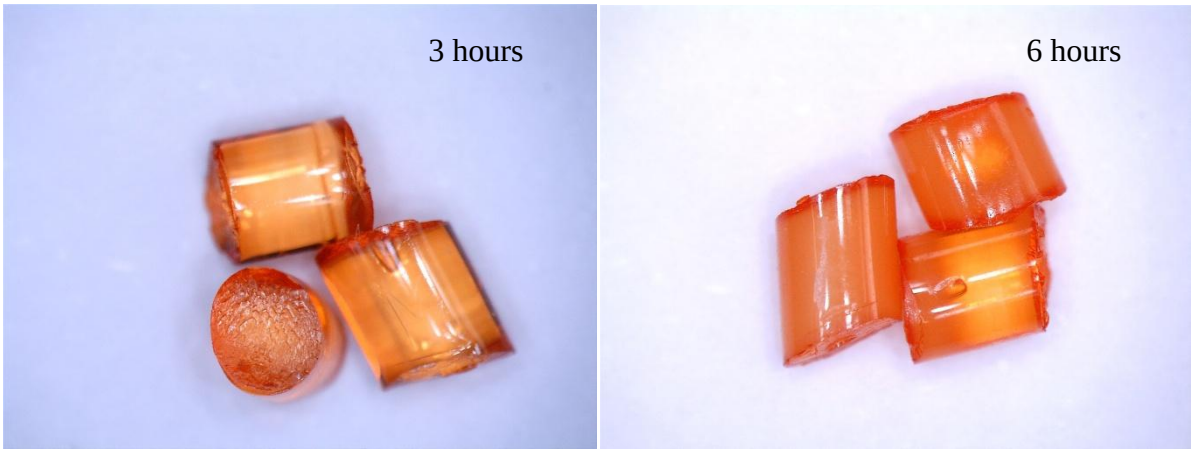

Figure 30: PC pellets impregnated with DR1 at 200 bar and 50°C for various sorption times

In spite of the coloring of PC by the use of DR1 was reported to be highly ineffective [74], it is proven here that by taking advantage from the tunable properties of $scCO_2$ (that is, varying sorption temperature and pressure), an entirely deep colored sample can be obtained with excellent dyeing fixation. The highest uptake of 0.1040 mg/g, obtained at 200 bar, 50°C and after six hours, corresponds to 0.010 wt% with respect to the mass of the polymer. This is fifty times lower than in case using PMMA for the impregnation which can be explained by the different behavior of the two polymers. In case of PMMA, specific π-interactions of polymer chains with CO_2 facilitates the mass transport within the polymer phase, which results in higher sorption amount, i. e. higher dye uptake. It is suggested, that kinetics of PC dyeing should not be investigated in case even when it is only partly crystallized because in those regions CO_2 sorption and mass transport does not necessarily follow the classical Fickian laws of diffusion. However, it should be noted, that crystallization occurs after dye sorption, therefore crystalline regions are already contain dye which does not desorbs when amorphous regions turns to crystalline. The degree of swelling does not seem to have an effect on the impregnation. This is not unexpected. First, the change in swelling in the investigated pressure and temperature range is not that remarkable, and as a second, CO_2 being a small molecule, could induce mass transport due to its benign properties discussed above, even without swelling the polymer.

1.5 Results obtained by DR13

1.5.1 Solubility measurements

Where literature data were not available, solubility of DR13 dyestuff was measured as it was described in the materials and methods section. These data were essential in order to calculate the equilibrium constants after the impregnation. Solubility data measured and taken from literature with the dye uptake obtained during experiments are shown in table 7.

Table 7: Tabulated data of dye uptake at various temperature and pressure, DR13 dyestuff

T (°C)	p (bar)	Dye solubility ($\times 10^{-7}$ mol/mol)	Dye uptake (mg/g)		
			3 hours	6 hours	24 hours
40	100	1.77	0.059	0.072	0.089
40	200	7.80	0.038	0.065	0.138[b] / 0.231
40	300	18.40	0.048	0.082	0.268
50	100	0.43 [a]	0.208	0.276	
50	200	52.59 [a]	**0.283±0.016**	0.453	
50	300	119.4 [a]	0.389/0.463 [c]	0.552	

[a] From reference [72]
[b] After 17 hours sorption time
[c] After 4 hours sorption time

1.5.2 Impregnation experiments

Due to the chlorine group, DR13 has an approx. 3-5 times higher solubility in $scCO_2$ than DR1 [71,72]. Therefore, in general, much better results were obtained by the use of DR13 in the investigated time and pressure range (see figure 31). The measurement at 200 bar 50°C and three hours sorption time was triplicate, and a standard deviation of 0.016 [$mg_{(dye)}/g_{(PC)}$] (5.6 %) was calculated. We consider this error constant for DR13 within our working pressure and temperature. This value is indeed higher than in case of DR1 but dye uptake also increased by an order of magnitude.

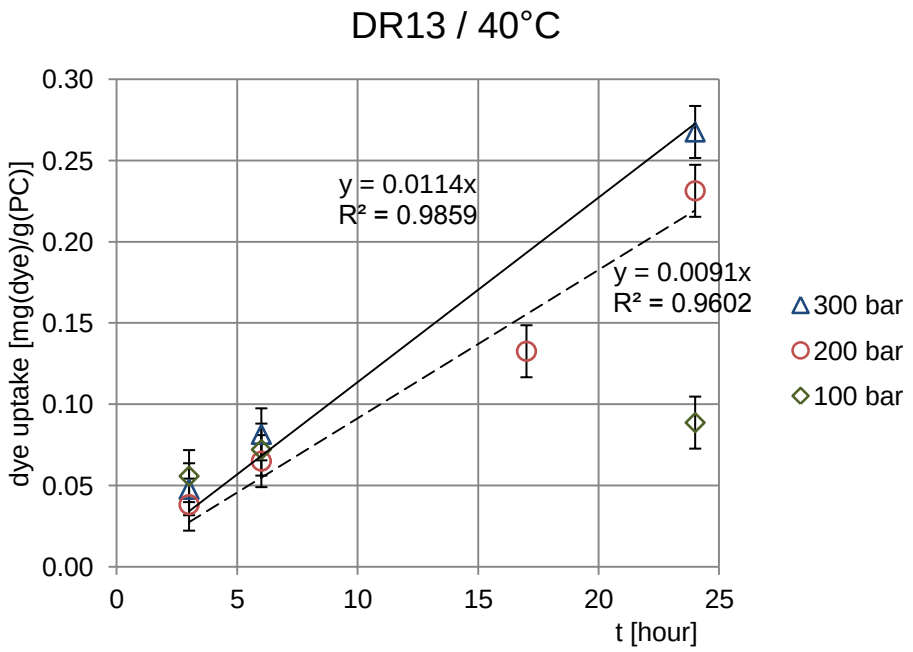

Figure 31: Effect of the CO_2 pressure on the DR13 uptake versus impregnation time, 40°C

In figure 31 and from the values in table 7 it can be seen, that equilibrium has been reached at 100 bar sorption pressure and at 40°C. From the final dye uptake here and solubility data measured (see table 6), the partitioning coefficient was calculated to be 111.1, remarkably higher than in case of DR1 at these conditions (56.7). Within the measured time range at 200 and 300 bar the equilibrium has not been reached. According to Tang *et al.* [56], a PC sample having a thickness of 0.5 mm reaches a maximum CO_2 sorption after 2 hours of impregnation time at 40 °C. Therefore, increment in the dye uptake on a fixed pressure cannot be accounted for increasing $scCO_2$ sorption. Rather, the diffusion of the dye within the polymer phase as a function of time can be observed here. Within this time range of 24 hours the first, linear part of a diffusion curve can be observed before it would level off due to saturation. In order to calculate the diffusion coefficients of the dye into the polymer phase, the maximum dye sorption amount in the polymer has to be known. In our experiments at 200 and 300 bar DR13 has not reached the saturation concentration, thus the maximum dye sorption is unknown and diffusion coefficients cannot be calculated. Again, as it was reported elsewhere [47,74], dye diffusion can last sometimes more than 72 hours to reach saturation. In experiments performed at 50°C, in particular the outer part and the corners of the pellets turned in some cases opaque after sorption just in case of DR1 impregnation, which is attributed to the $scCO_2$ induced crystallization of PC. After 3 hours of impregnation time at 200 and 300 bar at 50°C samples remain transparent, but somewhat opaque pellets were obtained after 6 hours of

sorption time. Therefore, no further experiments with longer sorption times than 6 hours at 50°C and than 24 hours at 40°C were performed. Figure 32 shows results measured at 50°C.

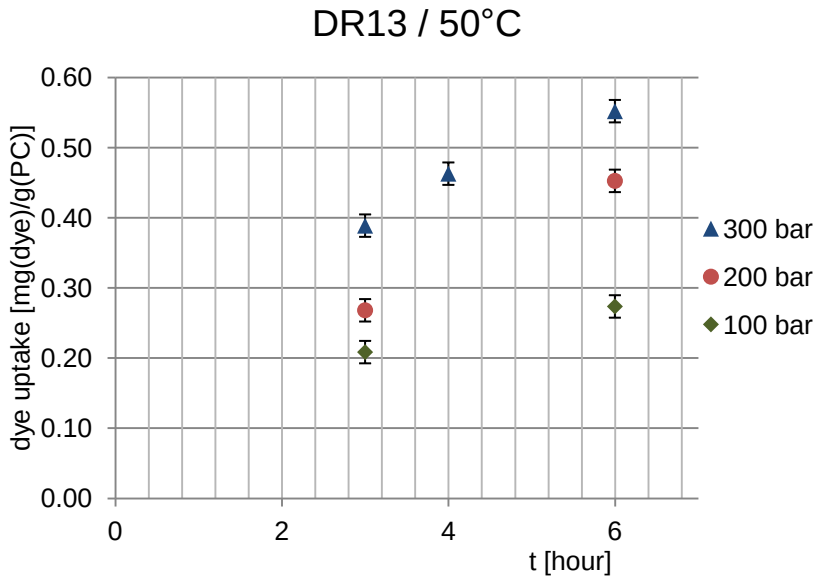

Figure 32: Effect of the CO_2 pressure on the DR13 uptake versus impregnation time, 50°C

The increase in the dye uptake at a given sorption time at various CO_2 pressures is related to the dye solubility, which increases at higher pressures (see table 7). Due to the higher temperature, *D* is increased and thus much better results were obtained here than at 40°C. Impregnation for 3 hours sorption time at 100 bar and 60°C resulted in really similar uptake to that of 100 bar and 50°C. An experiment at 200 bar and 60°C yielded a slightly opaque sample already after 3 hours, therefore no further experimentation on 60°C was performed.

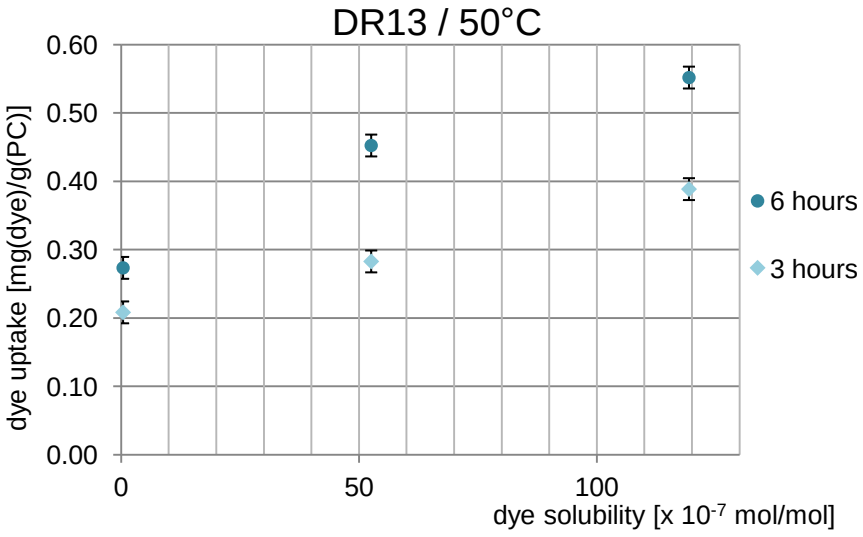

Figure 33: DR13 dye uptake of PC versus dye solubility at 50°C at various sorption times

In figure 33 a linear relationship can be observed between the dye uptake and its solubility at a given sorption time. It is assumed that after 3 and 6 hours PC pellet has reached the maximum CO_2 uptake and only dye sorption takes place. Therefore, on fixed pressure, temperature and time, only the concentration of the dye in the fluid phase determines the uptake. The higher is the solubility, the more dye is dissolved in the dye bath thus concentration increases. Figure 34 shows dyed PC pellets by the use of DR13. It can be observed that impregnation is deep and equal, just as in the case of using DR1. The highest dye uptake of 0.552 [$mg_{(dye)}/g_{(PC)}$] corresponds to 0.055 wt% with respect to the weight of the polymer.

Figure 34: PC pellets impregnated with DR13 at 200 bar, 50°C for 3 hours of sorption time

2. Polycarbonate modification with dithizone by SFI in $scCO_2$

This section focuses on the dithizone modification of PC (see figure 35), wherein the metal chelating capacities of the impregnated samples are also investigated. As it was pointed out earlier, since dithizone has a slight solubility in $scCO_2$ with a slight green color, it can be discussed as a dyestuff and its sorption kinetic in PC can be investigated just as in the case of using dyes (DR1 or DR13) for the impregnation.

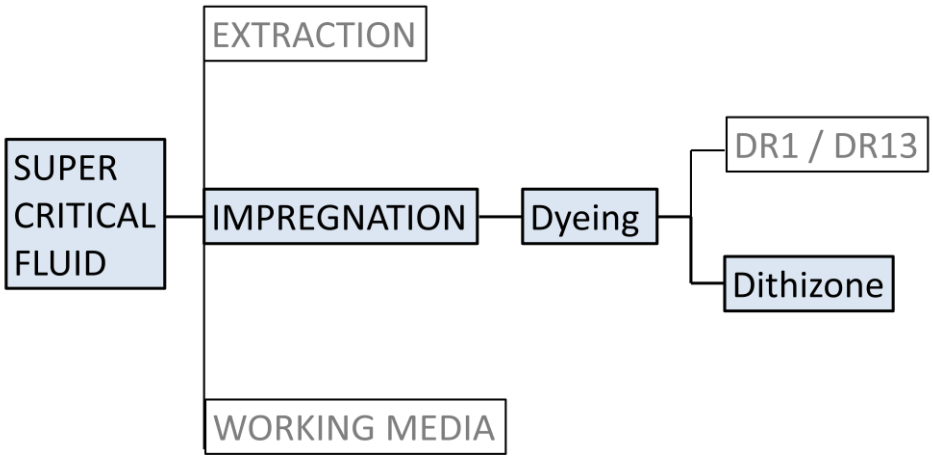

Figure 35: Application of $scCO_2$ for polymer dyeing dithizone

2.1 Solubility measurements

The solubility of the dithizone (DIT) was measured at the BUTE within the frame of DoHip. Measurements was carried out in the same apparatus and by the same method which was used for determining the solubility of DR13 and it was performed at 100 and 200 bar and at 40°C by applying 0.75 ml/min flow rate. At 100 bar the solubility turned to be almost negligible. The absorbance of the samples taken after the measurement has barely changed. Although, at 200 bar the solubility was measured twice and was determined to be 8.44×10^{-8} and 9.56×10^{-8} mol/mol, which is approximately only one order of magnitude lower that of the solubility measured for DR13 at these conditions (see table 7).

2.2 Impregnation experiments

Experiments were performed in the range of 100–200 bar at 40 and 50°C for 1 to 24 hours of sorption time. Impregnation was carried out by using the gear pump and spare parts nr. 3 shown in figure 17 in chapter II. With this arrangement, the impregnation vessel had a volume

of ~140 ml. The sorption experiment with ethanol as cosolvent at 100 bar, 40°C and for 2 hours of time (see figure 37) was triplicate and the standard deviation of this process was determined to be 11.2 %. This error is remarkably higher than in case of the dyeing experiments (5.6 and 6.2 %), which can be caused due to the mixing. By circulating the solution the impregnation efficiency is indeed higher by the increased diffusion in the fluid phase, but on the other hand, some dead zones may evolve where mixing is less effective, which results in different impregnation depth for the distinct pellets.

Generally, applying ethanol as a cosolvent provided far better results; almost two orders of magnitude higher dithizone load was achieved inside the polymer by applying cosolvent. This is not unexpected, since dithizone has a good solubility in ethanol [75] which, in turns, has good miscibility with $scCO_2$. At 40°C ethanol and $scCO_2$ become a one phase mixture above approx. 80 bar [91]. It has to be noted however, that having a one phase mixture does not necessarily mean that both compounds (in this case, ethanol and CO_2) present in supercritical state! The T_c of the ethanol is 248°C, which is far above the temperature applied here. Figure 36 represents vapor–liquid equilibria (VLE) data of ethanol and CO_2 system at 40°C [92]. Each point denotes the cloud point. This is the pressure at fixed temperature and composition above which the mixture is present as one single phase. On the abscissa xCO_2 denotes mole fractions of CO_2 in liquid, while yCO_2 denotes mole fractions in vapor phase. First experiments were performed at 100 bar and 40°C by applying 10.0 ml ethanol as a cosolvent. With 140 ml of vessel volume at these conditions, this means 7.87 n/n % of ethanol in CO_2, corresponding to xCO2 = 0.9213. This working condition is represented by a triangle in figure 36. Since this point is above the equilibrium points, it can be seen that at this condition the mixture of $scCO_2$ and liquid ethanol is only a one phase system inside the vessel.

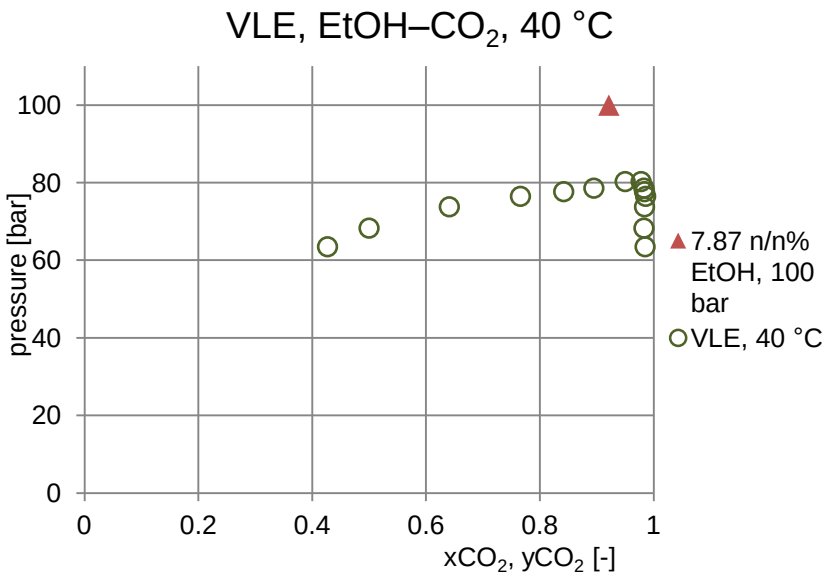

Figure 36: vapor liquid equilibria of $scCO_2$–ethanol system

From the preliminary experiments it was obvious that applying ethanol as a cosolvent, crystallization takes place within considerably lower sorption time. Although in the DR1 dyeing experiments a completely transparent sample was produced at 200 bar and 50°C after 3 hours of impregnation, the here obtained sample turned to opaque already after 2 hours at these conditions (see figure 39). The dithizone uptake using ethanol at 100 bar and 40°C as a function of time is plotted in figure 37 (st. dev.: 0.00845 [mg/g]). Not unexpected, that just as in the case of the dyeing experiments, uptake increases with time since more DIT can be accumulated as sorption proceeds. This increase seems to be linear, which can indicate that the points measured here are on the initial part of a diffusion curve, just like in case of the DR13 experiments at 200 and 300 bar (figure 31).

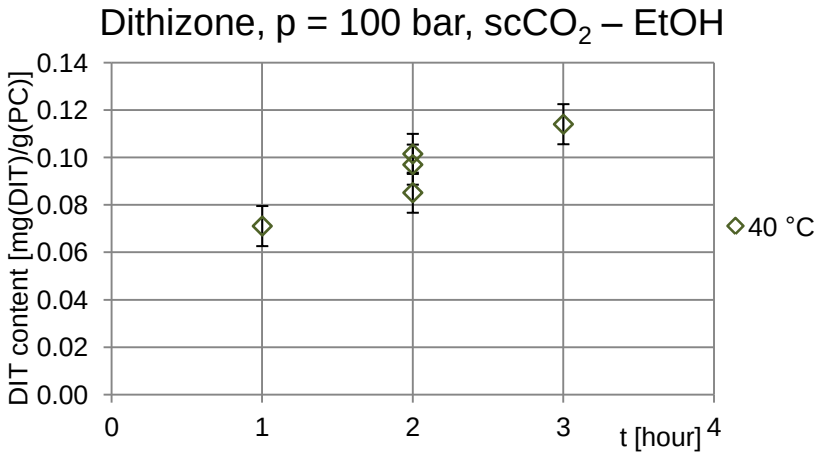

Figure 37: Effect of impregnation time on dithizone uptake at 100 bar and 40°C in scCO2–ethanol mixture

The pressure and the temperature effect on the impregnation was investigated at two hours of sorption time and is shown in figure 38.

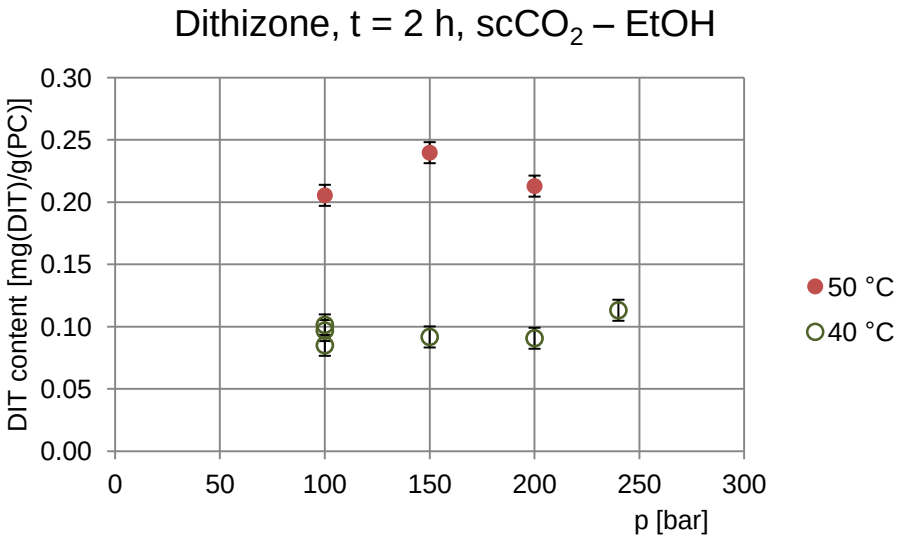

Figure 38: Effect of sorption temperature on dithizone uptake versus pressure

An experiment at 240 bar at 40°C yielded partly opaque samples. At 40°C pressure does not seem to have an effect on the impregnation. By changing the pressure, CO_2 density changes but apparently it does not result neither in an enhanced diffusivity nor in an increased solubility of dithizone in the $scCO_2$–ethanol mixture. The swelling of the polymer indeed enhances by pressure within this range (see table 6). However, just as in case of dyeing experiments, impregnation efficiency is not influenced by this increment in swelling. Experiments at 50°C yielded higher DIT uptake, which can be either due to the increased solubility of DIT in the mixture or the higher diffusivity. These effects were found to be important in the dyeing experiments as well. Moreover, elevated temperature results in higher chain mobility whereas the interchain distance can also be increased. All these factors are facilitating the impregnation process. Therefore, from 100 bar to 150 bar at 50°C there is a slight increase in uptake. It is possible, that at these conditions the T_g of the polymer is exceeded, which would mean an enhanced mass transport in the rubbery polymer phase and thus more dithizone content in the polymer. From 150 bar to 200 bar at 50°C uptake clearly decreases, however polymer's T_g should also be exceeded here. It can be assumed however, that this elevated pressure of 200 bar promotes crystallization phenomenon. Since in crystalline regions the mass transport is less favored than in glassy or in rubbery phase, the diffusion of the dithizone within the polymer matrix can be hindered, resulting in a slightly lower uptake. It should be noted however, that the differences between samples measured at

50°C are rather small and their standard deviation can be remarkably higher at 50°C than at 40°C.This can also be an explanation why sample obtained at 150 bar has higher dithizone content than the other two produced at 100 and at 200 bar. Impregnation was tried to be carried out also at atmospheric conditions. For this experiment the PC pellets were soaked in an ethanol solution of dithizone without using any CO_2. After several hours samples turned slightly green but this color effect disappeared when putting the PC samples again in clean ethanol. On the contrary, samples which were impregnated in $scCO_2$ or in $scCO_2$–ethanol mixture did not change the color after being soaked again in ethanol for 24 hours. Table 8 and 9 show tabulated data for dithizone uptake at various conditions while figure 39 shows the impregnated pellets.

Table 8: Dithizone uptake at various conditions by using ethanol as a cosolvent

T (°C)	p (bar)	Dithizone uptake (mg/g)		
		2 hours	3 hours	4 hours
40	100	**0.0945±0.00845**	0.1140	
40	150	0.0918/0.1100		0.1785
40	200	0.0908		
40	240	0.1133		
40	250	0.1179		
50	100	0.2056		
50	150	0.2398		

Table 9: Dithizone uptake at various conditions achieved by impregnation in pure $scCO_2$

T (°C)	p (bar)	Dithizone uptake (mg/g)		
		1.5 hours	3 hours	6 hours
40	100			0.00026
40	200	0.00015	0.00127	0.00270
50	100		0.00021	
50	200		0.00925	

Although impregnation proceeds also by using only $scCO_2$, in figure 39 it can be observed how strongly ethanol influences the sorption effect. From table 9 it can be seen that impregnation carried out in $scCO_2$ without ethanol at 100 bar produced very poor uptake even after 6 hours. This is not unexpected since dithizone solubility turned out to be negligible at these conditions. Therefore, when *not* using ethanol for the experiments, measurements were carried out at 200 bar in the range of 1.5 – 24 hours of sorption time. Since saturation has been achieved, from these experiments K_c was determined to be 10.8 and 12.2 (depending on which solubility data are taken for the calculation). Dithizone uptake versus impregnation time at 200 bar (without applying cosolvent) is shown in figure 40.

Figure 39: Dithizone impregnated PC at various conditions

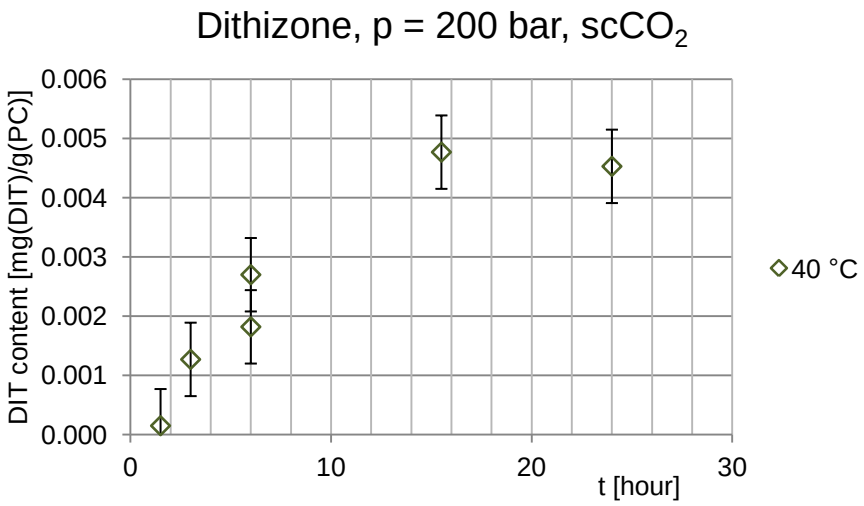

Figure 40: Effect of sorption time on dithizone uptake in $scCO_2$ at 200 bar and 40°C

In figure 40 it can be observed, that uptake increases with time and shows a typical sorption curve. In this case 15 hours proved to be enough to reach saturation within the polymer phase, therefore sorption diffusivity of the dithizone can be calculated by applying the same method which was used by Tang *et al.* and Sun *et al.* [56,57]. In this method, Fickian diffusion is assumed and the calculation is based on eq. (3) in chapter I. By plotting the sorption amount data $ln(1-M_s/M_\infty)$ collected before saturation against t_s/l^2 and applying a linear regression (figure 41), the slope of the linear plot gives the diffusion coefficient at given pressure and temperature conditions.

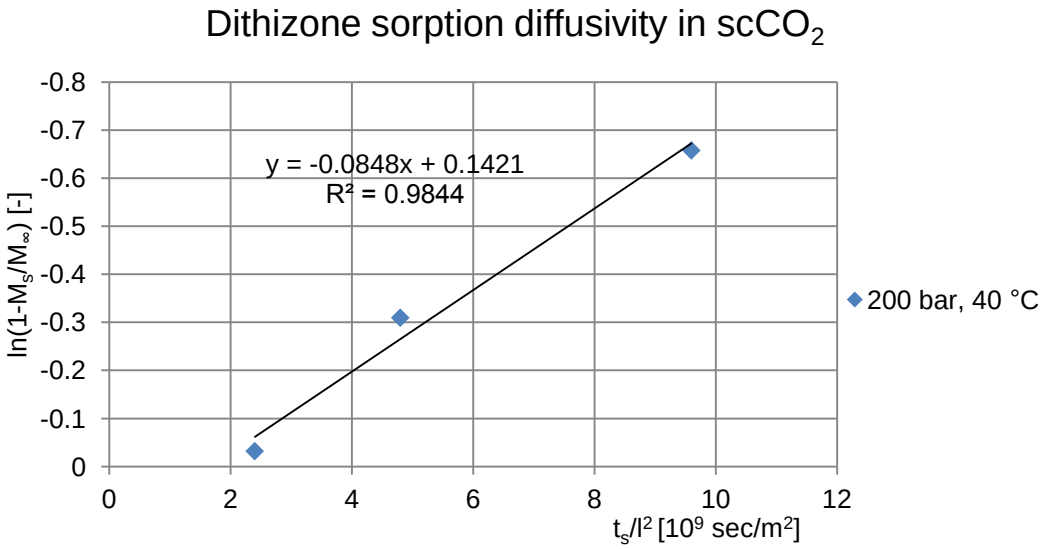

Figure 41: Plot of $ln(1-M_s/M_\infty)$ against t_s/l^2 based on experimental data at 200 bar, 40°C

By this, diffusivity of dithizone in PC matrix at 200 bar and 40°C was determined to be ~8.5×10^{-11} m^2/s. Tang [56] determined 1.22×10^{-11} m^2/s as a diffusion coefficient of $scCO_2$ in PC matrix at these conditions. CO_2 is a really small molecule and is expected to have better diffusivity than dithizone in the same PC matrix. Nevertheless experimental data show different results. This difference can arise from the sort of PC matrices used in this and in Tang's work. Due to the relatively low M_w of our PC, diffusion can be significantly higher. The second reason for the deviation is, that the D calculated here highly depends upon the geometrical size of the impregnated material. PC pellets used in this work have rather different diameter and for this calculation a rough estimation of an average diameter $l = 1.5$ mm was used. As a comparison, taking $l = 1.0$ mm as an average diameter for one pellet, D would result in a value of ~3.8×10^{-11} m^2/s. It has to be noted though, that the relatively high D is not unexpected since in this case the saturation of the polymer phase with dithizone has been reached relatively fast compared to other additives. For instance Schnitzler [47] reported up to 72 hours saturation times for some dye additives, while West [74] told about values as high as ~90 hours to reach maximal dye uptake into a polymer. Table 10 summarizes constants and solubility data.

Table 10: Summary of solubility, partitioning coefficient (K_c) and diffusivity (D) obtained upon dithizone impregnation of PC

T (°C)	p (bar)	dithizone solubility ($\times10^{-8}$ mol/mol)		K_c (-)		D ($\times10^{-11}$ m^2/sec)	
40	200	sample *a)*	8.44	sample *a)*	12.2	l = 1.5 mm	8.5
40	200	sample *b)*	9.56	sample *b)*	10.8	l = 1.0 mm	3.8

2.3 Analytical studies

In order to characterize the produced DPC pellets, some analytical measurements were performed in cooperation with UMB in Maribor, Slovenia. A sample which was produced as a preliminary experiment at 150 bar and 40°C for 4 hours of sorption time using ethanol as cosolvent was measured by TG and IR. This sample had a dithizone content of 0.1785 mg/g and the TG graph is shown in figure 42. Measurement was carried out from 30 to 300°C with a heating rate of 10°C/min.

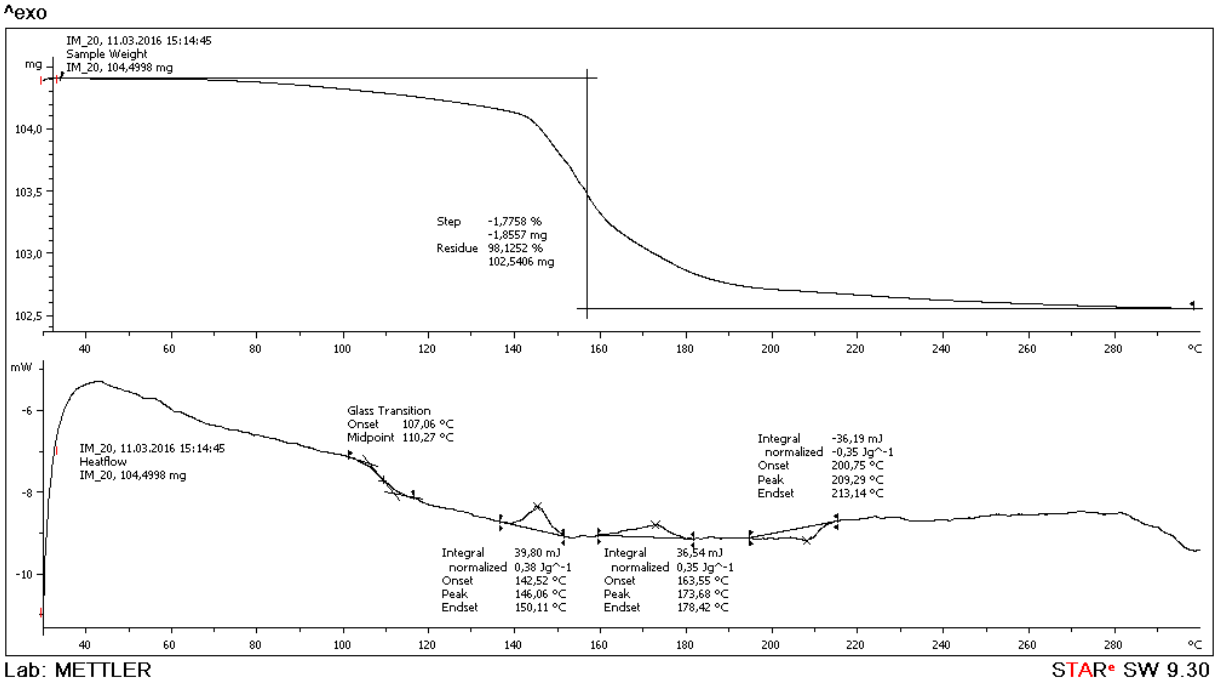

Figure 42: Thermogravimetric curve of DPC produced in scCO$_2$–ethanol mixture

The measurement showed 1.78 % mass loss. This is more than the amount of dithizone impregnated inside the polymer. This indicates that still some ethanol is present in the polymer, most probably entrapped in small clusters upon depressurization of the system after sorption. The two exothermal peaks of the DTA curve with onsets of ~142°C and ~163°C can indicate the burning of the ethanol upon leaving the pellets. It can also be observed, that the original T_g of PC decreased and shifted to temperatures as low as ~110°C after impregnation. It means that the original T_g could not be regained after sorption which can be due to the residual ethanol content of the sample.

IR measurements were performed by using a device with ATR extension and the spectra are shown in figure 43 and 44. Combining the spectra of raw and impregnated PC samples neither

new peak nor remarkable shifts can be observed. This indicates no formation of a new chemical bonding, thus there is no chemical reaction between the dithizone and PC occurred, independent which media (pure $scCO_2$ or $scCO_2$–ethanol mixture) was used for sorption. Therefore, only strong sorption of the dithizone took place within the polymer phase upon impregnation in $scCO_2$ and in $scCO_2$–ethanol mixture.

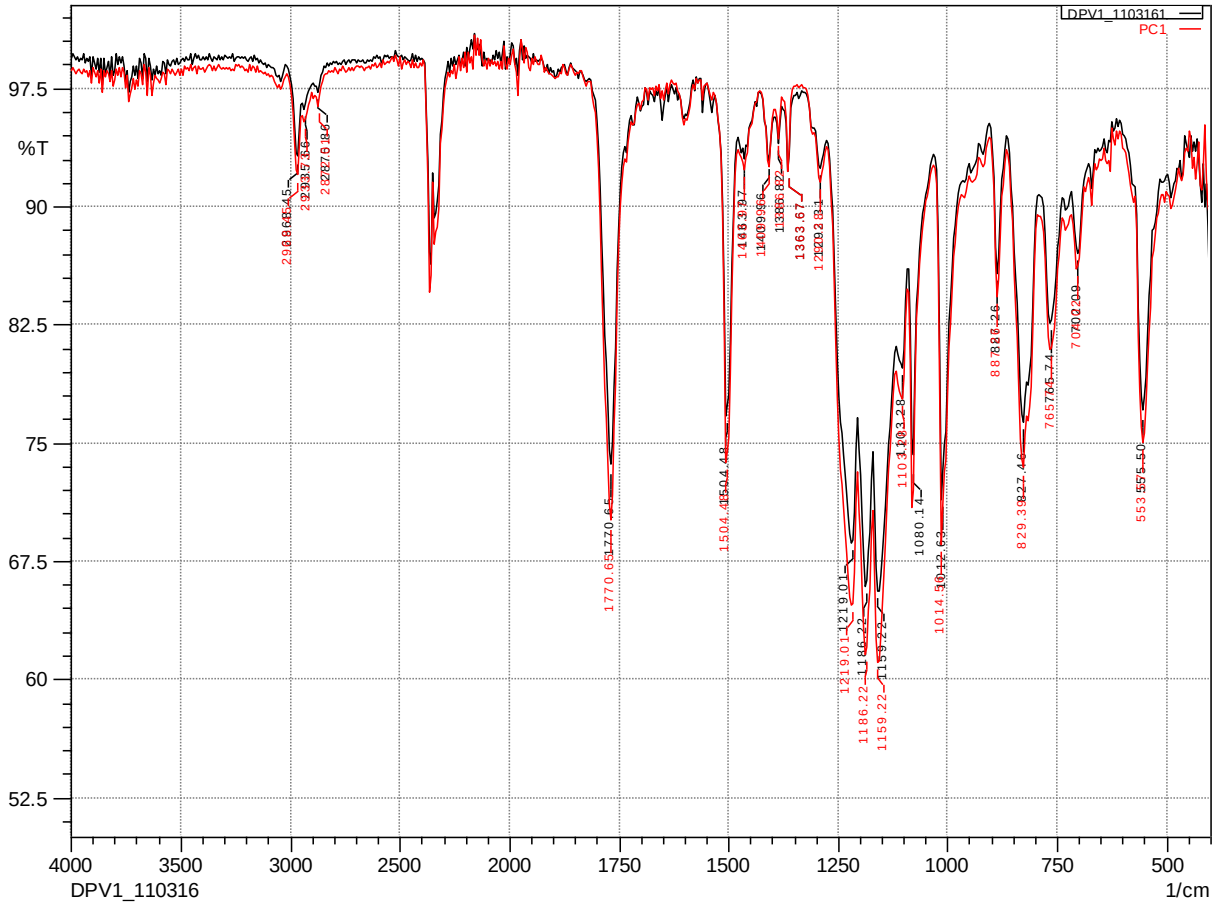

Figure 43: IR spectrum of untreated PC (red) combined with the spectrum of PC impregnated with dithizone (black) in $scCO_2$ at 200 bar, 40°C and 3 hours

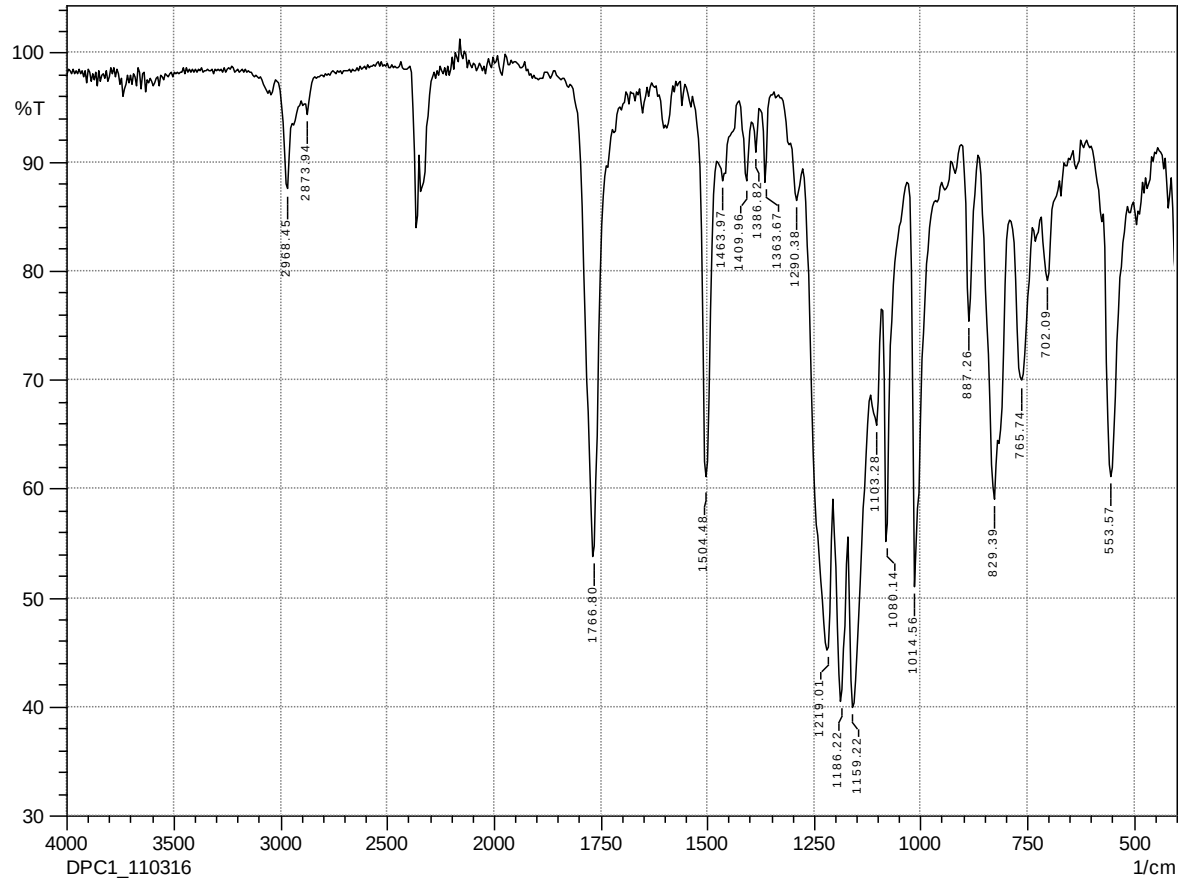

Figure 44: IR spectrum of PC impregnated with DIT in $scCO_2$–ethanol mixture at 150 bar 40°C and 4 hours

3. Polycarbonate modification with metal nanoparticles in $scCO_2$

Although PC is an important technical plastic, no reference could be found in literature for copper nanoparticle impregnation of PC matrix in supercritical media. Therefore, this chapter deals with investigations towards this direction by considering different ways for the modification.

3.1 Nanoparticle impregnation using DPC

First, the possibility of using DPC for copper capture within the polymer phase was taken into account, see figure 45.

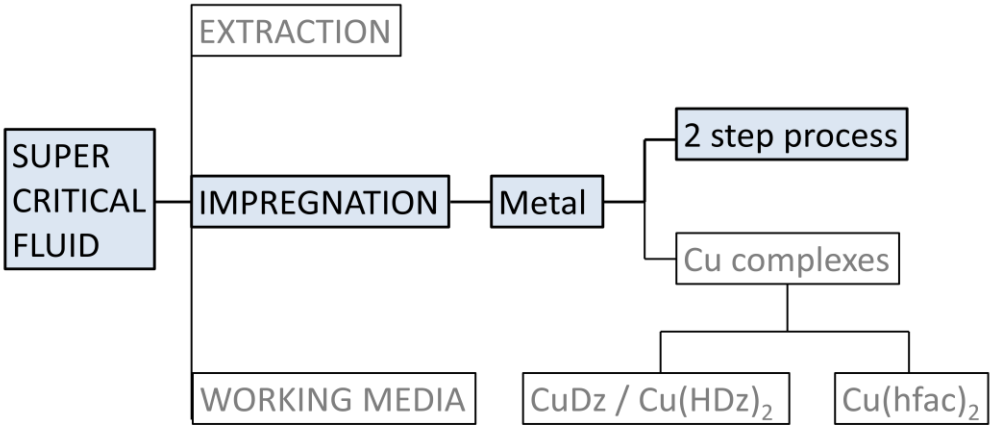

Figure 45: Application of $scCO_2$ for metal modification of PC by a two step process

3.1.1 Experiments with copper

Besides extraction of heavy metals from aqueous solution which can be carried out by chelating them by the use of dithizone [78], other studies reported that dithizone impregnated SG [76,77] or PVC [93] membranes can be used for heavy metal detection. Based on this, the goal was to investigate the applicability of the synthesized DPC pellets for heavy metal capture and by this creating nanoparticle modified plastic pellets. In this approach, DPC was taken as a matrix and a solution containing metal ions acted as impregnation material. Metal ions were obtained from copper nitrate trihydrate ($Cu(NO_3)_2 \bullet 3H_2O$) which was dissolved either in 10.0 ml ethanol or in 10.0 ml water. The pH of the aqueous solution was varied by adding small amounts (mostly 1.0 ml) of c = 0.1 mol/dm^3 KOH or HNO_3. Without the addition of KOH or HNO_3, the pH of the water was acidic (pH ~ 3) [94] in the impregnation vessel due to the formation of H_2CO_3 as water reacts with $scCO_2$. From the preliminary

experiments it was learned, that a successful impregnation could be carried out by using ethanol and water with KOH, whereas impregnation could not be realized in water without KOH addition or with HNO_3. Table 11 shows results from preliminary experiments measured by ICP-OES at the Institute of Analytical Chemistry and Food Chemistry. Results are presented in ppm units, that is, mg_{copper}/kg_{PC}. The raw, untreated PC pellet had a copper content of 0.07±0.01 ppm, determined by ICP-MS.

Table 11: DPC impregnation with solutions containing Cu^{2+}, preliminary results

sample ID	p (bar)	T (°C)	dithizone content of DPC (mg/g)	cosolvent	copper load (ppm)
IM_14_1	100	40	(no data)	EtOH	45±2
IM_21	100	40	0.1785	EtOH	10.9±0.3
IM_14_2	100	40	(no data)	water + KOH	109±2
IM_20	100	40	0.1785	water + KOH	90±3
IM_37	100	40	0.0970	water	< LOQ[a)]
IM_40	100	40	0.0033	water	< LOQ[a)]
IS_1	100	40	0.0033	water + HNO_3	< LOQ[a)]

a) Limit of Quantification, LOQ = 4 ppm (mg/kg) for ICP-OES

After these preliminary experiments, several impregnation were performed wherein the influence of mixing the impregnation solution by the gear pump, amount of dithizone in DPC, spare parts arrangement within the impregnation vessel, sorption pressure and temperature were investigated. Unfortunately, presumably due to the insufficient mixing inside the vessel, copper load obtained in different experiments had a really high standard deviation. Thus, in spite of impregnation was successful, reproducibility has turned out to be insufficient. For example, a measurement at 100 bar and 40°C using DPC with 0.0643 mg/g dithizone load carried out in water + KOH cosolvent was triplicate. The first sorption yielded 39±4 ppm copper load, while repeating the experiment using the very same conditions gave 85±34 ppm. In the third repetition, solution was not circulated by the gear pump and this time copper load was below LOQ (4 ppm). The poor mixing performance arises from the fact, that water has a really low solubility in $scCO_2$ (4.28×10^{-3} mol/mol at 101.3 bar and 40°C, determined by [95]). Therefore there are two distinct phases present in the vessel during impregnation. In this case, it is really hard to obtain uniform mass transfer for all the experiments.

In order to characterize the impregnated samples, some pellets were investigated by SEM. See figure 46 and 47 for sample IM_14_2 with 109±3 ppm copper load. Before the investigation, samples were cut and the surface was modified by carbon deposition in vacuum in order to obtain a conductive plane, thus taking SEM pictures and EDX measurements were possible.

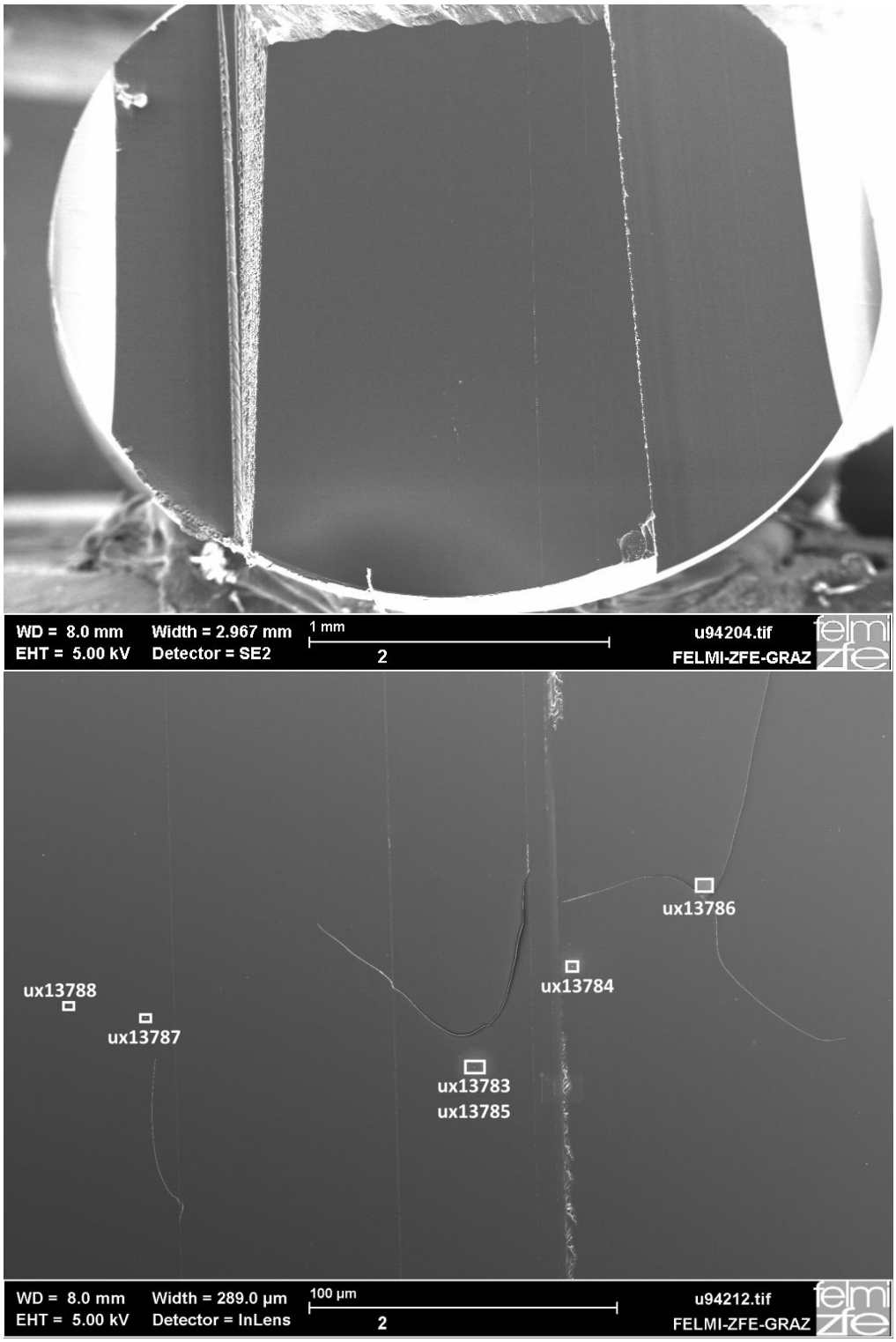

Figure 46: Cross section of IM_14_2 pellet (upper picture) and particles observed within the polymer matrix (picture below)

In figure 46 it can be observed that copper particles were evenly distributed inside the polymer matrix. At higher magnification it can be seen, that those pieces are bigger clusters in the nanometer range (up to approx. 400 nm) surrounded by smaller particles.

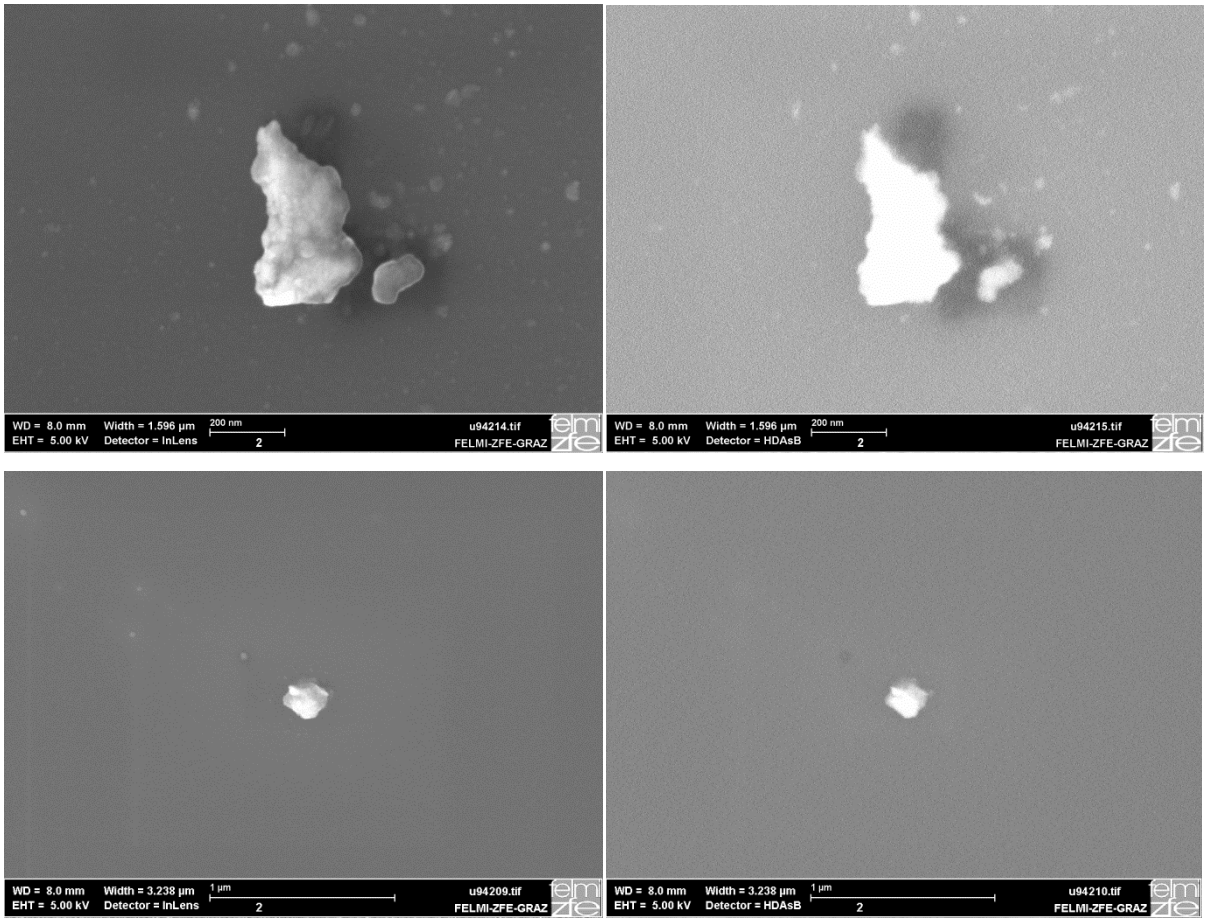

Figure 47: Copper nanoparticles in DPC matrix, sample: IM_14_2

In figure 47 single particles can be observed. On the left side pictures were made by using secondary electron ("in lens") detector, while particles on the right side were detected by applying the backscattered (BsE) detector. The latter one gives information for material contrast because metal particles appear with bright contrast in the matrix. Some of those metallic particles (marked with *ux13783–ux13788* in figure 46) were measured by EDX detector, which provided evidence for copper. EDX spectrum for particle *ux13783* is shown in figure 48.

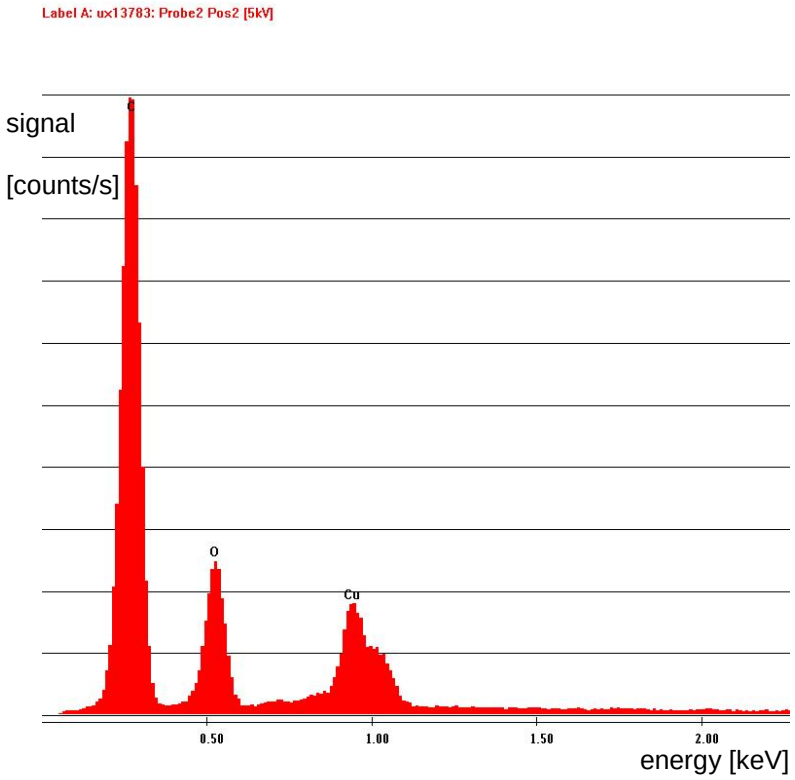

Figure 48: EDX spectrum for ux13783 particle

From the EDX spectrum (see fig. 48) it can be observed, that besides the polymer matrix which contains C and O, Cu is well present, and thus the presence of copper within the polymer is proved. Since this measurement does not provide information on the oxidation state of the metal, for the same sample an XPS analysis was performed. However, copper was detected also in the XPS measurements, the oxidation state of the metal could not be determined because of the weak signal obtained. This can be due to the small measurement depth (1.5 nm – 5.0 nm) which was used during the investigation. As it was shown above, copper presents in larger agglomerates sized from 5 to 400 nm and it is probable, that the local copper load at the measured point at this deepness was not enough to obtain strong signal. XPS spectrum is shown in figure 49, while figure 50 shows an enlarged part of the spectrum where copper was detected. From this measurement, an oxidation state of Cu^{2+} would be the most probable – however, it has to be stressed, that one should not draw comprehensive conclusions from this rather weak signal, which slightly differs from the noise of the spectrum.

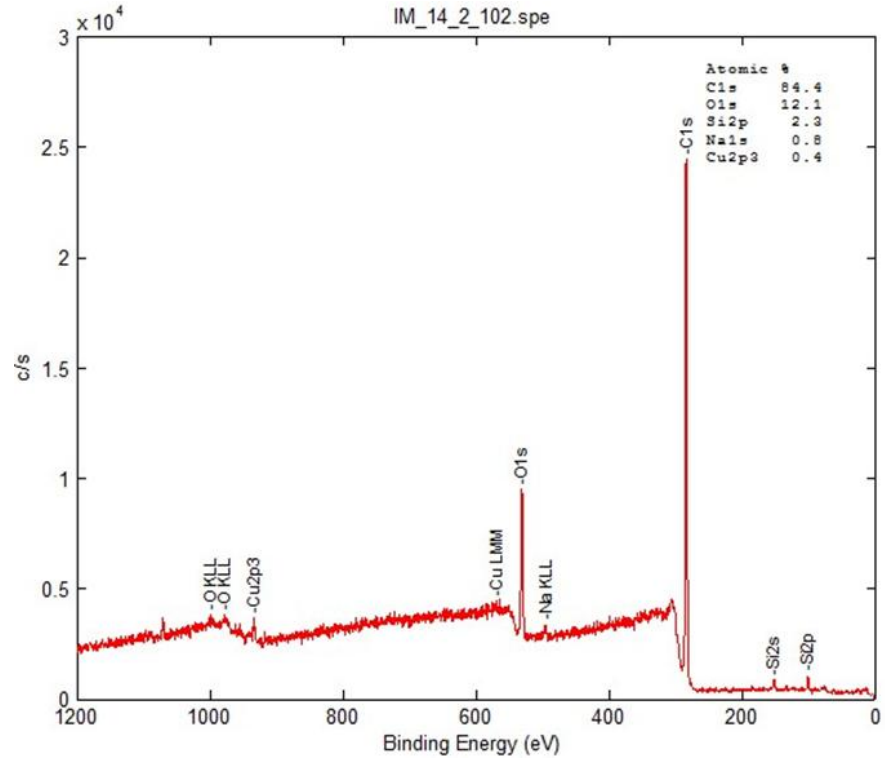

Figure 49: XPS spectrum of IM_14_2

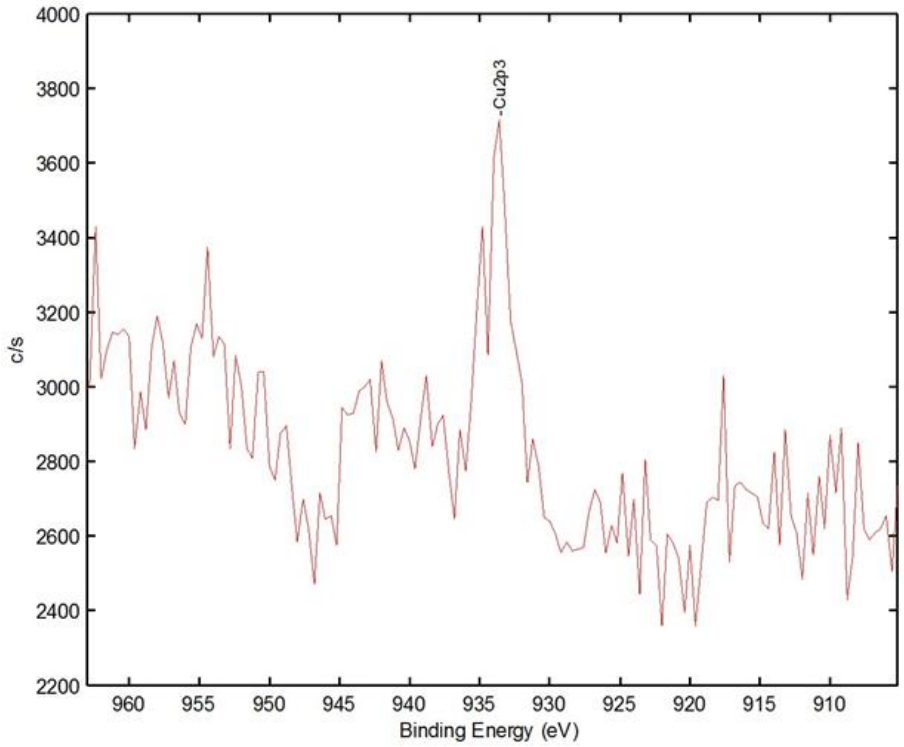

Figure 50: Enlarged XPS spectrum of sample IM_14_2 with the copper signal

As a conclusion, DPC was successfully used in order to modify PC by nanoparticles. It has to be noted however, that the standard deviation was really high and therefore detailed investigation with this process could not be carried out. For the same reason, it is also hard to

give a detailed explanation, how does impregnation in this case exactly proceeds. It is known, that dithizone has a capability of reacting to copper ions which can also take place within a SG membrane [77]. In that study, authors suggested that the adsorption of copper could be attributed to the formation of penta-heterocycles chelating complex between Cu^{2+} and the nitrogen and sulfur atoms of the dithizone. Authors made this assumption based on results obtained by IR spectroscopy; bending vibration for –N–H groups and stretching vibration for –N=N– group were shifted after dithizone modified SG membranes adsorbed copper ions. This means, that one dithizone molecule adsorbs one copper, thus the formation of bigger clusters in our experiments cannot be explained. Further on, a sample with a copper content of 90±3 ppm was analyzed by IR spectroscopy and no shifts from the original peaks of the DPC was observed. Therefore, it is not probable that a chelation within the polymer matrix occurred, or at least not with remarkable efficiency.

Impregnation was only successful when KOH was added to the aqueous solution, while adding HNO_3 or applying pure water provided copper load non detectable by ICP-OES. The pH of the aqueous solution mixed with the $scCO_2$ is around 3.2 at 100 bar and around 40°C [94]. Yu and coworkers [77] reported that dithizone in SG has the best copper chelating capacity around pH 4–6. However, varying the amount of KOH in our system did not cause remarkable changes in copper uptake. Therefore, it is suggested that KOH does not influence the impregnation via the pH value. The effect of the KOH can be explained though by another theory. It is known, that OH^- ions form copper hydroxide precipitate ($Cu(OH)_2$) when reacting to copper ions in a given solution (see eq. 9).

$$Cu^{2+} + 2OH^- \rightleftharpoons Cu(OH)_2 \quad (9)$$

$$CO_2 + H_2O \rightharpoonup H_2CO_3 \rightleftharpoons H^+ + HCO_3^- \quad (10)$$

This precipitate has a very low solubility in water and was formed under atmospheric conditions when preparing the aqueous impregnation solution. The pH of this solution decreases within the vessel due to the CO_2-water interaction and H_2CO_3 formation (which dissociates readily to H^+ and HCO_3^- see eq. 10). It is assumed that the equilibrium in equation 9 is influenced by this pH change, thus the solubility of $Cu(OH)_2$ increases. This is the role of the aqueous phase inside the vessel.

Another important factor is the polymer-$scCO_2$ interaction. According to Perman *et al.* [96], it is possible for the impregnation solute to penetrate inside the CO_2-swollen polymer matrix even if the applied solution is completely immiscible with $scCO_2$. Therefore, PC pellets being

simultaneously contacted with both the $scCO_2$ and with the aqueous phase containing copper ions, can partially adsorb from this solution; not only on the surface but also within the matrix. During decompression, CO_2 leaves the aqueous phase and desorbs from polymer matrix, thus pH increases again which brings $Cu(OH)_2$ to precipitate again; this time entrapped in the polymer phase. This theory explains the effect of KOH and the bigger clusters which were seen by SEM. However, should this be the driving force for the impregnation, than the role of the dithizone is not very clear. It is assumed, that dithizone helps the transportation or migration of the copper ions within the PC.

3.1.2 Experiments with zinc

In order to study the applicability for another metals, modification of DPC was tried to be carry out be applying zinc nitrate hexahydrate ($Zn(NO_3)_2 \cdot 6H_2O$) as an impregnation solution. Zinc was chosen as it has already been used in dithizone modified PVC membranes [93]. Just as in the case of copper impregnation, experiment was not successful by dissolving zinc nitrate only in water. However, when 1.0 ml c = 0.1 mol/dm^3 KOH was added to the aqueous solution, 21±3 ppm zinc load in PC matrix was achieved at 100 bar, 40°C and after 2 hours of sorption time. Therefore it is suggested, that DPC matrix can be modified with several other metals by using the method presented above.

3.2 Nanoparticle impregnation of PC using copper complexes

3.2.1 Primary copper (II)- and secondary copper (II) dithizonate

Since dithizone was proved to be readily soluble in $scCO_2$, it is suggested that metal dithizonates can also be used for the impregnation since the stability of the anion can determine the solubility of the complex. This assumption was investigated by synthesizing two copper dithizonate complexes; the primary ($Cu(HDz)_2$) and the secondary (CuDz) copper (II) dithizonate. The chemical structures of these molecules are shown in figure 51.

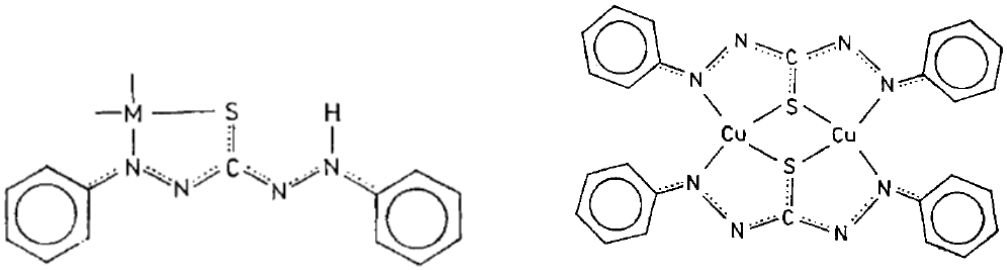

Figure 51: Chemical structure of $Cu(HDz)_2$ (left) and CuDz (right) [97]

Although the structure of CuDz was heavily discussed [85], Röbisch *et al.* [97] suggest that CuDz occurs in dimer form; therefore "Cu_2Dz_2" should be written to denote the structure. However, since the form of "CuDz" for secondary copper (II) dithizonate is consistently used in numerous publications, this abbreviation was adopted also in this work. The synthesized materials were characterized by UV-Vis spectroscopy. The absorbance maximum (measured in chloroform) for the CuDz was determined to be at $\lambda_{(max)}$ = 444 for concentrations within a broad absorbance range between A = 0.111 and 1.121. This correlates well with literature data of $\lambda_{(max)}$ = 445–450 nm given by [85]. For $Cu(HDz)_2$, $\lambda_{(max)}$ = 544 was measured which also matches literature's value ($\lambda_{(max)}$ = 545 by [85]). However, it has to be noted, that at higher absorbance values than A = 0.260 for $Cu(HDz)_2$, a peak at 445 nm also appears, which can be accounted for CuDz. It is known, that $Cu(HDz)_2$ transforms into CuDz in the presence of copper ions. $Cu(HDz)_2$ was synthesized by using $CuSO_4$ as a copper ion source and it is probable that its conversion to the complex was not complete. Thus the synthesized $Cu(HDz)_2$ could have some copper contamination, which at higher concentrations forms CuDz as suggested by [85] and thus yields a peak at 445 nm. In order to further characterize this material, $Cu(HDz)_2$ was measured by thermogravimetry, wherein enthalpy signal has also been recorded. Measurement result is shown in figure 52.

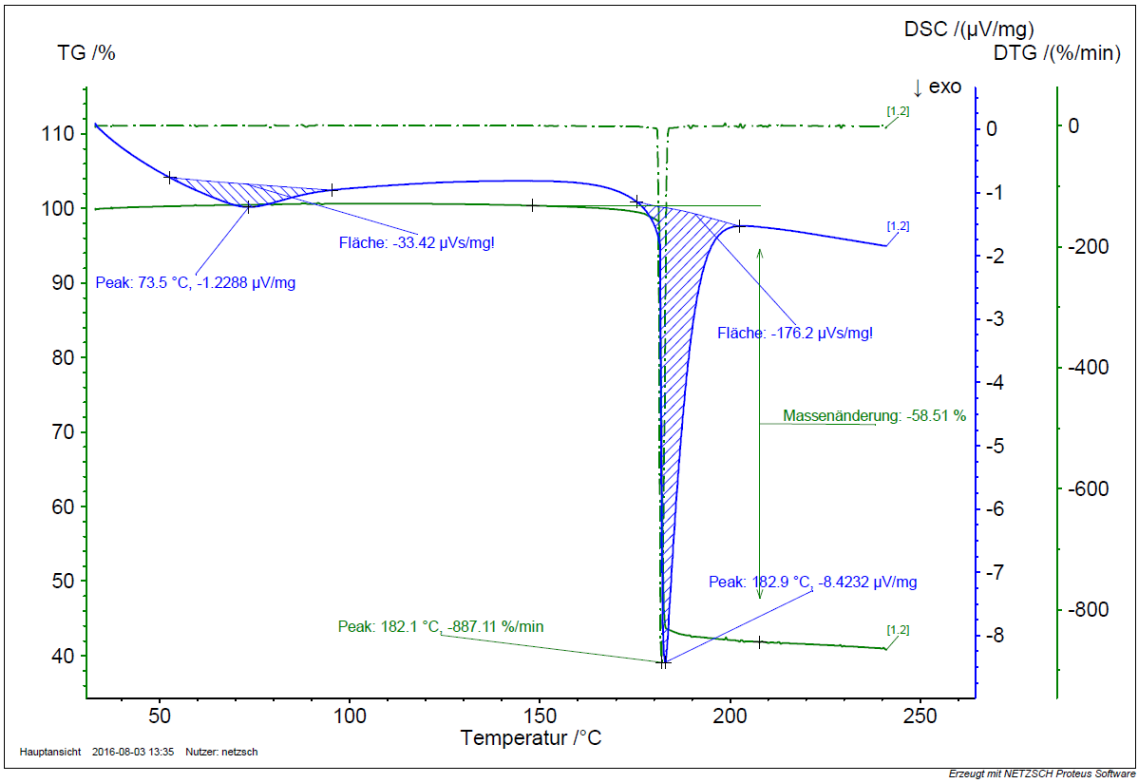

Figure 52: Mass change and DTA curve of $Cu(HDz)_2$

From the sudden mass change measured by thermogravimetric analysis it can be concluded, that the complex decomposes at 182°C without a melting point. Literature data [97] mention 174–176°C which not exactly matches our data, but it is not clear if this temperature is melting or decomposition temperature, hence the method used for the measurement is also unknown. The first peak of the blue DTA curve with a maximum of 73.5°C can indicate the leave of some chloroform contamination from the sample.

However, accurate solubility measurements were not performed, but according to high pressure view cell observations, $Cu(HDz)_2$ was soluble in $scCO_2$. The solubility of the complex makes it possible to exclude organic solvents from the process, therefore some experiments were carried out by not using any cosolvent. CuDz was also placed in the view cell to test the solubility, but a clear dissolution was not observed. CuDz and $Cu(HDz)_2$ are pretty well dissolve in DCM or in chloroform, but since these solvents also dissolve PC, they cannot be used as a cosolvent for the experimentation. As a comparison to sorptions performed only in $scCO_2$ media, some impregnations were carried out in $scCO_2$–ethanol mixture. Since the solubility of both complexes in ethanol was turned out to be poor, their dissolution was enhanced by using ultrasound. Table 12 contains impregnation data obtained by these in-lab synthesized complexes. Although the actual solubility of the complexes is

unknown, relatively high amounts were used (~ 0.015 g per experiment) in order to surely obtain a saturated phase inside the vessel.

Table 12: Results obtained by $Cu(HDz)_2$ and CuDz copper complexes

T (°C)	p (bar)	impr. time (hours)	complex	media	sonication (min)	copper load (ppm)*
40	200	2	CuDz	$scCO_2$	-	0.33±0.09[a)]
40	150	3	CuDz	$scCO_2$-ethanol	3	1.2±0.1[a)]
40	150	3	CuDz	$scCO_2$-ethanol	8	1.8±0.1[a)]
40	150	3	$Cu(HDz)_2$	$scCO_2$	-	0.7±0.2[a)]
40	150	3	$Cu(HDz)_2$	$scCO_2$-ethanol	6	5±1[b)]

*blind PC sample: 0.07±0.01 ppm
a) measured by ICP-MS
b) measured by ICP-OES

Sample impregnated by using CuDz and only $scCO_2$ as impregnation media showed almost no change in color and the copper content of 0.33 ppm with a relatively high standard deviation is almost negligible. However, because impregnation was possible, it has to be noted that CuDz has to have at least a very slight solubility in $scCO_2$. When using ethanol as cosolvent, remarkably higher results were achieved and hence the sample color has changed slightly to brown, significantly darker compared to raw PC pellets. Apparently, the usage of ultrasound also has an influence. Higher sonication time yielded in remarkably higher results. This is not unexpected since ultrasound helps small particles to be better dispersed in a given solvent, thus more Cu^{2+} is present in the impregnation solution causing higher copper uptake. From all the experiments, $Cu(HDz)_2$ provided the best result of ~ 5 ppm. This light brown sample is shown in figure 53. In this experiment, a gear pump was used to obtain mixing. All the other experiments were carried out without gear pump.

Figure 53: PC pellet impregnated by using $Cu(HDz)_2$ in $scCO_2$-ethanol mixture

As a conclusion, impregnation was possible by complexes synthesized in-lab, hence the assumption that they should be soluble in $scCO_2$ based on their anion (i. e, the dithizone) solubility, proved to be correct. Nevertheless, the copper uptake achieved up to ~ 5 ppm is indeed remarkably lower than results obtained by impregnation method using DPC and the solution of copper ions, it must not be neglected. Very recently, Mölders *et al.* coated PC strips with silver by using $AgNO_3$ for the impregnation carried out in $scCO_2$. Although samples had a very different silver content depending on the conditions were used, authors measured noteworthy antibacterial activity on PC samples having silver content as low as 2.3 ppm [98]. Since dithizone forms complexes with numerous metals, it is suggested that these chelates have a really high potential in metal modification of polymers.

3.2.2 Copper(hexafluoroacetylacetonate)-hydrate

In order to compare the impregnation results obtained by using copper (II) dithizonate complexes, copperhexafluoroacetylacetonate-hydrate ($Cu(hfac)_2$), a commercially available copper complex was used. $Cu(hfac)_2$ has already been used in some studies for copper deposition wherein it was reported to be a suitable material for copper modification of materials in $scCO_2$ [99,100,101]. Experimental results are shown in table 13. Experiments were carried out by circulating the content of the vessel by the gear pump and applying $Cu(hfac)_2$ in excess (three times as much as its maximum solubility at the given sorption conditions).

Table 13: Experimental results obtained by $Cu(hfac)_2$

T (°C)	p (bar)	impr. time (hours)	media	copper load (ppm)*
40	300	3	$scCO_2$	4.6±0.1[a)]
40	200	3	$scCO_2$	5±1[b)]
40	200	2	$scCO_2$-ethanol	0.85±0.03[a)]
40	100	1	$scCO_2$	5.0±0.7[a)]

*blind PC sample: 0.07±0.01 ppm
a) measured by ICP-MS
b) measured by ICP-OES

As it can be seen from table 13, very similar copper uptake compared to that of obtained by the use of copper (II) dithizonate complexes were achieved. Interestingly, performing the experiments only in $scCO_2$ atmosphere, copper uptake does not seem to change much, although pressure varied between 100–300 bar and for 1 to 3 hours sorption time. According to literature data, this complex has an outstanding solubility in $scCO_2$ [67]. This corresponds to observations made in the high pressure view cell, where very fast dissolution was noticed. It is suggested that due to the relatively high solubility of the $Cu(hfac)_2$ in the $scCO_2$ phase and to the low solubility in the polymer phase, its diffusion into the polymer matrix is not very favored and therefore reaches a maximum value around ~ 5 ppm. Impregnated samples are shown in figure 54.

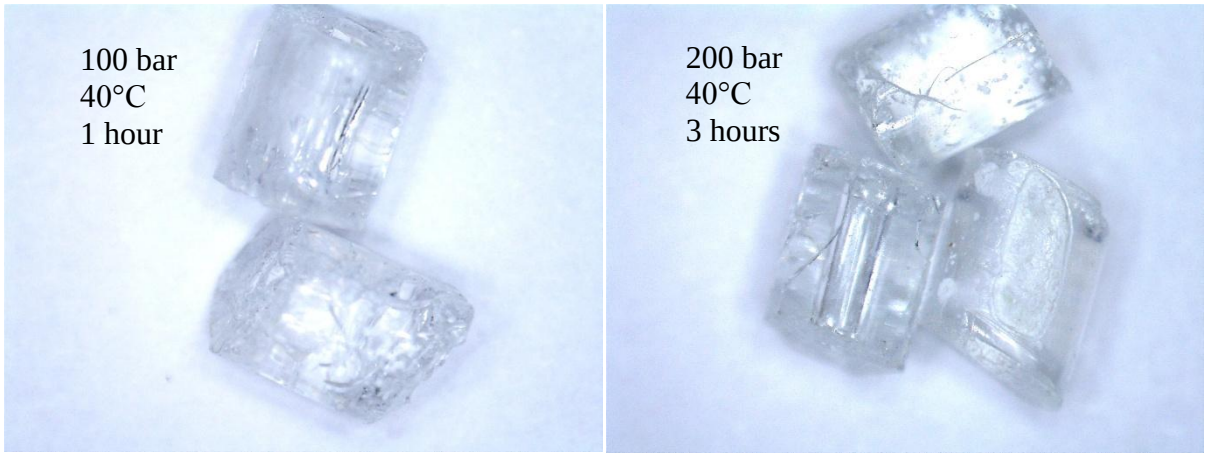

Figure 54: PC pellets impregnated by using $Cu(hfac)_2$ in $scCO_2$ media

Polymer pellets did not change in color, but a white precipitate on their surface was observed after every sorption. It is suggested, that during decompression the solubility of $Cu(hfac)_2$ decreased fast and therefore it precipitated onto the surface of the polymer. The hydrate complex itself is green in color and the anhydrous form is purple [101]. Accordingly, it is

probable that due to the dissolution in $scCO_2$ the material was chemically transformed and this precipitate can be seen on the PC's surface. Using $scCO_2$–ethanol mixture for the sorption resulted in much lower copper uptake. This can be explained by the higher solubility of the complex in this mixture than in the $scCO_2$. Due to this enhanced dissolution in $scCO_2$–ethanol mixture the partition of copper towards the polymer phase is even less favored, which results in a remarkably lower metal load.

4. Feasibility study of PC dyeing in $scCO_2$

Since the dyeing of PC by using dyestuff DR13 in $scCO_2$ provided convincing experimental data, a rough calculation for scaling up was made in order to study the feasibility of the process in an industrial scale. Since at 200 bar and at 50°C good results were achieved only after 3 hours of impregnation time, these conditions were considered to be suitable for an industrial process. Therefore the scaling up was designed at these circumstances and for a yearly production of 5 000 tons dyed PC. The 3 wt% dye to polymer ratio applied during DR13 experimentation was used here. However, the industrial plant was designed to re-use the dye remained in the impregnation vessel after sorption and only the dye taken up by the polymer was refilled after dyeing one charge. Although in the lab scale the vessel was not stirred, in the scaled up process a 0.001 m/s $scCO_2$ flow was considered in order to enhance the mass transfer. This was necessary, since in the lab scale vessel the diffusion path was only one centimeter, but in an industrial plant this can be up to some meter, which extremely influences the dye uptake. Therefore it was essential, to increase the diffusion in the industrial plant. The value of 0.001 m/s was taken from literature because this flow rate has already been used in scaled up dyeing processes and proved to be appropriate [28].

4.1 Scaling up of laboratory dyeing apparatus

As it is known in the chemical industry, in several cases a process cannot be scaled up only by applying the law of geometrical similarity (e.g. the length to the diameter ratio for a cylindrical part (in our case, the impregnation vessel) is to be kept constant) for the devices. Several other parameters (such as flow rate, pressure drop, mass transport, heat transfer, etc.) also have to remain unchanged for bigger devices. Generally, in fluid flow calculations for packed columns, two dimensionless characteristic numbers are considered to have the highest influence on the system; the Reynolds (Re) and the Euler (Eu) number. The Re number is defined as:

$$Re = \frac{dv\rho}{\eta} \tag{11}$$

Where d is the diameter of the vessel, v is the velocity, ρ is the density and η is the viscosity of the applied fluid. The applied velocity of 0.001 m/s yields a really low Reynolds number (virtually at any realistic d for a scaled up system), which is negligible and means a laminar

flow within the vessel. The effect of this laminar flow on the process can be described by the Eu number, which is used to determine the losses in fluid flow calculations and defined as:

$$Eu = \frac{pressure\ force}{inertial\ force} = \frac{\Delta p}{\rho v^2} = \frac{p_u - p_d}{\rho v^2} \tag{12}$$

where ρ is the density of the applied fluid, Δp is the pressure drop which is the difference between the upstream (p_u) and the downstream pressure (p_d). This Δp differs for lab scale and for the industrial scaled equipment, and can be calculated by using the Carman-Kozeny equation by assuming that the impregnation process in a continuously circulated CO_2 flow in a vessel containing PC particles can be treated as a filtration at a constant filtration rate or pressure. The Carman-Kozeny equation is defined as:

$$\frac{\Delta p}{L} = \frac{K V_0 \eta}{\Phi_s^2 D_p^2} \frac{(1-\varepsilon)^2}{\varepsilon^2} \tag{13}$$

where L is the total height of a bed, V_0 is the "empty tower" velocity (without PC charge), η is the viscosity of the fluid, ε is the porosity of the bed, Φ_s is the sphericity of the particles of the packed bed, D_p is the diameter of the equivalent spherical particle and K is an empirical constant [102]. The sphericity is defined as:

$$\Phi_s = \frac{{}^{6}/_{D_p}}{a_v} \tag{14}$$

where a_v is the surface to volume ratio of a particle. By taking 3.3 mm average height and 2.5 mm diameter for a single PC pellet, Φ_s = 1.089. The empirical constant was chosen as K = 150 as it was suggested in the literature [103]. Although, the lab scale high pressure vessel was not stirred, in order to compare the pressure losses to the scaled up system, for this calculation a 0.001 m/s CO_2 flow was assumed as the same was applied in the scaled up system. For porosity, ε = 0.47 was chosen (a value for cylinders with a height to diameter ratio = 1) [104].

Table 13: Parameters for pressure drop calculation by Carman-Kozeny equation

parameter	lab scale	industrial scale	unit
K	150	150	-
ε	0.47	0.47	-
V_0	0.001	0.001	m/s
D_p	0.0025	0.0025	m
Φ_s	1.089	1.089	-
η	6.867×10^{-5}	6.867×10^{-5}	Pa*s
L	0.03	3.0*	m
Δp	**0.5**	**45.3**	**Pa**

*rough preliminary estimation for the calculation

From equation (13) the pressure drop was calculated to be 0.5 Pa for the lab scale and approx. 45 Pa (4.5×10^{-4} bar) for the scaled up system by assuming a reliable, 3.0 meter of total height of bed. These pressures drops are negligible compared to the impregnation pressure of 200 bar. Therefore, the scaling up has been done by using only the law of geometrical similarity.

4.2 Industrial plant operation

Impregnation time of one charge was chosen as 3 hours while the dead time has been chosen as one hour. This time contains the decompression time of 30 minutes and the refill of the vessel. In order to optimize the efficiency and to perform the dyeing in semi-continuous process, it was decided to use 4 impregnation vessels. For achieving the yearly amount, vessels having a 0.5 m diameter with a 4.80 m height are necessary by applying 95 % PC load of one vessel. With the calculated height of 4.80 meter, the pressure drop on the bed calculated by eq. (13) is 72.6 Pa, which is also negligible.

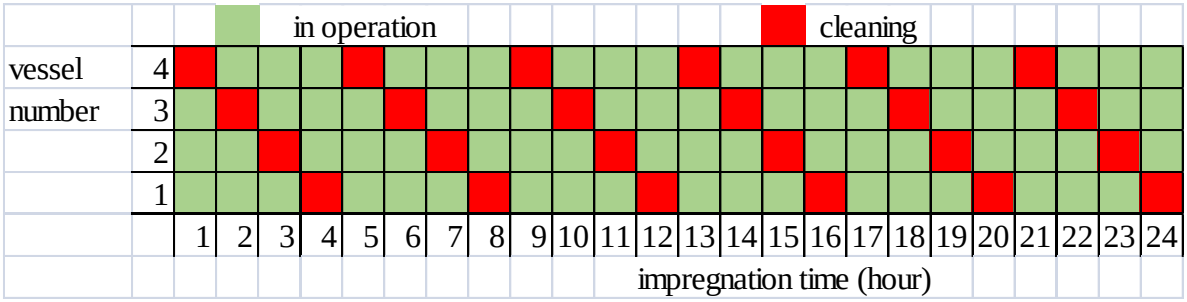

Figure 55: Operation method of the impregnation vessels

The operation method chosen for the four vessels is shown in figure 55 on the Gantt chart, where the operation / cleaning schedule of each vessel can be seen in flow shop mode. CO_2 is supplied from a storage tank where it is stored at 14°C and at 60 bar in liquid phase. It is compressed by a CO_2 liquid pump to 200 bar while temperature rises up to approx. 33°C upon compression. One of the preheated (50°C) vessels containing the dyestuff is filled with CO_2; once the pressure of 200 bar is reached, sorption starts and is performed for 3 hours. During sorption, a gear pump maintains the continuous circulation inside the vessel. After the three hours of impregnation time, the given tempered vessel is decompressed to 60 bar into a separator within 30 minutes by the use of a regulation valve.

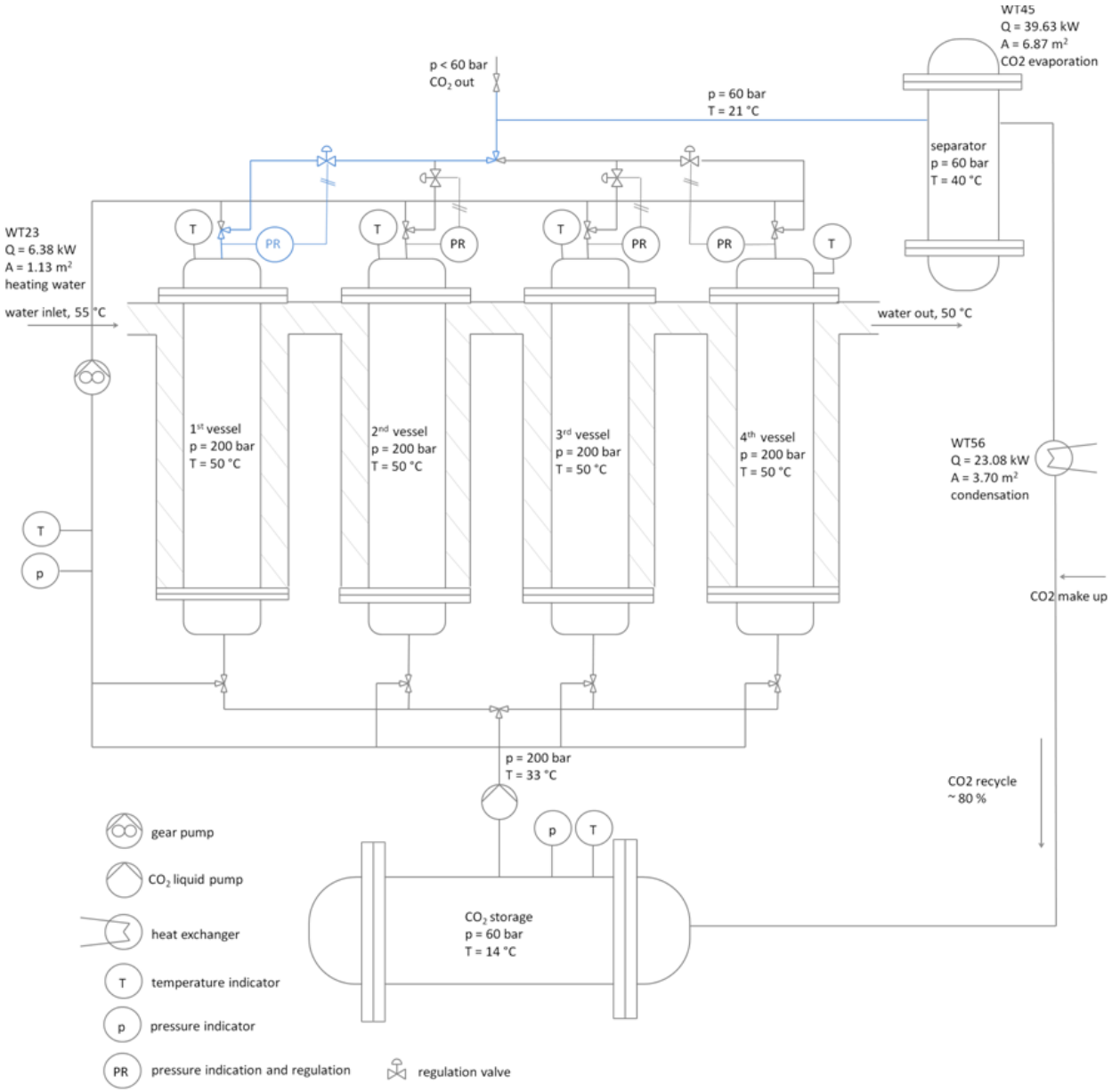

Figure 56: Flow sheet of the scaled up dyeing plant

In the separator, the DR13 content of the CO_2 is removed by heating it up to 40°C. Evaporated CO_2 is than being condensed again by cooling it down to 14°C and recycled into the storage tank. The CO_2 make up refills the circle with fresh CO_2 in order to replace the loss. Thereafter, the impregnation vessel is completely depressurized expanding the remaining CO_2 into atmosphere through a valve. Dyed PC is removed and the vessel is filled with raw PC and the dye amount which was taken by the polymer is replaced. By this, 83 % of the CO_2 can be re-used. However, due to additional losses, it was considered to calculate only with 80 % recirculation. A flow diagram of the process is shown in figure 56, where blue colored lines show the decompression route of the first vessel.

4.3 Thermodynamical calculations

As the first step, the energy consumption for the heat exchangers (WT) was calculated. First, impregnation vessels' temperature has to be kept constant. This is obtained by circulating warm water in the heating jackets of the vessels by using heat exchanger WT_{23}. The water enters into the jacket at 55°C and leaves at 50°C. Since the CO_2-circulation cycle is not tempered, it is assumed that the CO_2 which flows into the vessels by recirculation has the same temperature as the CO_2 in the pump, that is 33°C. WT_{45}, a second heat exchanger heats the CO_2 up for the gas-dye separation step to 40°C in the separator. The separator also has a cylindrical form with a volume of 0.8 m^3 and 1.6 meter height. The cleaned gas is then condensed by WT_{56} by cooling it again to 14°C at 60 bar. The heat flow for a given heat exchanger can be calculated by using the following equation:

$$\dot{Q} = \dot{m} * c_p * \Delta T_{log} \tag{15}$$

Where $\dot{Q}$ is the heat flow, $\dot{m}$ is the mass flow, c_p is the specific heat capacity for isobaric processes, and the logarithmic temperature difference, ΔT_{log} is calculated as:

$$\Delta T_{log} = \frac{T''_{out} - T'_{in} - (T''_{in} - T'_{out})}{ln\frac{T''_{out} - T'_{in}}{T''_{in} - T'_{out}}} \tag{16}$$

Where T''_{out} and T''_{in} is the outlet and inlet temperature of the CO_2, T'_{out} and T'_{in} is the outlet and inlet temperature of tempering media (i.e., of the water). The surface required for the applied heat exchanger can be calculated as:

$$A = \frac{\dot{Q}}{k * \Delta T_{log}} \tag{17}$$

Where k is the heat transfer coefficient and was chosen as 300 $Wm^{-2}K^{-1}$. The overall heat balance for the system can be expressed as:

$$\dot{Q} = \dot{m_1} * c_p^1 * (T''_{in} - T''_{out}) = -\dot{m}_2 * c_p^2 * (T'_{in} - T'_{out}) = k * A * \Delta T_{log} \tag{18}$$

where $\dot{m}_2$ and c_p^2 are the mass flow and the isobaric specific heat capacity of the water. The CO_2 mass flow ($\dot{m}_1$) for heat exchanger WT_{23} was calculated from the volume flow and from CO_2 density by taking 0.5 m for vessel diameter and the 0.001 m/s linear flow velocity. The mass flows for WT_{45} and WT_{56} was calculated from the CO_2 amount which has left the impregnation vessel meanwhile applying linear decompression from 200 to 60 bar within 21 minutes (overall decompression from 200 to 1 bar took 30 minutes). Mass flow $\dot{m}_2$ for cooling or heating water was calculated by

$$\dot{m}_2 = \frac{\dot{m}_1 * c_p^1 * (T''_{out} - T''_{in})}{c_p^2 * (T'_{in} - T'_{out})} \tag{19}$$

Table 14 shows the results for heat exchangers obtained by using eq. (15–19)

Table 14: Total energy balance for heat exchangers

	v (m/s)	CO_2 density [b)] (kg/m^3)	pressure (bar)	T_{in}'' (K)	T_{out}'' (K)	T_{in}' (K)	T_{out}' (K)	ΔT_{log}
WT_{23}	0.001 [a)]	875.76	200	306.15	323.15	328.15	323.15	-18.891
WT_{45}		767.79	60	294.15	313.15	318.15	313.15	-19.232
WT_{56}		149.26	60	313.15	287.15	282.15	287.15	20.770

[a)] literature value [28]
[b)] NIST Standard Reference Database

	volume flow (m^3/s)	mass flow $\dot{m}_1$ (kg/s)	mass flow $\dot{m}_2$ (kg/s)	k ($Wm^{-2}K^{-1}$)	$c_p^{1\ b)}$ ($Jkg^{-1}K^{-1}$)	$c_p^{2\ b)}$ ($Jkg^{-1}K^{-1}$)
WT_{23}	0.000196	0.1720	0.3052	300	2181.9	4179.4
WT_{45}	0.000630	0.4842	1.8946	300	4307.6	4183.4
WT_{56}	0.003244	0.4842	1.1046	300	1833.5	4179.4

	A (m^2)	$\dot{Q}$ (kW)
WT_{23}	1.1254	6.378
WT_{45}	6.8685	39.629
WT_{56}	3.7044	23.082

4.4 Cost estimation

In order to give a rough estimation for process costs, first, the costs of raw materials (P_M) were considered. The market price for the PC was approx. 2 USD/kg [2] in 2010. In calculations made here, the price of 2.00 €/kg was considered for PC and 80 € for 1000 kg of CO_2. The price of the dyestuff is not included in the calculations, since Sigma Aldrich did not provide offer for higher amounts. A calculation with a price for lab-scale amounts given by the producer (239.50 € for 25.0 g [105]) would be possible, but not reliable, because the price will be really different due to the high amounts ordered and to the long term contract between the supplier and the costumer. For the whole process, yearly 1 300 tons of CO_2 and 1 570 kg of DR13 are necessary, taking in assumption that the 80 % of the CO_2 is re-used after cleaning and for every experiment only the amount of dye which was taken by the polymer is refilled and the rest is not removed from the impregnation vessel.

The energy costs (P_E) were calculated from the power required for each device and by considering 0.04 €/kWh price of electricity [106]. For charging the vessels, a liquid CO_2 pump with a maximum feed rate of 38 l/min at 200 bar is used operating with 16.0 kW power [107]. The CO_2 storage tank is rented for 250 €/month. These expenses are summarized in table 15.

Table 15: operational costs for the industrial dyeing process

	Devices		
	power (kW)	working hours (h)	Cost (€/a)
CO_2 Pump	16.00	8760	5 578.37
WT_{23}	6.378	8760	2 223.75
WT_{45}	39.629	8760	13 816.59
WT_{56}	23.082	8760	8 047.60
	Raw materials		
	mass (t/a)	price (€/t)	costs (€/a)
CO_2	1300	80.00	104 000.00
Dyestuff DR13	1.570	not included	not available
Polycarbonate	5000	2000.00	10 000 000.00

The total purchase cost (TPC) for the plant was calculated by using two different methods. First, the method suggested by Douglas [108] was used. By this method, calculation was done by assuming 8 760 h/a operation. The purchase costs (Pc) in USD for a high pressure vessel can be calculated as:

$$Pc_{vessel}(\$) = \left(\frac{M\&S}{280}\right) * 101{,}9 * d^{1.066} * h^{0.82} * F_c \quad (20)$$

Where *M&S* is the Marshall and Swift cost index, (*M&S* = 1493.5 for the chemical industry [109]) *d* is the diameter and *h* is the height of the vessel in feet and F_c is a correlation factor calculated as:

$$F_c = F_m * F_p \quad (21)$$

Where F_m is a correlation factor for a given material and it is 3.67 for stainless steel and F_p is a correlation factor depends upon the applied pressure. The value for F_p was available only up to 1000 psi (approx. 70 bar) in literature, therefore the value for 2900 psi (200 bar) was extrapolated and thus F_p = 16.92 in case of the dyeing vessels. In case of the separator which operates at 60 bar, F_p = 2.29 [108]. The installed cost (IC) can be calculated as follows:

$$IC_{vessel}(\$) = \left(\frac{M\&S}{280}\right) * 101{,}9 * d^{1.066} * h^{0.82} * (2.18 + F_c) \quad (22)$$

Since the process consists of four impregnation vessels, IC and Pc for the impregnation vessels have to be multiplied by four in order to calculate the total cost for the high pressure vessels. From eq. 20–22 expenses of 4 466 249.62 USD for the four vessels and 112 470.80 USD for the separator were determined. The price of the heat exchangers can be expressed with the following equations:

$$Pc_{WT}(\$) = \left(\frac{M\&S}{280}\right) * 101{,}3 * A^{0.65} * F_c \tag{23}$$

where A is the area of the heat exchanger in square feet. F_c parameter here is calculated as:

$$F_c = (F_d + F_p) * F_m \tag{24}$$

Where F_d is a correlation factor for design type of the heat exchanger and equals to 1.35 for reboilers [108]. IC for a given heat exchanger can be determined as:

$$IC_{WT}(\$) = \left(\frac{M\&S}{280}\right) * 101{,}3 * A^{0.65} * (2.29 + F_c) \tag{25}$$

Table 16 contains the total price (Pc + IC) determined for heat exchangers used in the process.

Table 16: Total price of heat exchangers used in the process

	A (m^2)	A (ft^2)	price (USD)
WT_{23}	1.1254	12.11	33 941.95
WT_{45}	6.8685	73.93	109 987.90
WT_{56}	3.7044	39.87	73 628.69
		total	217 558.55

Summarizing every expenses by using the Douglas model, the TPC for high pressure vessels (4 impregnation vessels and one separator) and heat exchangers is 4 796 278.98 USD (4 316 651.08 € at a 0.9 € to $ change rate). In addition, the price of the high pressure liquid pump is 21 122.00 € [107].

TPC has also been calculated by using a different planning [110]. First, the production costs were evaluated. In order to estimate the costs for the vessels and the separator, the amounts of

stainless steel required for the production of the equipment were calculated from the geometrical sizes. After this, the production price was obtained by multiplying this raw materials' price by 30. The expenses for heat exchangers were determined by:

$$Pc'_{WT} = (-0.2152 * A_{WT}^2 + 256.25 * A_{WT})/1.95583 \quad (26)$$

Where *WT* indices the given heat exchanger, *A* is the area and the number 1.95583 is the change rate between Euro and Deutsche Mark. [111]. Afterwards, from Pc the installation costs were calculated by a method given by Ullrich [112]. In this approach, every type of device has an additional multiplication factor in percent regarding to the installation cost of the given device. The model includes the costs for planning and also calculates with unexpected costs. Performing all the calculations, the TPC for the industrial plant is 3 065 066 .29 €. Table 17 summarizes every expenses calculated for the scaling up.

Table 17: Overall costs for the industrial dyeing plant

	Calculation method	
Costs	J. M. Douglas [108], 1988	H. Ullrich [112], 1983
TPC (€)	4 337 773.08	3 065 066.29
raw materials (P_M, €/a)	10 104 000.00	
energy (P_E, €/a)	29 665.94	
overall, for the first year (€)	14 471 439.02	13 198 732.23

As it can be seen from table 17, costs for the dyeing plant calculated by the two different methods are not the same, but this difference of approx. 30 % is reliable. Afterwards, a minimum sale price (MSP) for the dyed PC product can be given by the use of the total utility cost (TUC) and the total annual cost (TAC), calculated as:

$$TUC = 1.2 * (P_M + P_E) \quad (27)$$

$$TAC = \frac{6.0 * TPC}{depreciation\ period} + TUC \quad (28)$$

$$MPS = \frac{TAC}{amount\ PC\ produced} \quad (29)$$

Calculations were done by considering 5 years of operation for the dyeing plant. Table 18 summarizes the results.

Table 18: overall costs and minimum sale price for the dyed PC

Costs	Calculation method	
	J. M. Douglas [108], 1988	H. Ullrich [112], 1983
TPC (€)	4 337 773.08	3 065 066.29
TUC (€)	12 160 398.00	
TAC (€)	17 365 725.60	15 838 477.20
MSP (€/kg)	**3.47**	**3.17**

The price of 3.47 € and 3.17 € per kg dyed PC is comparable to the estimated market price of the raw material (2.00 €/kg). This price can be further decreased if the operation time for the plant is prolonged. For instance, producing dyed PC for 10 years instead of 5 by using this scaled up method, MSP for the product changes to 2.95 € and 2.80 € per kg (depending on the method used [108, 112] for TPC calculation). MSP was calculated though by not considering expenses for the DR13 since the price given by the producer is for small amounts and it would not be realistic applying this for amounts which are several orders of magnitudes higher. Nevertheless, by taking the value of 239.50 € for 25.0 g DR13 [105], MSP of the dyed PC would be 7.08 € and 6.78 € by planning 5 years of production.

IV. Conclusions

Within the frame of this thesis, the modification of polycarbonate was carried out by using the supercritical fluid impregnation method. The procedure has been realized by using supercritical carbon dioxide as sorption media and took place in a high pressure vessel in batch mode. This method offers an alternative way for polymer modification in order to replace old technologies, which have several drawbacks.

Although several polymers and textile fibers have already been dyed in supercritical media, a dyeing procedure for polycarbonate, a technical plastic with high importance, was unknown. Therefore, the first part of the work focused on investigations towards this direction. For these experiments, two commercially available dyestuffs (disperse red 1 and disperse red 13) were used. Experiments were carried out in the range of 100–300 bar for 3–24 hours of sorption times at 40, 50 and 60°C. Upon investigation, the sorption kinetics were studied in detail and the effects of temperature, pressure, CO_2 density, sorption time and dye solubility in the fluid phase were explained. Moreover, equilibrium constants for the process were calculated and new solubility data for the dyes were reported. The impregnation resulted in an entirely, equally deep dyed polymer pellet with excellent dyeing fixation, solely by the use of supercritical carbon dioxide as the applied media. Impregnated samples were analyzed by UV-Vis spectroscopy. The highest dye uptakes achieved were 0.010 wt % and 0.055 wt % for disperse red 1 and disperse red 13, respectively, with respect to the mass of the polymer. Since these amounts caused very satisfactory changes in color, a study was carried out in order to examine the applicability of the process in an industrial scale. Within the frame of this work, theoretical calculations were performed in order to scale up the applied system for 5000 tons of dyed polycarbonate per year production. It was concluded, that by operating the industrial scale system for ten years, the minimum sale price has to be 3.47 €/kg polycarbonate, which is really comparable to the market price of the untreated polymer of approx. 2.0 €/kg. Therefore, the process has been considered to be also economically feasible.

The second part of the thesis was dedicated to explore different ways in order to create metal nanoparticle modified polycarbonate pellets. In the foremost approach, first, polycarbonate was impregnated with dithizone, a chelate ligand capable of reacting to several metal ions. Upon this experimentation, the sorption kinetics of dithizone into the polymer was investigated in detail. In addition, the solubility of the dithizone in supercritical carbon

dioxide and its diffusion coefficient in polycarbonate was determined. As a second step, the possible chelation or capture of metal ions using these impregnated pellets was investigated. This process was optimized for copper, wherein the effect of pressure, temperature, vessel size and stirring within the vessel were studied. By this technique, a maximum 109±3 ppm of metal load was obtained. Impregnated pellets were investigated by several analytical methods afterwards. Scanning electron microscopy investigations showed copper clusters having a size of 5 to 400 nanometers, equally distributed deeply inside in the entire polymer matrix. Preliminary experiments for zinc yielded in 21±3 ppm as the highest metal load. In a second, different method, two copper dithizonate complexes were synthesized in lab and were used for the modification afterwards. Polycarbonate has been successfully modified by the use of these raw materials and the highest metal load obtained was 5±1 ppm. In order to gather comparable data, impregnation has also been carried out by applying copper(hexafluoroacetylacetonate)-hydrate, a commercially available copper complex, which has been reported to be suitable for supercritical carbon dioxide media. By using this material, sorption yielded in maximum 5.0±0.7 ppm copper content in the polymer matrix.

Abbreviations

acac	acetylacetate
BsE	backscattered electron detector
BUTE	Budapest University of Technology and Economics
CuDz	secondary copper(II)dithizonate
$Cu(HDz)_2$	primary copper(II)dithizonate
$Cu(hfac)_2$	copper(hexafluoroacetylacetonate)-hydrate
DCM	dichloromethane
DIT	dithizone
DPC	dithizone impregnated polycarbonate
DR1	disperse red 1
DR13	disperse red 13
DSC	differential scanning calorimetry
DTA	differential thermal analysis
EDX	electron dispersive X-ray spectrophotometry
ESCA	electron spectroscopy for chemical analysis
HDPE	high density polyethylene
IC	investment cost
ICP–MS	inductively coupled plasma – mass spectrometry
ICP–OES	inductively coupled plasma – optical emission spectrometry
LDPE	light density polyethylene
MSB	magnetic suspension balance
MSP	minimum sale price
NRHB	non-random hydrogen bonding
PAR	polyarylate
Pc	purchase cost
PC	bisphenol A polycarbonate
P_E	energie cost
PET	polyethylene terephthalate
PGSS	particles from gas saturated solutions
P_M	raw materials' price
PMP	poly(4-metilpent-1-ene)
PMMA	poly(methyl methacrylate)

PP	polypropylene
PTFE	polytetrafluoroethylene
QCM	quartz crystal microbalance
RESS	rapid expansion of supercritical solutions
ROSE	residuum oil supercritical extraction
SAS	supercritical antisolvent
$scCO_2$	supercritical carbon dioxide
SCF	supercritical fluid
SCWO	supercritical water oxidation
SE	secondary electron detector
SEM	scanning electron microscopy
SFC	supercritical fluid chromatography
SFD	supercritical fluid dyeing
SFE	supercritical fluid extraction
SFEE	supercritical fluid extraction of emulsions
SFI	supercritical fluid impregnation
SG	silica gel
SIGT	sorption induced glass transition
TAC	total annual cost
TEM	transmission electron microscopy
T_g	glass transition temperature
TG	thermogravimetry
TPC	total purchase cost
TUC	total utility cost
UMB	University of Maribor
VLE	vapor liquid equilibria
WT	heat exchanger
XPS	X-ray photoelectron spectroscopy
XRD	X-ray diffraction

Nomenclature

a	constant for Chrastil equation (5)
a_v	surface to volume ratio
A	area
b	constant for Chrastil equation (5)
b	affinity constant (equation 1)
c	concentration
c_p	specific heat capacity for isobaric processes
C	sorption amount
C'_H	Langmuir capacity constant
cps	counts per second
d	diameter
D	sorption diffusivity
D_p	diameter of the equivalent spherical particle
Eu	Euler number
F_c	correlation factor
F_d	correlation factor for design type of a heat exchanger
F_m	correlation factor of a given material
F_p	correlation factor for a given pressure
h	height
k	crystallization kinetic constant (equation 4)
k	association number (equation 5)
k_D	Henry's law solubility coefficient
K	empirical constant
K_c	partition coefficient
l	planar thickness
L	total height of bed
$\dot{m}$	mass flow
M_A	molecular weight of the solute
M_B	molecular weight of gas
M_s	carbon dioxide sorption amount at a given impregnation time
M_w	weight average molecular weight
M_∞	equilibrium sorption amount of carbon dioxide

M&S	Marshall and Swift cost index
n	Avrami exponent
p	pressure
$\dot{Q}$	heat flow
R	ideal gas constant
Re	Reynolds number
t	time
t_0	induction time of crystallization
T	temperature
T’	temperature of tempering media
T”	temperature of CO_2
$T_{g(d)}$	depressed glass transition temperature
V_0	empty tower velocity
X_c	crystallinity

Greek symbols

ΔH	total reaction heat
ε	porosity
η	viscosity
λ	wavelength
ρ	density
ρ_p	polymer density
Φ_s	sphericity
ω	absorbed amount of carbon dioxide

Subscripts

aq	aqueous phase
c	critical
dye	dye
fluid	fluid phase
in	inlet
log	logarithmic
max	maximum
out	outlet
polym	polymer phase

References

[1] Metal-Polymer Nanocomposites, edited by L. Nicolais, G. Carotenuto. John Wiley & Sons, **2005**

[2] Report on polycarbonate within the ChemSystems Process Evaluation/Research Planning (PREP) Program, Nexant Inc., December **2011**

[3] V. Goodship, E. O. Ogur: Polymer Processing with Supercritical Fluids, Rapra Review Reports, 15, 8, (**2004)** ISBN 1-85957-494-7

[4] B. Simándi (Ed.): Vegyipari Műveletek II. Anyagátadó műveletek és kémiai reaktorok, Typotex, (**2011**) ISBN 978-963-279-487-7

[5] Gerd H. Brunner: Supercritical Fluids as Solvents and Reaction Media, Elsevier Science & Technology Books, (**2004)** ISBN 0444515747

[6] N. Maraschin: Ethylene Polymers, LDPE. Encyclopedia of Polymer Science and Technology, Vol. 2. (**2001)**

[7] Y. Oka, S. Koshizuka, Y. Ishiwatari, A. Yamaji: Super Light Water Reactors and Super Fast Reactors; Supercritical-Pressure Light Water Cooled Reactors, Springer, (**2010)** ISBN 978-1-4419-6035-1

[8] M. D. Bermejo, M. J. Cocero: Supercritical water oxidation: A technical review, AIChE Journal, 52 (11) (**2006**) 3933–3951

[9] F. Temelli: Perspectives on supercritical fluid processing of fats and oils, J. Supercrit. Fluids, 47 (3) (**2009**) 583–590.

[10] Y. Suehiro, M. Nakajima, K. Yamada, M. Uematsu: Critical parameters of {xCO2 + (1 - x)CHF3} for x = (1.0000, 0.7496, 0.5013 , and 0.2522), J. Chem. Thermodyn.**,** 28 (**1996)** 1153–1164.

[11] E. Schütz: Neues bei überkritischen Fluiden, 15th European Meeting on Supercritical Fluids, 8-11th May **2016**, Essen, Germany

[12] E. Reverchon, I. De Marco: Supercritical fluid extraction and fractionation of natural matter (review article), J. Supercrit. Fluids, 38 (2) (**2006)** 146–166

[13] R. Marr, T. Gamse: Use of supercritical fluids for different processes including new developments–a review, Chemical Engineering and Processing, 39 (**2000**) 19–28

[14] M. B. King, T. R. Bott (Ed.): Extraction of Natural Products Using Near-Critical Solvents, Chapman and Hall, (**1993**) ISBN 978-94-010-4947-4

[15] Natex Prozesstechnologie GmbH. homepage, www.natex.at **2016**

[16] C. Campos Domínguez, T. Gamse: Process intensification by the use of micro devices for liquid fractionation with supercritical carbon dioxide, Chemical Engineering and Research Design, 108 (**2016**) 139–145

[17] E. Székely: Reszolválás szuperkritikus szén-dioxidban, PhD. Thesis, Budapest University of Technology and Economics, **2003**

[18] D. Varga, Gy. Bánsághi, J. A. Martínez Pérez, S. Miskolczi, L. Hegedűs, B. Simándi, E. Székely: Chiral Resolution of Racemic Cyclopropanecarboxylic Acids in Supercritical Carbon Dioxide, Chemical Engineering and Technology, 37 (**2014**) 1885 – 1890

[19] Gy. Bánsághi, E. Székely, D. M. Sevillano, Z. Juvancz, B. Simándi: Diastereomer salt formation of ibuprofen in supercritical carbon dioxide, J. of Supercrit. Fluids, 69 (**2012**) 113–116

[20] C. Erkey: Supercritical carbon dioxide extraction of metals from aqueous solutions: a review, J. of Supercrit. Fluids, 17 (**2000**) 259–287

[21] A. W. Kjellow, O. Henriksen: Supercritical Wood Impregnation (Review article), J. of Supercrit. Fluids, 50 (**2009**) 297–304

[22] I. Kikic, F. Vecchione: Supercritical Impregnation of Polymers, Current Opinion in Solid State and Materials Science, 7 (**2003**) 399–405

[23] G. Tkalec, M. Pantic, Z. Novak, Z. Knez, Supercritical impregnation of drugs and supercritical fluid deposition of metals into aerogels, J. Mater. Sci. 50, 1 (**2015**) 1–12

[24] I. Smirnova, J. Mamic, W. Arlt, Adsorption of Drugs on Silica Aerogels, Langmuir 19 (**2003**) 8521–8525

[25] M. V. Fernández Cid, Cotton Dyeing in Supercritical Carbon Dioxide, Ph.D. Thesis, TU Delft, **2005** ISBN: 90-9019765-5

[26] S. G. Kazarian: Polymer Processing with Supercritical Fluids, Polymer Science, Ser. C, 42 (1) (**2000**) 78–101

[27] T. Gamse, R. Marr, C. Wolf, K. Lederer: Supercritical CO2 Impregnation of Polyethylene components for medical purposes, Hem. Ind., 61 (5) (**2007**) 229–232

[28] E. Bach, E. Cleve, E. Schollmeyer, Past, present and future of supercritical fluid dyeing technology – an overview, Rev. Prog. Color. 32, 1 (**2002**) 88–102

[29] W. Saus, D. Knittel, E. Schollmeyer, Dyeing of Textiles in Supercritical Carbon Dioxide, Text. Res. J. 63, 3 (**1993**) 135–142

[30] D. Knittel, W. Saus, S. Hoger, E. Schollmeyer: Färben in überkritischem CO_2: Bestimmung von Einflußgrößen auf das strukturelle Verhalten von Polyethyleneterephthalat-Fasermaterial, Die Angewandte Makromolekulare Chemie, 218 (1) (**1994**) 69–79

[31] K. W. Hutchenson, N. R. Forster (Ed.): Innovations in Supercritical Fluids, ACS Symposium Series, American Chemical Society, (**1995**) ISBN: 0-8412-3324-1

[32] M. Saito: History of supercritical fluid chromatography: Instrumental developement, Journal of Bioscience and Bioengineering (review article), 115, 6, (**2013**) 590–599

[33] J. L. Kendall, D. A. Canelas, J. L. Young, J. M. DeSimone: Polymerizations in Supercritical Carbon Dioxide, Chem. Rev. 99 (**1999**) 543–563

[34] P. G. Odell, G. K. Hamer: Polycarbonates via melt transesterification in supercritical carbon dioxide, Polym. Prep., 38 (**1997**) 470–471

[35] J. J. Watkins, T. J. McCarthy: Polymerization in Supercritical Fluid-Swollen Polymers: A New Route to Polymer Blends, Macromolecules, 27 (**1994**) 4845–4847

[36] A. H. Landrock (Ed.): Handbook of Plastic Foams, Types, Properties, Manufacture and Applications, Noyes Publications, (**1995**) ISBN: 0-8155-1357-7

[37] A. I. Cooper: Polymer synthesis and processing using supercritical carbon dioxide, Journal of Materials Chemistry, 10 (**2000**) 207–234

[38] E. Weidner: High pressure micronization for food applications, J. of Supercrit. Fluids 47 (**2009**) 556–565

[39] Gy. Lévai, Á. Martín, E. de Paz, S. Rodríguez-Rojo, M. J. Cocero: Production of stabilized quercitin aqueous suspensions by supercritical fluid extraction of emulsions, J. of Supercrit. Fluids, 100 (**2015**) 34–45

[40] Á. Martín, E. Weidner: PGSS-drying: Mechanism and modelling, J. of Supercrit. Fluids 55 (1) (**2010**) 271–281

[41] A. G. Wonders, D. R. Paul: Effect of CO_2 exposure history on sorption and transport in polycarbonate, Journal of Membrane Science, 5 (**1979**) 63–75

[42] W. J. Koros, A. H. Chan, D. R. Paul: Sorption and transport of various gases in polycarbonate, Journal of Membrane Science, 2 (**1977**) 165–190

[43] W. J. Koros, D. R. Paul, A. A. Rocha: Carbon dioxide sorption and transport in polycarbonate, Journal of Polymer Science, 14 (**1976**) 687–702

[44] A. R. Berens, G. S. Huvard, R. W. Korsmeyer, F. W. Kunig: Application of Compressed Carbon Dioxide in the Incorporation of Additives into Polymers, Journal of Applied Polymer Science, 46 (2) (**1992**) 231–242

[45] M. Pantoula, C. Panayiotou: Sorption and swelling in glassy polymer/carbon dioxide systems, Part I. Sorption, J. of Supercritical Fluids 37 (**2006**) 254–262

[46] M. Pantoula, J. von Schnitzler, R. Eggers, C. Panayiotou: Sorption and swelling in glassy polymer/carbon dioxide systems, Part II. Swelling, J. of Supercritical Fluids, 39 (**2007**) 426–434

[47] J. von Schnitzler, R. Eggers: Mass transfer in polymers in a supercritical CO_2-atmosphere, J. of Supercrit. Fluids, 16 (**1999**) 81–92

[48] S.-H. Chang, S.-C. Park, J.-J. Shim, Phase equilibria of supercritical fluid–polymer systems, J. of Supercritical Fluids, 13 (**1998**) 113–119

[49] R. G. Wissinger, M. E. Paulaitis: Swelling and sorption in polymer–CO_2 mixtures at elevated pressures, Journal of Polymer Science Part B: Polymer Physics, 25 (12) (**1987**) 2497–2510

[50] N. S. Kalospiros, M. E. Paulaitis: Molecular Thermodynamic Model for Solvent-induced Glass Transitions in Polymer-supercritical Fluid Systems, Chemical Engineering Science, Vol. 49, 5, (**1994**) 659

[51] J. D. Yoon, S. W. Cha: Change of glass transition temperature of polymers containing gas, Polym. Testing 20 (3) (**2001**) 287–293

[52] E. Beckman, R. S. Porter: Crystallization of Bisphenol a Polycarbonate Induced by Supercritical Carbon Dioxide, Journal of Polymer Science, Part B: Polymer Physics, 25 (**1987**) 1511–1517

[53] P. Neogi (Ed.): Diffusion in Polymers, Marcel Dekker (**1996**) ISBN: 0-8247-9530-X

[54] A. R. Berens: Analysis of transport behavior in polymer powders, Journal of Membrane Science, 3 (**1978**) 247–264

[55] K. F. Webb, A. S. Teja: Solubility and diffusion of carbon dioxide in polymers, Fluid Phase Equilibria, 158 (**1999**) 1029–1034

[56] M. Tang, Tz-Bang Du, Y.-P. Chen: Sorption and diffusion of supercritical carbon dioxide in polycarbonate, J. of Supercrit. Fluids, 28 (2-3) (**2004**) 207–218

[57] Y. Sun, M. Matsumoto, K. Kitashima, M. Haruki, S. Kihara, S. Takishima: Solubility and diffusion coefficient of supercritical-CO2 in polycarbonate and CO2 induced crystallization of polycarbonate, J. of Supercrit. Fluids, 95 (**2014**) 35–43

[58] Y. Sato, T. Takikawa, A. Sorakubo, S. Takishima, H. Masuoka, M. Imaizumi: Solubility and Diffusion Coefficient of Carbon Dioxide in Biodegradable Polymers, Ind. Eng. Chem. Res, 39 (**2000**) 4813–4819

[59] Y. Sato, K. Fujiwara, T. Takikawa, S. Takishima, H. Masuoka: Solubilities and diffusion coefficients of carbon dioxide and nitrogen in polypropylene, high-density polyethylene, and polystyrene under high pressures and temperatures, Fluid Phase Equilibria, 162, (1-2) (**1999**) 261–276

[60] S. Areerat, E. Funami, Y. Hayata, D. Nakagawa, M. Ohshima: Measurement and Prediction of Diffusion Coefficients of Supercritical CO_2 in Molten Polymers, Polymer Engineering and Science, 44 (10) (**2004**) 1915–1924

[61] Y. Sato, T. Takikawa, S. Takishima, H. Masuoka: Solubilities and diffusion coefficients of carbon dioxide in poly(vinyl acetate) and polystyrene, J. of Supercrit. Fluids, 19 (2) (**2001**) 187–198

[62] J. S. Chiou, J. W. Barlow, D. R. Paul: Plasticization of Glassy Polymers by CO_2, Journal of Applied Polymer Science, 30 (**1985**) 2633–2642

[63] L. Mascia, G. Del Re, P. P. Ponti, S. Bologna, G. di Giacomo, B. Haworth, Crystallization Effects on Autoclave Foaming of Polycarbonate Using Supercritical Carbon Dioxide, Advances in Polymer Technology, 25, 4, (**2006**) 225-235

[64] S. M. Gross, G. W. Roberts, D. J. Kiserow, J. M. DeSimone, Crystallization and Solid-State Polymerization of Poly(bisphenol A carbonate) Facilitated by Supercritical CO2, Macromolecules, 33 (**2000**) 40–45

[65] Z. Zhang, Y. P. Handa, An in-situ study of plasticization of polymers by high-pressure gases, J. Polym. Sci. Pol. Phys., 36 (6) (**1998**) 977–982

[66] M. Banchero: Supercritical fluid dyeing of synthetic and natural fibers – a review, Coloration Technology, 129 (**2012**) 2–17

[67] R. B. Gupta, J-J. Shim: Solubility in Supercritical Carbon Dioxide, CRC Press (**2007**) ISBN: 0-8493-4240-6

[68] J. Chrastil: Solubility of Solids and Liquids in Supercritical Gases, J. Phys. Chem, 86 (15) (**1982**) 3016–3021

[69] T. Gamse, F. Steinkellner, R. Marr, P. Alessi, I. Kikic: Solubility Studies of Organic Flame Retardants in Supercritical CO_2, Ind. Eng. Chem. Res., 39 (12) (**2000**) 4888–4890

[70] D. E. Knox: Solubilities in supercritical fluids, Pure Appl. Chem., 77 (3) (**2005**) 513–530

[71] S. L. Draper, G. A. Montero, B. Smith, K. Beck, Solubility relationships for disperse dyes in supercritical carbon dioxide, Dyes and Pigments 45 (**2000**) 177-183

[72] T. Shinoda, K. Tamura, Solubilities of C.I. Disperse Red 1 and C.I. Disperse Red 13 in supercritical carbon dioxide, Fluid Phase Equilibria 213 (**2003**) 115–123

[73] T. Ngo, C. Liotta, C. A. Eckert, S. G. Kazarian: Supercritical fluid impregnation of different azo-dyes into polymer: in situ UV/Vis spectroscopic study, J. of Supercrit. Fluids, 27 (**2003**) 215–221

[74] B. L. West, S. G. Kazarian, M. F. Vincent, N. H. Brantley, C. A. Eckert, Supercritical fluid dyeing of PMMA films with azo-dyes, J. Appl. Polym. Sci. 69, 5 (**1998**) 911–919.

[75] G. Iwantscheff: Dithizon-Verfahren in der chemischen Analyse, Überblick über die Entwicklung der letzten 15 Jahre, Angewandte Chemie 69 (13/14) (**1957**) 472–477

[76] O. Zaporozhets, N. Petruniock, V. Sukhan: Determination of Ag(I), Hg(II) and Pb(II) by using silica gel loaded with dithizone and zinc dithizonate, Talanta 50 (**1999**) 865–873

[77] H.-M. Yu, H. Song, M-Li Chen: Dithizone immobilized silica gel on-line preconcentration of trace copper with detection by flame atomic absorption spectrometry, Talanta 85 (**2011**) 625–630

[78] J. Halili, A. Mele, T. Arbneshi, I. Mazreku: Supercritical CO_2 extraction of heavy metals Cu, Zn and Cd from aqueous solution using dithizone as chelating agent, American Journal of Applied Sciences 12 (**2015**) 284–289

[79] Y. Zhang, C. Erkey: Preparation of supported metallic nanoparticles using supercritical fluids: A review. J. of Supercrit. Fluids 38 (**2006**) 252–267

[80] J. J. Watkins, T. J. McCarthy: Polymer/Metal Nanocomposite Synthesis in Supercritical CO_2, Chemistry of Materials, 7 (11) (**1995**) 1991–1994

[81] C. Erkey: Preparation of metallic supported nanoparticles and films using supercritical fluid deposition, J. of Supercrit. Fluids 47 (**2009**) 517–522

[82] E. Said-Galiyev, L. Nikitin, R. Vinokur, M. Gallyamov, M. Kurykin, O. Petrova, B. Lokshin, I. Volkov, A. Khoklov, K. Schamburg: New Chelate Complexes of Copper and Iron: Synthesis and Impregnation into a Polymer Matrix from Solution in Supercritical Carbon Dioxide, Ind. Eng. Chem. Res., 39 (**2000**) 4891–4896

[83] T. Hasell, L. Lagonigro, A. C. Peacock, S. Yoda, P. D. Brown, P. J. A. Sazio, S. M. Howdle: Silver Nanoparticle Impregnated Polycarbonate Substrates for Surface Enhanced Raman Spectroscopy, Adv. Funct. Mater. 18 (**2008**) 1265–1271

[84] A. Sharma, S. Bahniwal, S. Aggarwal, S. Chopra, D. Kanjilal: Synthesis of copper nanoparticles in polycarbonate by ion implantation, Bull. Mater. Sci., 34 (4) (**2011**) 645–649

[85] H. M. N. H. Irving, A. M. Kiwan: Studies with dithizone, pt. XXV: Secondary and Primary Copper(II)Dithizonate, Analytica Chimica Acta, 56 (**1971**) 435–446

[86] R. W. Geiger, E. B. Sandell: Copper(II)-Dithizonate Equilibria in Water-Carbon Tetrachloride, Analytica Chimica Acta, 8 (**1953**) 197–308

[87] Ronald F. Sieloff: Method for color dyeing polycarbonate, US Patent, US5453100, 26th Sept. **1995**

[88] J. Bianco, V. Humphreys: Method of dyeing shaped polycarbonate resins, US Patent, US3514246, 26th May **1970**

[89] J. P. Mercier, R. Legras: Correlation between the enthalpy of fusion and the specific volume of crystallized polycarbonate of bisphenol A, Polymer Letters, 6 (**1970**) 645–650

[90] S. N. Young, K-P. Yoo: Solubility of Disperse Anthraquinone and Azo Dyes in Supercritical Carbon Dioxide at 313.15 to 393.15 K and from 10 to 25 MPa, J. Chem. Eng. Data, 43 (**1998**) 9–12

[91] T. Suzuki, N. Tsuge, K. Nagahama: Solubilities of ethanol, 1-propanol, 2-propanol and 1-butanol in supercritical carbon dioxide at 313 K and 333 K, Fluid Phase Equilibria, 67 (**1991**) 213–226

[92] J. S. Lim, Y. Y. Lee, H. S. Chun: Phase Equilibria for Carbon Dioxide–Ethanol–Water System at Elevated Pressures, J. of Supercrit. Fluids, 7 (**1994**) 219–230

[93] V. K. Gupta, A. K. Jain, G. Maheshwari: A New Zn^{2+}-Selective Potentiometric Sensor Based on Dithizone – PVC Membrane, Chemia Analityczna, 51 (**2006**) 889–897

[94] B. Meyssami, M. O. Balaban, A. A. Teixeira: Prediction of pH in Model Systems Pressurized with Carbon Dioxide, Biotechnol. Prog., 8 (**1992**) 149–154

[95] M. B. King, A. Mubarak, J. D. Kim, T. R. Bott: The mutual solubilities of water with supercritical and liquid carbon dioxides, J. of Supercrit. Fluids, 5 (4) (**1992**) 296–302

[96] C. A. Perman, M. E. Riechert: Methods of Polymer Impregnation, (**1994**) U.S. Patent 5.340.614.

[97] G. Röbisch, W. Herrmann, R. Stösser, R. Szargan: Zur Existenz und Struktur der sekundären Dithizonate, Zeitschrift f. anorg. und allg. Chemie, 515 (**1984**) 230–240

[98] N. Mölders, M. Renner, C. Errenst, E. Weidner: Impregnation of polycarbonate surfaces with silver nitrate using compressed carbon dioxide, 15th European Meeting on Supercritical Fluids, (**2016**) Essen, Germany

[99] E. Kondoh, H. Kato: Characteristics of copper deposition in a supercritical CO2 fluid, Microelectronic Engineering, 64 (**2002**) 495–499

[100] R. M'Hamdi, J. F. Bocquet, K. Chhor, C. Pommier: Solubility and Decomposition Studies on Metal Chelates in Supercritical Fluids for Ceramic Precursor Powders Synthesis, J. of Supercrit. Fluids, 4, (**1991**) 55–59

[101] R. Garriga, V. Pessey, F. Weill, B. Chevalier, J. Etourneau, F. Cansell: Kinetic study of chemical transformation in supercritical media of bis(hexafluoroacetylacetonate)copper (II) hydrate, J. of Supercrit. Fluids, 20 (**2001**) 55–63

[102] B. Kruczek: *Carman–Kozeny Equation* in E. Drioli, L. Giorno (Ed.): Encyclopedia of Membranes, (**2014**) Springer, ISBN: 978-3-642-40872-4

[103] J. D. Seader, E. J. Henley: Separation Process Principles, (**2006**) John Wiley & Sons, ISBN: 978-0-471-46480-8

[104] M. Zogg: Einführung in die Mechanische Verfahrenstechnik, (**1993**) B. G. Teubner Stuttgart, ISBN: 3-519-16319-5

[105] Sigma Aldrich Austria homepage (http://www.sigmaaldrich.com/austria.html) product search: *„disperse red 13"* 1st Sept. **2016**

[106] Energie-Control Austria homepage (www.e-control.at), *Auswertung der Industriepreiserhebung Strom Jänner 2016*, 1st Sept. **2016**

[107] Official price offer from Speck Triplex Pumpen GmbH & Co. KG, Bielefeld, Germany. Received on 22th March, **2016**

[108] J. M. Douglas: Conceptual Design of Chemical Processes, (**1988**) McGraw-Hill, ISBN: 0-07-100195-6 (0-07-017762-7)

[109] Equipment Cost Index database, (www.equipment-cost-index.com/eci), data given for year **2010** second quarter

[110] R. Halb, L. Koller (supervised by D. Varga and T. Gamse): Imprägnierung im überkritischem CO2, „Konstruktsionsübung", performed at the Graz University of Technology, summer semester **2016**

[111] M. Gebhardt, H. Kohl, Th. Steinrötter: Preisatlas, (**2002**) Institut für Energie- und Umwelttechnik e. V., Duisburg

[112] H. Ullrich: Anlagenbau, (**1983**) Georg Thieme Stuttgart, ISBN: 978-3-136-42301-1

J. of Supercritical Fluids 116 (2016) 111–116

Contents lists available at ScienceDirect

The Journal of Supercritical Fluids

journal homepage: www.elsevier.com/locate/supflu

Supercritical fluid dyeing of polycarbonate in carbon dioxide

Dániel Varga [a,*], Simon Alkin [a], Peter Gluschitz [a], Barbara Péter-Szabó [b], Edit Székely [b], Thomas Gamse [a]

[a] Institute of Chemical Engineering and Environmental Technology, Graz University of Technology, Graz, Austria
[b] Institute of Chemical Engineering and Environmental Technology, Budapest University of Technology and Economics, Budapest, Hungary

ARTICLE INFO

Article history:
Received 19 November 2015
Received in revised form 23 May 2016
Accepted 23 May 2016
Available online 24 May 2016

Keywords:
Polymer dyeing
Impregnation
Supercritical carbon dioxide
Polycarbonate

ABSTRACT

In this work, the applicability of the supercritical CO_2 dyeing process on polycarbonate pellets was investigated by the use of two azo-disperse dyes; disperse red 1 (DR1) and disperse red 13 (DR13). Experiments were performed in the range of 100–300 bar and 40 °C–60 °C with 3–24 h of impregnation time. Dyeing took place in a high pressure vessel and kinetics was studied and explained. Impregnation efficiency on the polymer pellets was measured by UV–vis spectroscopy. The process was successfully applied and resulted in an entirely, equally deep-dyed polymer with excellent dyeing fixation. Arising from the different solubility and chemical structure of the dyes, their sorption kinetics was found to be different. Maximal dye uptake obtained with DR1 and DR13 were 0.010 wt% and 0.055 wt% respectively, with respect to the mass of the polymer. New solubility data for DR13 in supercritical CO_2 has also been measured and partition coefficients (K_c) for the dyes between the fluid and the polymer phase were calculated.

© 2016 Elsevier B.V. All rights reserved.

1. Introduction

Supercritical (sc.) fluid impregnation technique is used in several fields of the chemical industry. Most common examples are wood impregnation [1], sc. fluid deposition aerogel impregnation [2,3] and polymer dyeing [4].

The conventional dyeing of different natural products and polymers demands enormous amount of water, which contains at the end of the process large quantities of chemicals, salt and alkali [5]. This becomes a chemical waste, which is difficult to treat. By using a particular case of solute impregnation, the supercritical fluid dyeing (SFD), both the water consumption and the waste production can be eliminated. The sc. dyeing of textile yarns (such as cotton) and synthetic fibers (e.g. polyethyleneterephthalat (PET), polypropylene and aramides) have already been put into practice [5,6] and applied in the industry.

Dyes and pigments are conventionally incorporated into polycarbonate (PC) resins during their manufacture. This method suffers from two general drawbacks. First, the high melt viscosity of the resin makes it difficult to disperse the color uniformly and second, the high temperatures used in molding the resin exclude the use of thermally labile dyes. Processes invented to overcome these disadvantages consume high amount of organic solvent (containing carriers and surfactants) and hence an additional drying step has to be involved at the end of the dying process [7,8]. Our goal is to apply the SFD method for polycarbonate to overcome all the above mentioned drawbacks that conventional techniques have.

In the SFD process, a disperse dye is dissolved in a sc. fluid and by simultaneously contacting this solution with a polymer matrix in a high pressure vessel the dye penetrates into the polymer. Due to its feasible properties (it is nontoxic, nonflammable and relatively cheap) mostly $scCO_2$ is used as dyeing media. The dye uptake proceeds in four steps: (1) the dissolution of the dye in CO_2, (2) dye transport to the material, (3) adsorption on the surface and finally (4) the diffusion of the dye into the matrix [4]. $ScCO_2$ dissolved in glassy polymers increases the diffusivities of additives in the polymer matrix because of its plasticization effect [9]. SFD is mainly controlled by diffusion, which is described by the Fick law [10]. Pressure, temperature, impregnation time, stirring and the amount of dye also influence the mass transport. The fluid phase has always to be saturated and cannot be exhausted by the uptake of the polymer during the impregnation. This is achieved by creating a saturated phase in the impregnation vessel with high excess of dye. Although the solubility of both, here applied dyes in $scCO_2$ is rather low [11], the high partition coefficient between the polymer and the fluid phase can drive the dye into the polymer matrix. As a result, the dye concentration in the applied polymer can be remarkably higher than in the dye bath [4]. Since CO_2 is a gas under ambient conditions its removal from the product is very easy, avoiding the cost intensive processes of drying or organic sol-

* Corresponding author.
E-mail address: vdani_1@hotmail.com (D. Varga).

http://dx.doi.org/10.1016/j.supflu.2016.05.018
0896-8446/© 2016 Elsevier B.V. All rights reserved.

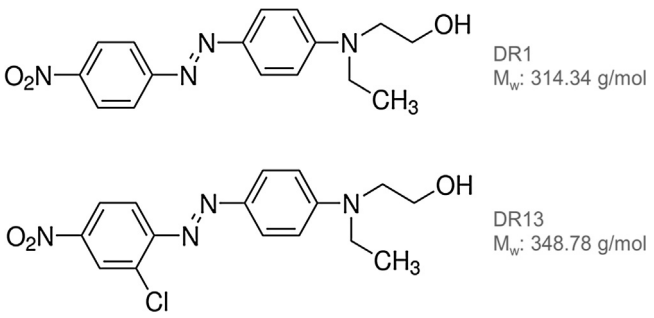

Fig. 1. Chemical structure of dyes DR1 and DR13.

vent removal. Its mild critical temperature (31.1 °C) enables also the use of thermal labile dyes. In the literature many commercially available disperse dyes suitable for $scCO_2$ dyeing are mentioned [4]. Although several polymers had already been colored by SFD [12], to our best knowledge, there is no detailed experimental data in the open literature on successful PC dyeing by SFD technique. However, the work of West et al. [13] should be noted who reported the dye impregnation of poly(methyl methacrylate) (PMMA) films with two disperse dyes. These authors achieved remarkable dye uptake (approx. 0.5 wt%) of the PMMA film at 40 °C and 91 bar. However, they could only achieve very poor coloring on PC sample at these conditions. They mention, that by the use of disperse red 1 dyestuff PC samples were colored slightly pink contrary to PMMA's dark red color. Therefore, in that article the dyeing of PC turned out to be complicated which was explained by the relatively nonpolar environment [13].

2. Materials and methods

2.1. Prime materials and reagents

Disperse red 1 (*N*-Ethyl-*N*-(2-hydroxy ethyl)4-(4-nitrophenylazo)aniline) and disperse red 13 (2-[4-(2-Chloro-4-nitrophenylazo)-*N*-ethylphenylamino]ethanol), DR1 and DR13, respectively, were supplied from Sigma Aldrich. They are common chromophores for nonlinear optic (NLO) materials and only differ in one chlorine group (see Fig. 1). Since it is known that the presence of halogen groups increases the solubility in $scCO_2$ atmosphere [14], we suggested them to be appropriate for a comparison in their dyeing efficiency. Polycarbonate (LEXAN® resin 121) was kindly provided by Saudi Basic Industries Corporation (SABIC) in pelletized form with a diameter of approx. 1.5 mm and a length of 3 mm. Carbon dioxide was ordered from Linde Gas GmbH. and had a purity of 99.5%. Other reagents (e. g. cleaning ethanol and dichloromethane) were supplied from Sigma Aldrich and had a purity of >99.5%.

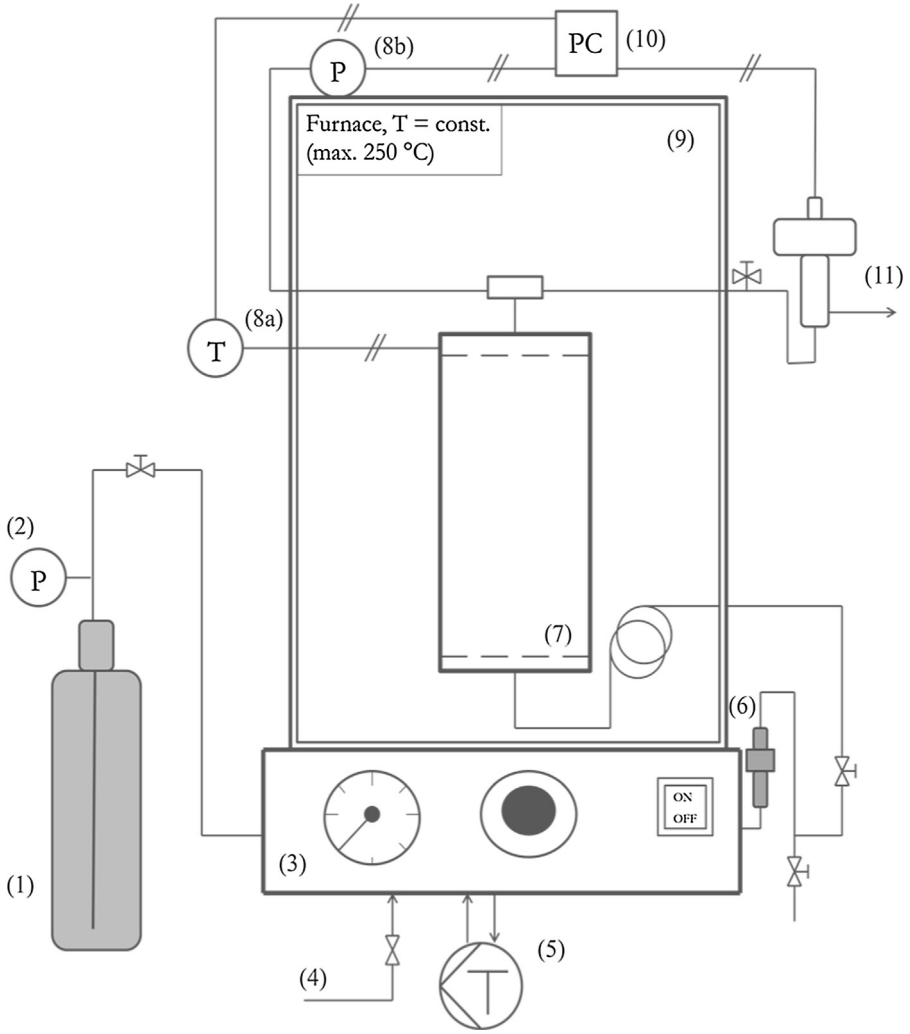

Fig. 2. Experimental SFD apparatus. Carbon dioxide cylinder (1), manometer (2), CO_2 liquid pump (3), pressurized air (4), recirculation cooling bath (5), check valve (6), high pressure vessel (7), temperature and pressure indicators (8a and 8b respectively), heating chamber (9), computer (10), metering valve (11).

2.2. The experimental apparatus

The impregnation equipment is shown on Fig. 2. Carbon dioxide is stored in cylinders equipped with a dip tube and a manometer in a safety box (not pictured). It enters into the system via a liquid CO_2 pump (Haskel ASF-100, USA), which operates with pressurized air. CO_2 is cooled below 5 °C by a recirculation cooling bath in order to maintain it in liquid form. Pressurized CO_2 leaves the pump through a check valve and flows into the high pressure vessel which is placed inside a thermostated heating chamber (*Spe-ed SFE*, Applied Separations, USA, T_{max} 250 °C). The useful volume of the vessel used was 140 ml. Temperature and pressure were monitored by indicators and data are transmitted into the computer via an interface (not pictured). The use of a metering valve (Kämmer Typ KA, Flowserve ltd. Germany) connected to the regulators and controlled by the computer allows a controlled depressurization at the end of the process.

2.3. Solubility measurements of DR13

A simplified version of a flow type apparatus [15] was used to measure the solubility of DR13 in some cases where literature data were not available. A CO_2 liquid pump (JASCO Pu-2080-CO2 Plus) was connected to an extraction column placed in a tempered water bath. The column was filled with 0.020 g dye mixed with 0.150 g Perfil 100™, a porous inert supporting material in order to obtain a uniform flow distribution of the $scCO_2$. At the end of the column, a filter (pore size 0.5 μm) was placed. Underneath and above the dye-Perfil package, small amount of cotton-wool was placed in order to avoid the possible blocking of the filter. Inner diameter of the column was 4.0 mm and the package length was 9.6 cm. The filled column was pressurized and a sample from the CO_2 phase was taken by firmly opening a needle valve placed after the column while pressure and temperature were kept constant. During sample taking 0.75 ml/min CO_2 flow was maintained by the JASCO pump. Average residence time in the packed part of the column was then calculated as 0.64 min assuming 0.4 relative void volume. Each sample was collected for 15 min in a liquid ethanol trap. After every sample the needle valve was carefully cleaned and the dye precipitated in the valve upon sample taking was washed into the collected sample by known amount of ethanol. After this, dye content was determined by UV–vis spectroscopy upon its calibration by using the Lambert-Beer law. According to the data given for a flow type apparatus constructed by [15], the average residence time was calculated to be 0.45 min and authors stated that by this time a saturation of the fluid phase with the dye was achieved. Moreover, one solubility measurement was carried out in our stirred high pressure view cell in a non-continuous flow type apparatus where the dye-$scCO_2$ (without Perfil) system was held for 120 min, thus equilibrium was surely evolved. The result obtained by using the view cell correlated fairly well with literature data and with the solubility measurement carried out in the flow type apparatus, therefore solubility data measured by our apparatus was accepted as a technical solubility data for DR13 in $scCO_2$.

2.4. Impregnation parameters

Experiments were performed in the range of 100–300 bar. Determining the optimum residence time and working temperature, the following points had to be taken into account. It is well known, that CO_2 acts as a plasticizing agent for polymers and reduces their glass transition temperature (T_g) remarkably [12]. Schnitzler [10] determined the glass transition temperature of PC at 300 bar to be around 70 °C. Tang et al. [18] suggests that on 400 bar T_g can be below 60 °C. Zhang and Handa [16] determined the T_g of polycarbonate by high pressure DSC up to 90 bar from ambient pressure. Authors observed a linear decreasing trend by increasing the pressure. The lowest depressed T_g value was 80 °C below the T_g measured at atmospheric conditions (145 °C). It is known, that PC becomes crystalline in the presence of $scCO_2$ above the glass transition temperature [17,18]. This means an irreversible change in the polymer structure, which has to be avoided, because crystalline regions are difficult to impregnate. Therefore, in our experiments temperature was fixed at 40 °C and 50 °C to stay surely below the depressed T_g of the polymer. According to Schnitzler [10], polycarbonate reaches its equilibrium sorption amount under $scCO_2$ within 3–6 h (depending on the temperature) and from 8 to 72 h for some dyes. Tang et al. [18] investigated the PC behavior in $scCO_2$ and reported that a 0.5 mm thick polycarbonate sample reaches the maximum carbon dioxide uptake after approx. 2 h at 40 °C, measured at 200, 300 and 400 bar. This uptake is diffusion controlled. Our cylindrical, pellet samples, have a remarkably bigger size (approx. 1.5 mm in diameter and 3 mm in length), thus presumably require more time to reach the equilibrium in $scCO_2$. Therefore a minimum impregnation time of three hours was chosen. According to West et al. [13], PMMA has a dye uptake of 0.5 wt% at 40 °C and 91 bar. To ensure that the dye is present in high excess 3 wt% of dye with respect to the polymer mass was applied (2.00 g PC and 0.0600 g dyestuff inside the high pressure vessel).

2.5. Impregnation experiments

The materials were used as received. The glass transition temperature of polycarbonate was measured by DSC and was determined to be around 148 °C. Samples of PC and dye were weighted on an analytical balance and placed in the high pressure vessel separated from each other. The dye was placed at the bottom, underneath the polymer, which was situated on an upper sieve approx. 1 cm above the dyestuff. After sealing and connecting the vessel it was heated up to impregnation temperature in the oven. When temperature was reached, the vessel was pressurized up to the desired pressure and the experiment started. After a given impregnation time, it was depressurized applying linear decompression within 30 min by using the metering valve. The dyed PC samples were cleaned with ethanol to remove the precipitated dye from the PC surface. The high pressure vessel was disassembled and thoroughly cleaned with ethanol.

2.6. Analytics

After every experiment, eight pellets (approx. 0.15 g, measured on analytical balance) of the dyed PC were dissolved in 2.000 ml dichloromethane (DCM) and the solution was measured by a double beam UV–vis spectrophotometer (UV-1800, SHIMADZU Handels GesmbH, Austria). UV measurements were triplicate to ensure the accuracy. The measured absorbance of these three different samples (each of them containing eight pellets) taken from one experiment correlated reasonably well, indicating the uniformity of the impregnation. UV–vis instrument was calibrated by known amount of dye dissolved in DCM. The dye concentration of the impregnated PC samples was calculated by the Lambert-Beer law. Dissolving untreated PC samples in dichloromethane did not change its absorbance in the 400–600 nm wavelength range thus clean DCM was used as a reference sample. The absorbance maximum was 484 nm and 503 nm for DR1 and DR13, respectively. Dye concentrations measured at absorbance maximum are given in $[mg_{(dye)}/g_{(PC)}]$ unit.

Table 1
Dyes solubility in $scCO_2$ and PC swelling at various pressures and temperatures.

T (°C)	p (bar)	CO_2 density (mol/L)[a]	Solubility ($\times 10^{-7}$ mol/mol)		Swelling V/V%[d]
			DR1	DR13	
40	100	14.283	0.81[b]	1.77	~6.0
40	150	17.729	3.41[b]	(no data)	
40	200	19.082	6.44[b]	7.80	
40	250	19.984	8.25[b]	(no data)	
40	300	20.675	(no data)	18.40	~9.5
50	100	8.7328	0.16[c]	0.43[c]	~5.9
50	200	17.821	15.78[c]	52.59[c]	
50	300	19.778	48.09[c]	119.4[c]	~9.2

[a] NIST standard reference database.
[b] From reference [19].
[c] From reference [11].
[d] From reference [10].

Table 2
Tabulated data of dye uptake at various temperature and pressure, DR13 dyestuff.

T (°C)	p (bar)	Dye solubility ($\times 10^{-7}$ mol/mol)	Dye uptake (mg/g)		
			3 h	6 h	24 h
40	100	1.77	0.059	0.072	0.089
40	200	7.80	0.038	0.065	0.138[b]/0.231
40	300	18.40	0.048	0.082	0.268
50	100	0.43[a]	0.208	0.276	
50	200	52.59[a]	0.283 ± 0.016	0.453	
50	300	119.4[a]	0.389/0.463[c]	0.552	

[a] From reference [11].
[b] After 17 h sorption time.
[c] After 4 h sorption time.

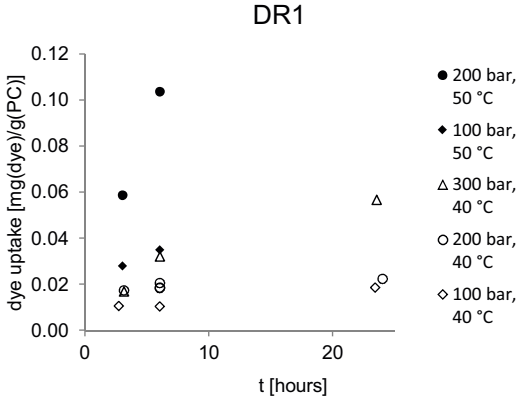

Fig. 3. Effect of the CO_2 pressure and temperature on the DR1 dye uptake versus impregnation time.

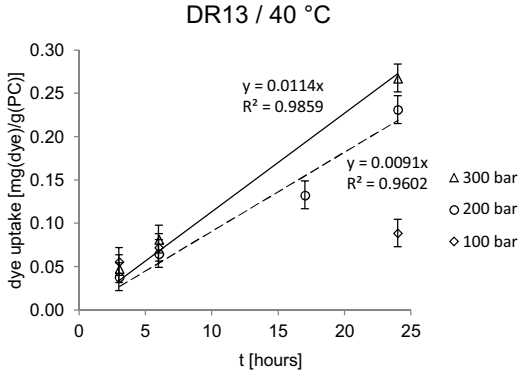

Fig. 4. Effect of the CO_2 pressure on the DR13 dye uptake versus impregnation time, 40 °C.

3. Results and discussion

3.1. Results obtained by the use of DR1

Experiments were performed first on 40 °C. The dye uptake versus time is shown in Fig. 3. The experiment at 200 bar and 40 °C and 6 h was triplicate, the standard deviation was determined as 0.0012 [$mg_{(dye)}/g_{(PC)}$] (6.2%, not pictured in Fig. 3). We consider this error constant within our working pressure and sorption time range in case of DR1. At 100 bar the impregnation is low, experiments performed at 200 bar result in a slightly better dye uptake. At these pressures $scCO_2$ swells the polymer remarkably (min. ~6.0 vol%, measured by Schnitzler et al. [10]). Since from 6 h to 24 h the uptake did not change remarkably neither at 100 nor at 200 bar, we assume that equilibrium of dye sorption in the polymer phase has been reached. In the equilibrium, the partitioning coefficient, K_c, which is the ratio of the saturated concentration of the dye in the polymer phase to the saturated concentration of the dye in the fluid phase, determines the final dye uptake. K_c was calculated from the solubility data of the dyes taken from [19] and from the measured dye concentration in the polymer after 24 h. They were determined to be 56.7 and 6.2 at 100 and at 200 bar, respectively. These values are low. The coloring of PC is rather poor as it was previously reported [13]. For PMMA-DR1 system, West et al. [13] determined the K_c to be ~10^5 at 91 bar and 40 °C. For DO25 dyestuff in PMMA matrix, a similar value at this pressure and temperature for K_c of 5.29×10^4 was found [20]. The calculated partition coefficient is lower at higher pressure. This is expected, because as CO_2 density increases, the solubility of the dye in the fluid phase increases, thus its partition in the polymer phase compared the fluid phase decreases. This correlates to literature data reported elsewhere [13,20]. The diffusion coefficient (D) in $scCO_2$ at a constant temperature increases with pressure [17] thus D is higher at 200 bar then at 100 bar. This increased D led to a faster process, thus equilibrium has been reached already after 6 h at 200 bar (Fig. 3). At 300 bar

much better results were observed after 24 h and it is probable, that equilibrium has not been reached. Here the diffusion governs the process and dye uptake can increase by impregnation time and reaches remarkably higher values than on 200 bar – meanwhile dye solubility and polymer behavior under $scCO_2$ do not change much within this range (see Table 1. which contains literature data of the dyes' solubility and swelling of the polymer at various pressures and temperatures). In general, applying the higher temperature (50 °C, Fig. 3, full markers) resulted in a better uptake. After six hours of impregnation time, similar dye uptake was achieved at 100 bar, 50 °C and at 300 bar, 40 °C. The difference between samples measured at these conditions is even higher after three hours. In the former case at 100 bar and 50 °C, the concentration of the dye in the polymer phase is higher than in the vessel. There are no literature data available for the solubility of DR1 at 300 bar and 40 °C (see Table 1). However, generally, the solubility of a given dye increases with the CO_2 density [11,14,19]. Therefore, we assume, that the solubility is higher at 300 bar and 40 °C ($\rho_{(CO2)}$ = 20.647 mol/l) than at 100 bar and 50 °C ($\rho_{(CO2)}$ = 8.732 mol/l). Tang et al. [18] measured the diffusion coefficients in PC at temperature ranges from 40 to 60 °C and pressure ranges from 100 to 400 bar. The authors pointed out, that $scCO_2$ sorption diffusivities increased with temperature and are the highest at lowest pressures. Nevertheless, by temperature increase the chain mobility and the kinetic motion of the $scCO_2$ within the polymer phase increases. These factors strongly affect the uptake and the effect of temperature seems to be more important that of pressure and CO_2 density. At 200 bar and 50 °C after six hours, an entirely colored but somewhat opaque sample was obtained. This behavior of PC has already been observed in the literature and was attributed to the $scCO_2$ induced crystallization phenomenon [17,18,21].

3.2. Results with dyestuff DR13

Due to the chlorine group, DR13 has an approx. 3–5 times higher solubility in $scCO_2$ than DR1 [11,14]. Therefore, in general, much better results were obtained by the use of DR13 in the investigated time and pressure range (Fig. 4). The measurement at 200 bar 50 °C and three hours sorption time was triplicate, and a standard deviation of 0.016 [$mg_{(dye)}/g_{(PC)}$] (5.6%) was calculated. We consider this error constant for DR13 within our working pressure and temperature. In Fig. 4 it can be seen, that equilibrium has been reached at 100 bar sorption pressure and at 40 °C. From the final dye uptake here and solubility data measured (see Table 1.), the partitioning coefficient was calculated to be 111.1, remarkably higher than in case of DR1 at these conditions. Within the measured time range at 200 and 300 bar the equilibrium has not been reached. According to Tang [18], a PC sample having a thickness of 0.5 mm reaches a maximum CO_2 sorption after 2 h of impregnation time at 40 °C. Therefore, increment in the dye uptake on a fixed pressure cannot be accounted for increasing $scCO_2$ sorption. Rather, the diffusion of the dye within the polymer as a function of time can be observed here. Within this time range of 24 h the first, linear part of a diffusion curve can be observed before it would level off due to saturation. In order to calculate the diffusion coefficients of the dye into the polymer phase, the maximum dye sorption amount in the polymer has to be known. In our experiments at 200 and 300 bar DR13 has not reached the saturation concentration, thus the maximum dye sorption is unknown and diffusion coefficients cannot be calculated. As it was reported elsewhere [10,13], dye diffusion can last sometimes more than 72 h to reach saturation. Literature data [22] also reported that the crystallization of polycarbonate in $scCO_2$ is not only dependent on sorption temperature but highly on sorption time as well. The higher is the temperature and impregnation time, the earlier the crystallization occurs. In our experiments performed at 50 °C, in particular the outer part and the corners of the pellets

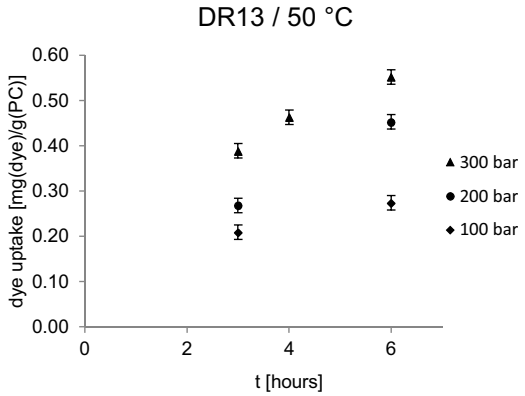

Fig. 5. Effect of the CO_2 pressure on the DR13 dye uptake versus impregnation time, 50 °C.

turned in some cases opaque after sorption. Based on literature data reported elsewhere [17,18,21], we also attribute this phenomenon to the $scCO_2$ induced crystallization of PC. After 3 h of impregnation time at 200 and 300 bar at 50 °C samples remain transparent, but somewhat opaque pellets were obtained after 6 h of sorption time. Therefore, no further experiments with longer sorption times than 6 h at 50 °C and than 24 h at 40 °C were performed. Fig. 5 shows results measured at 50 °C. The increase in the dye uptake at a given sorption time at various CO_2 pressures is related to the dye solubility, which increases at higher pressures (see Table 2). Due to the higher temperature, D is increased and thus much better results were obtained here than at 40 °C. Impregnation for 3 h sorption time at 100 bar and 60 °C resulted in really similar uptake to that of 100 bar and 50 °C. An experiment at 200 bar and 60 °C resulted in a slightly opaque sample readily after 3 h, therefore no further experimentation on 60 °C was made.

4. Conclusions

In spite of the relatively low partitioning coefficients of the dyes between the PC and the fluid phase, both dyes DR1 and DR13 proved to be appropriate for dyeing polycarbonate in $scCO_2$. Thus the SFD method for PC was successfully applied. Equilibrium concentration of the DR1 in PC was achieved at 100 and 200 bar at 40 °C within 24 h. In case of DR13, equilibrium was reached only at 100 bar and 40 °C. From the saturation sorption and solubility data it was calculated that the partitioning coefficient between the polymer and the fluid phase was much higher in case of DR13 than in case of DR1, this caused a better coloring using DR13. This can be due to the presence of a chlorine group in DR13. In case of the equilibrium has not been achieved yet, during impregnation the diffusion coefficient influences the process. The dye uptake here was found to be a linear function of sorption time and was increasing with temperature. Maximal uptake of the polycarbonate sample obtained with DR1 and DR13 in our investigated range were 0.010 wt% and 0.055 wt%, respectively. As it was reported earlier in the literature, we also observed the crystallization of polycarbonate in $scCO_2$ and we suggest this phenomenon can be a limitation for impregnation time, as crystalline regions of polymers are generally harder to impregnate.

Acknowledgements

This work was financially supported by the Marie Curie Initial Training Networks (ITN) via "DoHip – Training Program for the Design of Resource and Energy Efficient Products by High Pressure Processes", project number PITN-GA-2012-316959. The authors would like to acknowledge Candela Campos Domínguez for her valuable assistance during the experimental work. The work of E.

Székely was supported by János Bolyai research grant of the Hungarian Academy of Sciences.

References

[1] A.W. Kjellow, O. Henriksen, Supercritical wood impregnation (Review), J. Supercrit. Fluids 50 (2009) 297–304.
[2] G. Tkalec, M. Pantic, Z. Novak, Z. Knez, Supercritical impregnation of drugs and supercritical fluid deposition of metals into aerogels, J. Mater. Sci. 50 (1) (2015) 1–12.
[3] I. Smirnova, J. Mamic, W. Arlt, Adsorption of drugs on silica aerogels, Langmuir 19 (2003) 8521–8525.
[4] E. Bach, E. Cleve, E. Schollmeyer, Past, present and future of supercritical fluid dyeing technology—an overview, Rev. Prog. Color. 32 (1) (2002) 88–102.
[5] M.V. Fernández Cid, Cotton Dyeing in Supercritical Carbon Dioxide, Ph.D. Thesis, TU Delft, 2005, ISBN: 90-9019765-5.
[6] W. Saus, D. Knittel, E. Schollmeyer, Dyeing of textiles in supercritical carbon dioxide, Text. Res. J. 63 (3) (1993) 135–142.
[7] Ronald F. Sieloff, Method for color dyeing polycarbonate, US, Patent US5453100, 26th Sept. 1995.
[8] Joseph Bianco, Victor T. Humphreys, Method of dyeing shaped polycarbonate resins, US, Patent, US3514246, 26th May, 1970.
[9] I. Kikic, F. Vecchione, Supercritical impregnation of polymers, Curr. Opin. Solid State Mater. Sci. 7 (2003) 399–405.
[10] J. von Schnitzler, R. Eggers, Mass transfer in polymers in a supercritical CO_2-atmosphere, J. Supercrit. Fluids 16 (1999) 81–92.
[11] T. Shinoda, K. Tamura, Solubilities of C.I. disperse red 1 and C.I. disperse red 13 in supercritical carbon dioxide, Fluid Phase Equilib. 213 (2003) 115–123.
[12] S.G. Kazarian, Polymer processing with supercritical fluids, Polym. Sci. Ser. C 42 (1) (2000) 78–101.
[13] B.L. West, S.G. Kazarian, M.F. Vincent, N.H. Brantley, C.A. Eckert, Supercritical fluid dyeing of PMMA films with azo-dyes, J. Appl. Polym. Sci. 69 (5) (1998) 911–919.
[14] S.L. Draper, G.A. Montero, B. Smith, K. Beck, Solubility relationships for disperse dyes in supercritical carbon dioxide, Dyes Pigm. 45 (2000) 177–183.
[15] T. Shinoda, K. Tamura, Solubilities of C.I. disperse orange 25 and C.I. disperse blue 354 in supercritical carbon dioxide, J. Chem. Eng. Data 48 (2003) 869–873.
[16] Z. Zhang, Y.P. Handa, An in-situ study of plasticization of polymers by high-pressure gases, J. Polym. Sci. Pol. Phys. 36 (6) (1998) 977–982.
[17] Y. Sun, M. Matsumoto, K. Kitashima, M. Haruki, S.-I. Kihara, S. Takishima, Solubility and diffusion coefficient of supercritical-CO2 in polycarbonate and CO_2 induced crystallization of polycarbonate, J. Supercrit. Fluids 95 (2014) 35–43.
[18] M. Tang, Tz.-B. Du, Y.-P. Chen, Sorption and diffusion of supercritical carbon dioxide in polycarbonate, J. Supercrit. Fluids 28 (2004) 207–218.
[19] S.N. Joung, K.-P. Yoo, Solubility of disperse anthraquinone and azo dyes in supercritical carbon dioxide at 313.15–393.15 K and from 10 to 25 MPa, J. Chem. Eng. Data 43 (1998) 9–12.
[20] T.T. Ngo, C.L. Liotta, C.A. Eckert, S.G. Kazarian, Supercritical fluid impregnation of different azo-dyes into polymer: in situ UV/vis spectroscopic study, J. Supercrit. Fluids 27 (2003) 215–221.
[21] E. Beckmann, R. Porter, Crystallization of bisphenol a polycarbonate induced by supercritical carbon dioxide, J. Polym. Sci. Pol. Phys. 25 (7) (1987) 1511–1517.
[22] S. Gross, G. Roberts, D. Kiserow, J. DeSimone, Crystallization and solid-state polymerization of poly(bisphenol a carbonate) facilitated by supercritical CO_2, Macromolecules 33 (1) (2000) 40–45.